

**FAKULTÄT MASCHINENBAU**

Master of Science in Manufacturing Technology

Fachgebiet Werkstoffprüftechnik

Prof. Dr.-Ing. habil. Frank Walther

**Master Thesis**

**Layshaft Design & Material Characterization of a Heavy  
Duty Vehicle's Manual Transmission**

by

Gökhan Alkan

Matriculation Number: 173201

Supervisor(s):

1. Prof. Dr-Ing. Habil. Frank Walther
2. Assist. Prof. Dr. Mehmet Ipekoglu

Submitted on 10.07.2017



**TURKISH-GERMAN UNIVERSITY**  
**INSTITUTE FOR GRADUATE STUDIES IN SCIENCE AND ENGINEERING**  
**MASTER'S PROGRAM IN MECHANICAL ENGINEERING**  
**(MANUFACTURING TECHNOLOGY)**  
**THESIS PRESENTATION PROTOCOL**

13.09.2017

The result of the thesis presentation of Gökhan ALKAN, who is registered in the joint graduate program Manufacturing Technology between Turkish-German University and Technical University Dortmund with the registration number 1361011101, titled "Layshaft Design & Material Characterization of a Heavy Duty Vehicle's Manual Transmission" held on 13.09.2017 at 12.00 is presented below.

<input checked="" type="checkbox"/> Successful	<input type="checkbox"/> Extension (3 months)	<input type="checkbox"/> Unsuccessful
--	---	---------------------------------------

Thesis Presentation Committee:



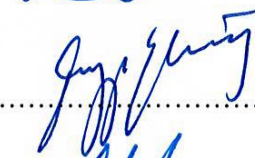


Prof. Dr.-Ing. habil. Frank WALTHER  
(Co-advisor)

Assist. Prof. Dr. Mehmet İPEKOĞLU  
(Co-advisor)

Assist. Prof. Dr. Duygu EKİNCİ  
(Member)

Assist. Prof. Dr. Alpay ORAL  
(Member)

Assist. Prof. Dr. Naime Özben ÖNHON  
(Member)

  
.....  
  
.....  
  
.....  
  
.....  
  
.....



## Master thesis

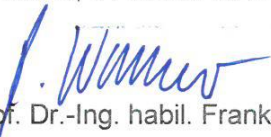
Name: **Gökhan Alkan**  
Supervisor: **M.Sc. Shafaqat Siddique**  
Topic: **Layshaft design and material characterization of a heavy duty vehicle's manual transmission**

Power train transmission unit of a heavy duty vehicle is subjected to excessive and variable loadings and it should function safely for the vehicle's predetermined operation life. In order to ensure a durable vehicle, the installed powertrain unit takes a vital role. This work is designed to obtain optimum design of the layshaft of manual transmission system of TÜMOSAN tractor. Therefore transmission development and its detail design needs to be carried out with reliable characteristics with a goal to define an optimum load bearing and fatigue resistant design of the layshaft.

The work will start from investigating state of the art design of manual transmission, durability, optimization and fatigue theory for component base. Forces and torques acting on the investigated component will be determined, and the corresponding stresses will be investigated by finite element modelling (FEM). Loading cases and expected component life will be considered. Initial design of the part will be examined by KISSsoft and KISSsys softwares by determination of reaction forces on the boundaries of the investigated part. Material properties for the alternative material will be determined by tensile and fatigue testing, and determination of the fatigue durability will be carried out utilizing FEMFAT software. Based on the simulations, structure of the component will be redesigned for optimal mechanical properties which will be finally manufactured as prototype.

All the practical work will be carried out at TÜMOSAN motor and tractor company in Turkey.

Dortmund, 01 March 2017

  
(Prof. Dr.-Ing. habil. Frank Walther)



**Declaration of Originality**

I hereby declare that this master thesis entitled

**“Layshaft Design & Material Characterization of a Heavy Duty Vehicle's Manual Transmission”** submitted as the final thesis of the master program Master of Manufacturing Technologies at Dortmund Technical University is written on my own and not made use of the work of any other party or students past or present without acknowledgement, except those indicated by referencing.

---

Istanbul, 10.07.2017

Gökhan Alkan







## ACKNOWLEDGEMENT

This thesis was prepared in a private company under the cooperation with Technical University of Dortmund and Turkish-German University. The thesis has been completed under constant supervision of Prof. Dr.-Ing. Habil. Frank Walther (Head of Department of Materials Test Engineering, TU Dortmund) and Assist. Prof. Dr. Mehmet Ipekođlu (Dept. of Mechatronic Systems Engineering, Turkish-German University). Taking this as an advantage, I would like to express my sincere gratitude to all of my colleagues at the Transmission Development Department.

I would like to convey my gratefulness to Mr. Shafaqat Siddique for his time, guidance and invaluable help. It was a great pleasure for me to conduct this with his valuable comments.

I want to express my gratitude to Assist. Prof. Murat Baydogan from ITU Metallurgical & Material Engineering Department and Mr. Alper Bayrak who is the manager of the MATIL (Material Testing and Innovation Laboratories AŞ.) for making available of material mechanical testing equipments. I also would like to thank to Cengiz Limerer who is the owner of Limoz Machine & Gear Co. and Mr Bülent Bolat the Purchasing Department Manager of TŪMOSAN Motor & Tractor Co. for raw material supply.

Lastly but not least, I would like to thank to my parents Mustafa and Ayfer Alkan for supporting me through all these years and my girlfriend Hazal Büyükbayram for her patience through this thesis work. I am sincerely grateful for their invaluable support.

Istanbul, 10.07.2017

Gökhan Alkan



## ABSTRACT

This thesis is oriented to be a guidance for optimum material selection and design optimization for heavy duty manual transmission's counter shaft which is also called as layshaft. In scope of the thesis, designing procedure of the intended manual transmission is described and the work is mainly focused on material testing, conducting FEA stress analysis and post FEA fatigue simulation of layshaft.

The main goal is to obtain durable and fatigue free design for the layshaft. In order to achieve this purpose three different widely used case hardening steel was examined as candidate material. The purpose is to be able to determine which material is best to choose for this particular development project by considering to be competitive in the market and reliable component design.

Material characterization was performed to obtain mechanical properties, by tensile and fatigue testing.

During the thesis work, structured work plan was followed as by making literature survey acquiring the state of knowledge regarding transmission design and fatigue theory. With the acquired knowledge, manual transmission architecture is determined and utilizing KissSoft and KissSys machine elements software preliminary transmission design is obtained with gear tooth count and shaft central distances. For further calculations, reaction forces on the boundaries of layshaft such as gear forces are calculated with maximum input torque from the internal combustion engine. These obtained forces are used as input for FEA analysis by utilization of available softwares outcome of FEA is input data for post fatigue analysis simulation. In parallel with computer simulations, chemical metallurgy, tensile test and fatigue test are performed on alternative candidate materials. The obtained strength of materials and their fatigue behaviour are fed to FEMFAT software. The results of fatigue software is compared with required duty cycle of the transmission and a proposed design is manufactured for first prototype of manual transmission. The success of the project will be evaluated after complete transmission test both on rig and field tests.

**Keywords:** Fatigue, FEA, FEMFAT, Case Hardening Steel, Manual Transmission.



## Table of contents

<b>ACKNOWLEDGEMENT</b>	<b>iii</b>
<b>ABSTRACT</b>	<b>v</b>
<b>Table of contents</b>	<b>vii</b>
<b>Formula symbols and abbreviations</b>	<b>ix</b>
<b>List of Figures</b>	<b>1</b>
<b>List of Tables</b>	<b>4</b>
<b>List of Equations</b>	<b>5</b>
<b>1 Introduction</b>	<b>7</b>
1.1 Background .....	7
1.2 Aim of the Thesis.....	7
1.3 Delimitation of the Thesis .....	8
<b>2 State of the Art</b>	<b>9</b>
2.1 Automobile Power Transmission .....	9
2.1.1 Manual Transmissions MT.....	11
2.2 Fatigue Theory .....	16
2.2.1 History of Fatigue Theory.....	16
2.2.2 Fatigue Failure Phases.....	19
2.2.3 Mean Stress Effect .....	19
2.2.4 Fatigue Life Models in Fatigue Design.....	21
2.2.5 Fatigue Design Criteria .....	21
2.2.6 Generation and Standard Load – Time Histories for Fatigue Investigation.....	23
2.2.7 Fatigue Stress Life (S-N) Approach .....	23
2.2.8 Damage Accumulation Theories.....	24
2.2.9 Fatigue Limit Testing & S-N Curve Generation .....	26
2.2.10 Post Investigation of Fatigue Failed Surface.....	26
2.2.11 Using FEMFAT Post FEA for Fatigue Life Estimation .....	26
2.2.12 Current Fatigue Related Researches.....	27
2.3 Choice of Material & Its Characterization.....	29
2.3.1 Tensile Test.....	29
2.3.2 Material Fatigue Testing .....	30
2.4 Shaft Hub Connections.....	34
2.4.1 Keyway Connection .....	34
2.4.2 Interference Fit Connection.....	35

---

2.4.3	Splined Connection.....	37
2.5	Key Aspects of FE Modelling .....	38
2.5.1	Deciding Element Type for the Analysis.....	38
2.5.2	Validating The Accuracy of the Results.....	40
<b>3</b>	<b>8+1 Manual Transmission Preliminary Design</b>	<b>41</b>
3.1	Concept and Benchmarking.....	41
3.2	Gear Count & Ratio Determination .....	45
<b>4</b>	<b>Layshaft Design Alternatives</b>	<b>49</b>
4.1	Splined layshaft CAD design .....	50
4.2	Interference Fit Layshaft CAD Design.....	52
<b>5</b>	<b>Material Selection</b>	<b>55</b>
5.1	Material Cost Analysis .....	57
<b>6</b>	<b>Experimental Investigation</b>	<b>58</b>
6.1	Chemical Metallurgy .....	58
6.2	Tensile Test.....	60
6.3	Rotating Bending Fatigue Testing.....	66
<b>7</b>	<b>Numerical Modelling</b>	<b>73</b>
7.1	Utilized Hardware Specification .....	73
7.2	Commercial Softwares for Analytical Calculation & FEA.....	73
7.3	Modelling of Rotating Bending Fatigue Test .....	73
7.3.1	Analytical Calculation of Bending Stress.....	77
7.3.2	FEA and FEMFAT Modelling of Rotating Bending Test.....	77
7.4	FEA Model for Layshaft Stress Analysis .....	80
7.4.1	Force Extraction of Transmission.....	81
7.5	CAE Analysis of Layshaft Designs.....	84
7.5.1	FEA Gear Loading Model .....	84
7.5.2	Layshaft assembly comparison.....	91
7.5.3	Mission Profile of Transmission .....	92
7.5.4	Post Fatigue Life Analysis.....	94
<b>8</b>	<b>Results &amp; Discussion</b>	<b>101</b>
8.1	Future Work.....	102
<b>9</b>	<b>Bibliography</b>	<b>103</b>

## Formula symbols and abbreviations

### Formula Symbols

<b>Symbol</b>	<b>Unit</b>	<b>Description</b>
$r$	mm	Radius
$d$	mm	Diameter
$\sigma_{max}/S_{max}$	MPa	Higher stress in stress cycle
$\sigma_{min}/S_{min}$	MPa	Lower stress in stress cycle
$\sigma_a/S_a$	MPa	Stress amplitude
$E$	MPa	Elastic modulus
$\Delta\sigma/\Delta S$	MPa	Difference between max and min stress
$R_s$	-	Stress ratio of min to max stress
$R_m$	MPa	Ultimate tensile stress
$N$	-	Number of cycles
$N_f$	-	Fatigue life endurance
$\sigma_N$	MPa	Fatigue strength at N cycles
$\varphi$	-	Strain
$\sigma$	MPa	Stress

---

## Indices

<b>Indice</b>	<b>Description</b>
<i>t</i>	<i>Thickness</i>
<i>l</i>	<i>Length</i>
<i>b</i>	<i>Width</i>

## Abbreviations

<b>Abbreviation</b>	<b>Description</b>
<i>AMT</i>	<i>Automated Manual Transmission</i>
<i>AT</i>	<i>Automatic Transmission</i>
<i>CAD</i>	<i>Computer Aided Design</i>
<i>CAE</i>	<i>Computer Aided Engineering</i>
<i>CH</i>	<i>Case Hardening</i>
<i>CHD</i>	<i>Case Hardening Depth</i>
<i>COF</i>	<i>Coefficient of Friction</i>
<i>DEM</i>	<i>Discrete Element Method</i>
<i>ECU</i>	<i>Engine Control Unit</i>
<i>FEA</i>	<i>Finite Element Analysis</i>
<i>FKM</i>	<i>Forschungskuratorium Maschinenbau</i>
<i>ICE</i>	<i>Internal Combustion Engine</i>
<i>IF</i>	<i>Interference Fit</i>
<i>ITU</i>	<i>Istanbul Technical University</i>
<i>MT</i>	<i>Manual Transmission</i>
<i>OES</i>	<i>Optical Emission Spectrometer</i>
<i>TCC</i>	<i>Torque Converter Clutch</i>
<i>TCU</i>	<i>Transmission Control Unit</i>



## List of Figures

FIGURE 2.1 POWERTRAIN ARRANGEMENT IN A VEHICLE (BMW) (FISCHER, ET AL., 2015).....	9
FIGURE 2.2 FIRST HYDRA-MATIC ON DISPLAY AT YPSILANTI AUTOMOTIVE MUSEUM .....	10
FIGURE 2.3 OPERATION FOR A CVT TRANSMISSION (NAUNHEIMER, ET AL., 2011).....	10
FIGURE 2.4 ILLUSTRATION OF DISENGAGED & ENGAGED CLUTCH (YAO, 2008) .....	11
FIGURE 2.5 SCHEMATIC DIAGRAM AND ACTUATION PRINCIPLE OF A SYNCHROMESH.....	12
FIGURE 2.6 ILLUSTRATION OF 4 SPEED TRANSMISSION WITH RESPECT TO THEIR STAGES	13
FIGURE 2.7 DIESEL ENGINE TORQUE-POWER CURVE (IN COURTESY OF COMPANY).....	14
FIGURE 2.8 A) TRACTION FORCE GAP B) POWER GAP (FISCHER, ET AL., 2015) .....	15
FIGURE 2.9 DESIGNS TO ACHIEVE MAXIMUM SPEED (FISCHER, ET AL., 2015) .....	15
FIGURE 2.10 FAILURE OF A CONSTRUCTION TRUCK TRANSMISSION LAYSHAFT .....	16
FIGURE 2.11 SIMULATION BASED FATIGUE INVESTIGATION (SOCIE, 2002) .....	18
FIGURE 2.12 SLIP BAND FORMATION UNDER CYCLIC LOADING (LEE, ET AL., 2005) .....	19
FIGURE 2.13 ALTERNATING AND MEAN STRESS COMBINATION ACCORDING TO GOODMAN	20
FIGURE 2.14 A) SODERBERG, B) GOODMAN, C) GERBER AND D) MORROW APPROACHES ..	20
FIGURE 2.15 FATIGUE DESIGN FLOW CHART (FATEMI, ET AL., 2001).....	21
FIGURE 2.16 CONSTANT AMPLITUDE LOADING .....	24
FIGURE 2.17 LINEAR VS. NONLINEAR DAMAGE FRACTION (STEPHENS, ET AL., 2001) .....	25
FIGURE 2.18 S-N TESTING WITH SMALL SAMPLE BATCH (LEE, ET AL., 2005) .....	26
FIGURE 2.19 FEMFAT MODULES (GAIER, 2010).....	27
FIGURE 2.20 TENSILE TEST SPECIMEN (BUDYNAS, 2006).....	29
FIGURE 2.21 TENSILE STRENGTH REPRESENTATION OF MATERIALS (BUDYNAS, 2006) .....	30
FIGURE 2.22 EXAMPLE OF TYPE-A TEST SPECIMEN PER DIN 50125.....	30
FIGURE 2.23 CANTILEVER ROTATING BENDING .....	31
FIGURE 2.24 ROTATING PURE BENDING.....	32
FIGURE 2.25 FOUR POINT BENDING WITH PARALLEL SPECIMEN (BS ISO 1143:, 2010).....	32
FIGURE 2.26 CYLINDRICAL SMOOTH SPECIMEN AS PER (BS ISO 1143:, 2010) .....	33
FIGURE 2.27 KEY ELEMENT FOR TORQUE TRANSMISSION (TEMIZ, N.D.) .....	34
FIGURE 2.28 PRESS FIT SHAFT AND HUB SIZE WITH TOLERANCE (TEMIZ, N.D.) .....	35
FIGURE 2.29 CONICAL PRESS FIT CONNECTION (TEMIZ, N.D.) .....	35
FIGURE 2.30 BOLT PRELOADED SHAFT – HUB CONNECTION (TEMIZ, N.D.).....	36
FIGURE 2.31 IF PARAMETERS (KLEBANOV, ET AL., 2007).....	36
FIGURE 2.32 SHAFT - HUB CONNECTIONS A) DIN5480 SPLINE, B)DIN5481 C)DIN32711 .....	37
FIGURE 2.33 FIRST AND SECOND ORDER TETRAHEDRAL ELEMENTS .....	39

---

FIGURE 3.1 A) GEOMETRIC GEAR RATIO DESIGN (FISCHER, ET AL., 2015).....	46
FIGURE 3.2 B) PROGRESSIVE GEAR RATIO DESIGN (FISCHER, ET AL., 2015) .....	46
FIGURE 3.3 GEAR RATIO TO SCAN ENGINE'S EFFECTIVE TORQUE RANGE .....	47
FIGURE 3.4 THE MANUAL 8+1 TRANSMISSION LAYOUT.....	48
FIGURE 3.5 8+1 MT 3D ROUGH SIZING USING KISSYS, COURTESY OF THE COMPANY .....	48
FIGURE 4.1 KEYWAY SLOTTED LAYSHAFT, THE MANUFACTURER IS UNKNOWN .....	49
FIGURE 4.2 VARIOUS SHAFT DESIGNS IN MECHANIC WORKSHOP .....	49
FIGURE 4.3 INTERFERENCE FITTED GEARS AND FLAT SURFACE LAYSHAFT (ZF) .....	50
FIGURE 4.4 DIN 5480 SPLINED LAYSHAFT.....	50
FIGURE 4.5 SPLINED LAYSHAFT ASSEMBLY WITH GEARS.....	51
FIGURE 4.6 TORQUE TRANSMISSION ON LAYSHAFT SPLINED CONNECTIONS.....	51
FIGURE 4.7 SPLINE SAFETY CALCULATION FOR THE SHORTEST FACE WIDTH.....	52
FIGURE 4.8 SMOOTH INTERFERENCE FIT LAYSHAFT DESIGN .....	53
FIGURE 4.9 INTERFERENCE FIT LAYSHAFT MODEL WITH GEAR HUB.....	54
FIGURE 4.10 IF FEA STRESS RESULT .....	54
FIGURE 5.1 SECTION VIEW OF 8+1 MT GEAR TRAIN (COURTESY OF THE COMPANY) .....	55
FIGURE 6.1 MATERIAL SAMPLES FOR CHEMICAL METALLURGY .....	58
FIGURE 6.2 SAMPLES AFTER CHEMICAL ANALYSIS.....	59
FIGURE 6.3 TENSILE TEST PIECE "A 6 × 30" PER DIN EN ISO 6892-1 .....	60
FIGURE 6.4 HARDNESS SCAN INSPECTION REPORT FOR TEST SPECIMENS .....	60
FIGURE 6.5 ZWICK/ROELL Z600 600KN TENSILE TEST MACHINE WITH CLAMPED SPECIMEN	61
FIGURE 6.6 MANUFACTURED TENSILE TEST SPECIMENS .....	61
FIGURE 6.7 TENSILE TEST GRAPH OF CASE HARDENED 18CRNIMO7-6.....	62
FIGURE 6.8 TENSILE TEST GRAPH OF CASE HARDENED 20NICRMO2-2.....	62
FIGURE 6.9 TENSILE TEST GRAPH OF CASE HARDENED 20MNCR5.....	63
FIGURE 6.10 TENSILE TEST GRAPH OF 18CRNIMO7-6 WITHOUT CH.....	64
FIGURE 6.11 TENSILE TEST GRAPH OF 20NICRMO2-2 WITHOUT CH.....	64
FIGURE 6.12 TENSILE TEST GRAPH OF 20MNCR5 WITHOUT CH.....	64
FIGURE 6.13 ALL TEST RESULTS ARE SUPERIMPOSED ON ONE GRAPH.....	65
FIGURE 6.14 TENSILE SPECIMENS, LEFT TO RIGHT 18CRNIMO7-6, 20MNCR5, 20NICRMO2-2	65
FIGURE 6.15 FRACTURE SURFACE LEFT TO RIGHT 18CRNIMO7-6, 20MNCR5, 20NICRMO2-2	65
FIGURE 6.16 RB FATIGUE TEST BENCH WALTER+BAI AG UBM 5-200NM .....	66
FIGURE 6.17 A CLAMPED SPECIMEN FOR RB FATIGUE TESTING .....	66
FIGURE 6.18 INTERCHANGEABLE WEIGHTS TO CREATE CONSTANT BENDING STRESS .....	67

---

FIGURE 6.19 MOMENT ARMS 400 MM FOR CREATING BENDING MOMENT ON SPECIMEN .....	67
FIGURE 6.20 ROTATING BENDING FATIGUE TESTING SAMPLE PER (BS ISO 1143:, 2010) .....	68
FIGURE 6.21 SPECIMENS FOR EACH MATERIAL GROUP BEFORE HEAT TREATMENT .....	68
FIGURE 6.22 20NICRMO2-2 RB TEST RESULTS WITH ENDURANCE VS. FEMFAT .....	69
FIGURE 6.23 20MNCR5 RB TEST RESULTS WITH ENDURANCE VS. FEMFAT .....	70
FIGURE 6.24 18CRNIMO7-6 RB TEST RESULTS WITH ENDURANCE VS. FEMFAT .....	71
FIGURE 6.25 RB TEST RESULT COMPARISON BETWEEN MATERIALS .....	72
FIGURE 7.1 MESH SIZE COMPARISON .....	74
FIGURE 7.2 DISPLACEMENT VALUE COMPARISON AFTER 10NM BENDING MOMENT .....	75
FIGURE 7.3 EQUIVALENT STRESS COMPARISON AFTER 10NM BENDING MOMENT .....	76
FIGURE 7.4 MESH CONVERGENCE ON RB BAR .....	77
FIGURE 7.5 LEFT MODEL: LOAD CASE 1, RIGHT MODEL: LOAD CASE 2 .....	78
FIGURE 7.6 LINEAR STATIC STRESS ANALYSIS RESULTS FOR REVERSED LOADING .....	78
FIGURE 7.7 FEMFAT RESULT OF RBF SPECIMEN FOR 20NICRMO2-2 MATERIAL .....	79
FIGURE 7.8 FEMFAT RBT WITH 13NM BENDING MOMENT WITH 20NICRMO2-2 SN .....	80
FIGURE 7.9 CTETRA ELEMENTS ON SPLINED LAYSHAFT .....	81
FIGURE 7.10 CTETRA ELEMENTS ON IF LAYSHAFT .....	81
FIGURE 7.11 INPUT & LAYSHAFT WITH ROUGH DIMENSIONS .....	81
FIGURE 7.12 FORCES ON LAYSHAFT .....	82
FIGURE 7.13 CONSTRUCTED SIMULATION MODEL .....	85
FIGURE 7.14 LAYSHAFT COMPRESSION STRESS ON THE SURFACE .....	91
FIGURE 7.15 TORSIONAL LOADING OF 4TH GEAR, TENSION AT SPLINE ROOTS .....	91
FIGURE 7.16 ESTIMATED DUTY CYCLE OF TRANSMISSION .....	93
FIGURE 7.17 LEFT THE FIRST ANALYZED LAYSHAFT, RIGHT IMPROVEMENT PROPOSAL ...	100
FIGURE 8.1 MANUFACTURED PROTOTYPE LAYSHAFT WITH SPLINE CONNECTION .....	101

## List of Tables

TABLE 2.1 GEAR RATIOS AND ITS INTERPRETATION.....	14
TABLE 2.2 FATIGUE PHASES .....	17
TABLE 2.3 OCCURRED FATIGUE FRACTURE AT TORSIONAL LOAD (FATEMI, ET AL., 2001)....	23
TABLE 2.4 RECOMMENDED DIMENSIONS FOR TEST SPECIMEN PER (BS ISO 1143:, 2010) ....	33
TABLE 2.5 FEA ACCURACY CHECK .....	40
TABLE 3.1 INDUSTRIAL VS. AUTOMOBILE TRANSMISSION (NAUNHEIMER, ET AL., 2011).....	41
TABLE 3.2 BENCHMARKED TRANSMISSIONS FOR MANUAL 8+1 TRANSMISSION.....	42
TABLE 3.3 8+1 TRANSMISSION GEAR RATIOS .....	47
TABLE 5.1 COMPOSITION OF STEEL GRADE 1.7147 (20MNCr5).....	56
TABLE 5.2 COMPOSITION OF STEEL GRADE 1.6523 (20NiCrMo2-2).....	56
TABLE 5.3 COMPOSITION OF STEEL GRADE 1.6587 (18CrNiMo7-6).....	56
TABLE 5.4 MATERIAL COST PER TON (ASIL ÇELİK SAN. & TIC. AŞ.).....	57
TABLE 6.1 AVAILABLE TESTING EQUIPMENT IN THE COMPANY .....	58
TABLE 6.2 PROVIDED CHEMICAL COMPOSITIONS BY MANUFACTURER .....	59
TABLE 6.3 OBTAINED CHEMICAL COMPOSITIONS BY SPECTROSCOPY .....	59
TABLE 6.4 HEAT TREATED CARBURIZED (CHD:1.2MM) TEST RESULTS.....	62
TABLE 6.5 TEST SPECIMENS WITHOUT HEAT TREATMENT .....	63
TABLE 6.6 ROTATING BENDING TEST RESULTS FOR 20NiCrMo2-2 AT 50HZ.....	69
TABLE 6.7 ROTATING BENDING TEST RESULTS FOR 20MNCr5 AT 50HZ.....	70
TABLE 6.8 ROTATING BENDING TEST RESULTS FOR 18CrNiMo7-6 AT 50HZ.....	71
TABLE 7.1 MESH INFORMATION OF RBF BAR.....	76
TABLE 7.2 EXTRACTED GEAR FORCES FOR LAYSHAFT BY ACTIVE GEARS.....	84
TABLE 7.3 APPLIED BOUNDARY CONDITIONS.....	85
TABLE 7.4 SPLINED LAYSHAFT STRESS ANALYSIS RESULT TABLE .....	87
TABLE 7.5 IF LAYSHAFT STRESS ANALYSIS RESULTS TABLE .....	89
TABLE 7.6 ESTIMATED DUTY CYCLE OF OFF ROAD VEHICLE AND ITS DRIVELINE.....	92
TABLE 7.7 LAYSHAFT DUTY CYCLE WITH TORQUE FLOW.....	93
TABLE 7.8 STATIC SPEEDS AT 1700 RPM FOR EACH GEAR SELECTION.....	94
TABLE 7.9 FEMFAT MATERIAL DEFINITION PARAMETERS .....	95
TABLE 7.10 FEMFAT LAYSHAFT IF WITH 18CrNiMo7-6.....	96
TABLE 7.11 FEMFAT LAYSHAFT IF WITH 20NiCrMo2-2.....	97
TABLE 7.12 FEMFAT LAYSHAFT SPLINED WITH 18CrNiMo7-6 .....	98
TABLE 7.13 FEMFAT LAYSHAFT SPLINED WITH 20NiCrMo2-2 .....	99

---

## List of Equations

EQUATION 2.1.....	12
EQUATION 2.2.....	12
EQUATION 2.3.....	13
EQUATION 2.4.....	13
EQUATION 2.5.....	19
EQUATION 2.6.....	20
EQUATION 2.7.....	20
EQUATION 2.8.....	20
EQUATION 2.9.....	23
EQUATION 2.10.....	23
EQUATION 2.11.....	23
EQUATION 2.12.....	24
EQUATION 2.13.....	24
EQUATION 2.14.....	24
EQUATION 2.15.....	24
EQUATION 2.16.....	25
EQUATION 2.17.....	25
EQUATION 2.18.....	29
EQUATION 2.19.....	29
EQUATION 2.20.....	34
EQUATION 2.21.....	34
EQUATION 2.22.....	35
EQUATION 2.23.....	36
EQUATION 2.24.....	37
EQUATION 2.25.....	37
EQUATION 3.1.....	45
EQUATION 3.2.....	45
EQUATION 3.3.....	46
EQUATION 3.4.....	46
EQUATION 3.5.....	47
EQUATION 5.1.....	55
EQUATION 7.1.....	77

---

EQUATION 7.2 .....	83
EQUATION 7.3 .....	83
EQUATION 7.4 .....	83
EQUATION 7.5 .....	92
EQUATION 7.6 .....	93



# **1 Introduction**

## **1.1 Background**

This thesis work prepared within a company which currently manufactures agricultural tractors and machineries in various sizes, diesel engines and agricultural tractor transaxles.

Transmission development is not a new business for the Company, however it is specialized only in agricultural tractor's transmissions so far. By the developing business model, company decided to widen its business with off-road vehicles and especially powertrain of heavy duty ones. This self-reliance allowed the company to create new projects such as MT - manual, AMT - automated and AT - automatic transmissions. Manual Transmission is the first step to be taken to gain experience and create solid base knowledge for the company. In May 2016, company initiated its first commercial manual transmission project which also shaped the subject of this thesis.

## **1.2 Aim of the Thesis**

This thesis is aimed to research on manual transmission's layshaft design, material selection and characterization from the available standard steel alloys. The priority is to guarantee the component durability of the transmission system. Later on the gained know how and practice would be applied on every vital component to ensure reliable system design.

In scope of the work, although, the thesis will not cover the complete manual transmission development process, there will be a brief information of the system design and it focuses on the detailed layshaft design of the intended 8+1 MT.

Company's future mission and governmental grants allowed research and development teams work more passionately and apply state of art technology in their related field. Additional outcome of this thesis, it contributes to company's know-how improvement and assist to acquire governmental monetary support for the project.

### 1.3 Delimitation of the Thesis

The transmission's layout and the gear ratios were determined by Transmission basic design team. This includes modelling of transmission by using KissSoft and KissSys softwares with respect to expected power input-output and the required gear ratios.

The following steps are performed within this thesis.

The thesis is mainly focused on manual transmission's layshaft design, design improvement, material selection and its durability prediction. With this regard, engineering tools such as CATIA V5 is used for CAD data and manufacturing drawing generation. The preliminary design output obtained from Kisoft is only the minimum diameter of the shaft for critical sections. Therefore CAD software is used to develop the released data.

Chemical metallurgy is performed to identify delivered material's composition. Tensile testing, fatigue testing and hardness measurement are done to extract mechanical behaviour of candidate materials.

Finite Element Analysis is performed both on the rotating bending testing sample and the layshaft component by using HyperWorks Optistruct. Post fatigue investigation is done with FEM-FAT software.

In order to investigate the component, prior to production both by analytically and numerically FEA approach was utilized. A CEA model was developed to simulate loads acted on layshaft for each selected gears. Correlation is performed between CAE and the experiment, in order to make sure the developed CAE approach, is representing enough the physical situation. Once the validation between CAE model and test results is achieved, using the same methodology, a design life is predicted for the original design and optimization is done with the outcomes of the initial design to have more durable and fatigue free component.



## 2 State of the Art

### 2.1 Automobile Power Transmission

Powertrain unit of an automobile is very crucial topic to be investigated and it could be considered as the backbone of a car. In other words it could be characterized as vehicle's muscular system as in human body. With the invention of internal combustion engines, passenger cars by Karl Benz in 19<sup>th</sup> century and the first massive car production by Henry Ford in 20<sup>th</sup> century, automotive industry initiated compact in size and mobile gearbox units unlike the heavy gearboxes which are needed until that time period. Power transmission from engine to wheels created endless competition between companies and pushed companies to introduce new types of transmissions.

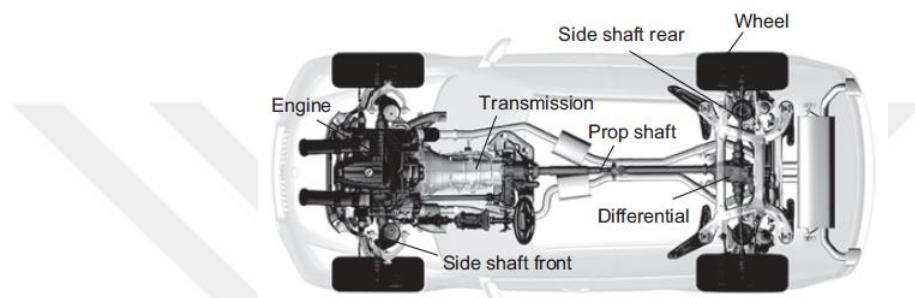


Figure 2.1 Powertrain arrangement in a vehicle (BMW) (Fischer, et al., 2015)

The first type of transmission was manual transmission which is still in service and widely installed on automobiles. Basically, a manual transmission powertrain system has a coupling called clutch and driver must disengage the clutch to disconnect transmission from engine for shifting from one to another gear (Yao, 2008). This system requires attention of driver and driver should follow the engine rpm and vehicle's speed to make the necessary gear change. Especially inexperienced drivers are mostly faced with problems for the first movement of vehicle and gear changes which requires brain-foot-hand coordination.

Gear changes on first manual transmissions was considerably difficult. Driver must arrange the timing and angular speed of the next gear. Because the gear in usage and the next one to be engaged are not rotating at the same speed without any synchronizer. Those manual transmission types called as Unsynchronized Manual Transmissions and no more in production due to unpractical functionality.

Unsynchronized manual transmissions eventually succeeded by synchronized manual transmissions. These types of transmissions have an additional frictional mechanism between sequential shifts such as 1<sup>st</sup> -2<sup>nd</sup>, 3<sup>rd</sup> -4<sup>th</sup> and 5<sup>th</sup> -6<sup>th</sup>. When the driver desires to engage to next gear from idle position, he/she simply moves the shifting knob which means shifting fork in gearbox. Shifting fork is connected directly to synchromesh and movement of the fork to the desired gear, pushes the dog clutch and compresses the conical shape friction component which is connected to the gear. This mechanical assembly equalize the speed of main shaft and desired gear and makes the gear changes smoothly and quiet.

The second type of transmission is conventional automatic transmissions. Despite the introduction of first type of AT by General Motors in 1937 which still needed to be operated by driver. The first mass produced fully automatic transmission was introduced by General Motors in 1939 named Hydra-Matic.

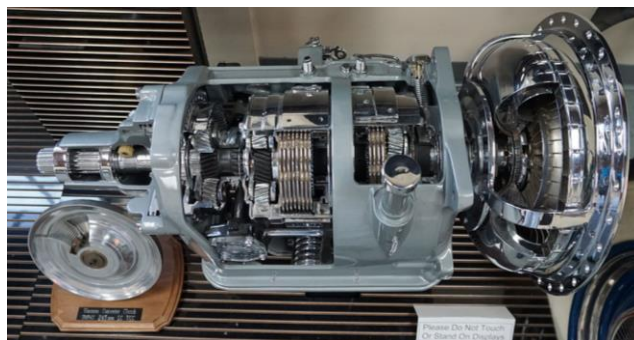


Figure 2.2 First Hydra-Matic on display at Ypsilanti Automotive Museum

A traditional automatic transmission has several subsystem, such as a torque converter, planetary gears in place of gear couples and internal wet-clutches for couplings of ring gears to allow shifting. Complete shifting mechanism actuated by a hydraulic system.

Continuously Variable Transmission shortly CVT unlike the MT and AT, has no gears couplings for speed ratio. Instead of the gears CVT transmissions use two pulleys and a belt or chain for power transmission and to create speed ratio. While shifting, CVT does not need disengage – engage movement of belt or pulleys. Hence belt and pulleys are always in contact. These type of transmissions creates a huge difference from other transmission types, because it is operated without power interruption see Figure 2.3.

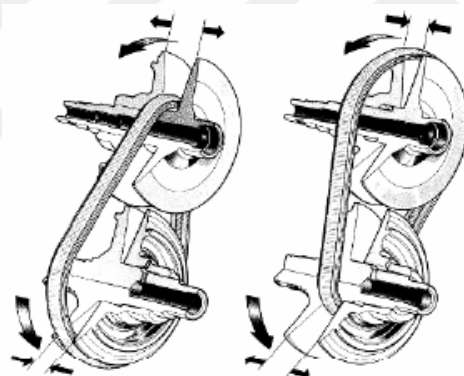


Figure 2.3 Operation for a CVT transmission (Naunheimer, et al., 2011)

The first commercially feasible CVT was Van Doorne's Variomatic and its production took place in the Nederland in 1958 and introduced by DAF Company. Company called its new product as *Variomatic* which was installed on DAF 600 passenger car. The transmission had a rubber V-belt and its pulleys varied diameter for the V-belt was established by axial movement of pulley's conical components. Rubber V-belt limited the transmitted power as for the input torque.

In today's world, development goals of a new transmission includes several criteria. For example transmission durability and comfort are must, reduction of maintenance and repair costs, creation a solid brand image and perception, weight and space reduction, reduction of fuel consumption and exhaust gas emissions while increasing efficiency (Naunheimer, et al., 2011).

Different continents and countries have their own dominant preferences when it comes to vehicles and specific power trains. For example in Japan and NAFTA (**N**orth **A**merican **F**ree

Trade Agreement among the United States, Canada, Mexico) mostly gasoline engine and conventional AT is preferred by household. However in Europe people tend to have a diesel car with manual transmission. The reason for this difference occurred, gasoline prices are higher in EU than in the USA considering the ICE selection, the case of transmission diversity between two markets depends on the habit and marketing strategies and comfort expectancy from a vehicle.

### 2.1.1 Manual Transmissions MT

As it mentioned manual transmissions are the ancestors of the all types of automobile transmissions. Although in American continent people mostly prefer to have an automatic or automated transmissions, MTs are still preferred especially in Europe with a big market share. MTs are dominant in developing or underdeveloped countries like they are in Europe.

A simple modern manual transmission has components such as gearwheels, shafts, synchronizers, bearings, clutches, boosters, TCU (transmission control unit) and with many small important components. These subsystems are all have their specialized research area. It requires decisive and highly specialized engineering teams to handle the complete transmission assembly. Nevertheless it is beneficial to provide brief description regarding the MT's subsystems.

Starting with the clutch system which has the first interaction unit of transmission with the engine. In a power train system on conventional automobile powered with ICE, there must be a coupling unit between engine and transmission for launching a vehicle. This can be established by an intermediate torque transmitter as listed below;

- Wet or dry friction clutches
- Hydrodynamic torque converters.

Torque transfer from one shaft to another can be established by different types of clutch couplings. These clutches can be categorized as shift-able friction clutches, shift-able dog clutches and no shiftable elastic clutches. The most common solution for MT road vehicles are dry friction clutches. See Figure 2.4 for its engaged and disengaged position. It is controlled by driver with a clutch pedal placed far left of the pedal set.

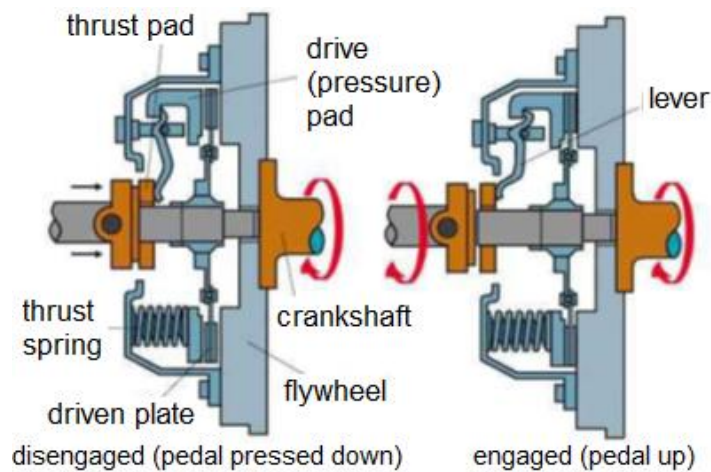


Figure 2.4 Illustration of disengaged & engaged clutch (Yao, 2008)

Transmitted torque is determined for clutch connection design can be formulated as in Equation 2.1

Clutch torque transmission:

$$M_K = \mu F_N r_m \quad \text{Equation 2.1}$$

A clutch might be considered as special type of a brake system. Both systems have a coupling task of two coaxial shafts. Only difference is clutch launches the vehicle by letting the power flow and brake enforces vehicle to stop by the friction occurred between tire and ground. Because of the similarities occurred on both systems, clutches faces the wear phenomenon as well. Therefore, clutch friction component must be periodically changed on a vehicle to have efficient torque flow.

Another important component of the MTs are synchronizers. This component wasn't exist on old manual transmissions however, it is impossible to see a MT in today's automobile market without synchronizers. Synchronizer units in gearboxes known as synchro meshes. Its genius design allows gear engagement quiet and with less effort. In a MT, with the first movement of gear change synchro mesh's sleeve starts its axial move on the shaft axis and pushes main functional element towards synchronizer hub with selector teeth and friction cone. This friction creation conical structure can be seen in Figure 2.5. A wet friction clutch located between these two conical components creates friction which helps the target gear to reach equivalent rotational speed of previously selected gear. Eventually the gear shifting achieved with the positive locking of the target gear. As a result, after the gear shifting operation, previously selected gear now rotates idle on main shaft by needle gear and torque transmission realized by the selected gear to main shaft.

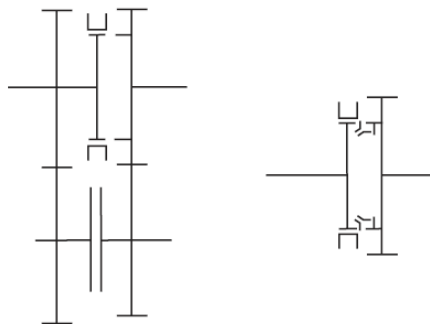


Figure 2.5 Schematic diagram and actuation principle of a synchromesh

One of the main challenge for a transmission is defining the transmission layout and the gear ratios for efficiency and engine compatibility. In general gear ratio symbolized by  $i$ , at this ratio the angular velocity is  $\omega_i$ , revelation of the gearwheel per second  $n_i$ . With these symbols the basic formulation of the calculation for transmitting movement can be found (Fischer, et al., 2015)

Gear ratio formulation

$$i = \frac{w_1}{w_2} = \frac{n_1}{n_2} \quad \text{Equation 2.2}$$

By neglecting the losses, the output torque could be estimated by using Equation 2.3. The total gear ratio  $i$ , creates torque difference between input and output shafts, when it is different than one. This created torque difference must be compensated by housing or supports. From the simplified torque equilibrium the required torque can be estimated as in Equation 2.4 (Fischer, et al., 2015).

Torque output formulation

$$M_2 = iM_1 \quad \text{Equation 2.3}$$

Actuated torque to transmission housing

$$M_3 = M_2 - M_1 = (i - 1)M_1 \quad \text{Equation 2.4}$$

Gearbox concepts can be categorized by their number of stages as listed below. The word stage here refers the power flow one shaft to another shaft which means number of shafts from input to output. (Naunheimer, et al., 2011)

- Single stage transmissions
- Two stage transmissions
- Multi stage transmissions

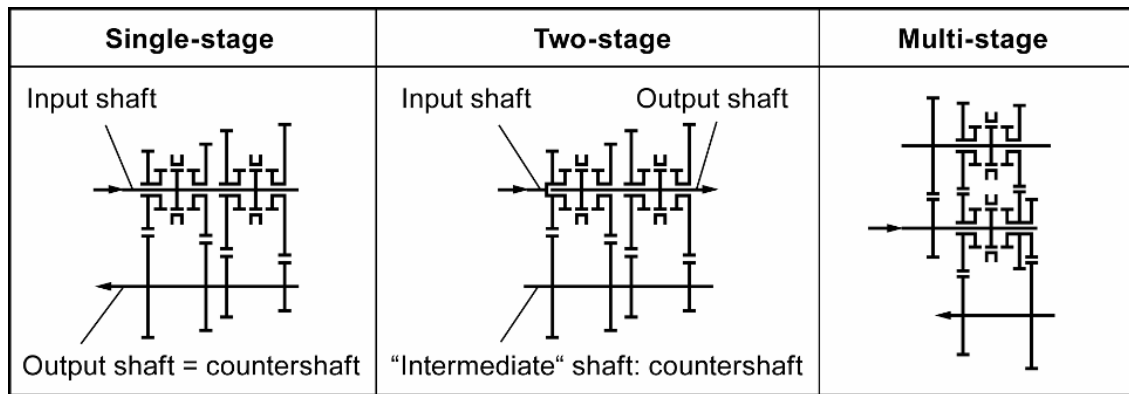


Figure 2.6 Illustration of 4 speed transmission with respect to their stages

Each of the transmission types has its application area, for example one stage transmission found its application area on front wheel drive vehicles. The multistage transmissions are compatible with front drive vehicles as well. The multistage design allows short transmission designs. Two stage transmissions are the most common types of transmissions on vehicles which has engine and transmission unit in front portion of the vehicle and the drive from the rear axle. In these type of transmissions input and the output shafts are lined up coaxially as seen in Figure 2.6. (Naunheimer, et al., 2011)

For a new transmission design, among the three types of transmission line-up architecture, a designer first determine the adequate gear-shifting numbers to fully benefit the power and the torque generated from the ICE. (Naunheimer, et al., 2011)

ICE produces power and torque between engine specific crankshaft rpm interval and this is almost unique to an engine. Engine itself cannot overcome the driving resistance occurred by driving experience. Driving resistance is a general expression which covers wheel resistance, air resistance, gradient resistance of the driving area and acceleration resistance of vehicle. (Naunheimer, et al., 2011)

Determination of transmission ratios is highly depends on the specific engine map. Because an efficient transmission must optimally utilize the engine power by converting it to traction force which is demanded on the wheel to overcome the driving resistance phenomenon. Table 2.1 shows the meaning of the transmission ratios.

Table 2.1 Gear ratios and its interpretation

$i > 0$	Input & output shafts rotate in the same direction
$i < 0$	Input & output shafts rotate in opposite direction
$ i  > 1$	Speed reducing ratio
$ i  < 1$	Speed increasing ratio

As we already mentioned, scanning the efficient portion of the engine by the transmission ratios is possible unless the following design steps are utilized.

- The lowest gear ratio is determined by allowing the intended vehicle to be able to overcome the driving resistance at with an expected highest velocity on ground level by excluding acceleration.

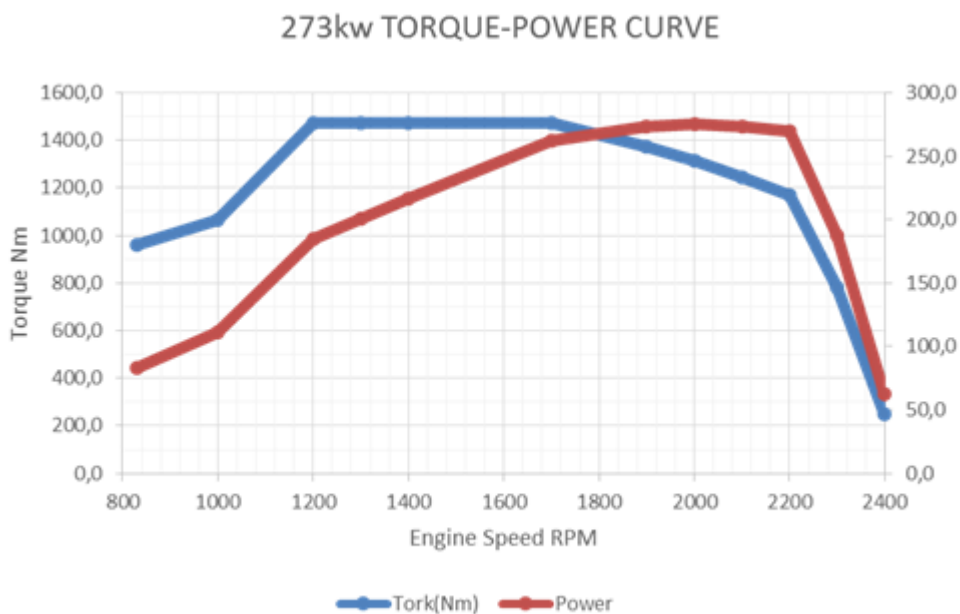


Figure 2.7 Diesel engine torque-power curve (in courtesy of Company)

- Gear ratios must be wisely selected in order to utilize the efficient engine operation points, by considering fuel consumption at minimum.
- The gear ratios must be plausible while acceleration, which means driver should not be forced to shift in short time intervals.
- Transmission Vehicle must have sufficient climbing ability to the intended roads, and should provide acceleration and top speed values indicated in catalogue values. Creep speed which is gas pedal activation free velocity, must be taken into account.
- Traction force gap indicated in Figure 2.8 reduces the drivable range of the engine so that it must be kept as small as possible. With more number of gear ratios these unusable areas of traction could be reduced to ideal map. This is an optimization problem. Because more selectable gear means more shifting effort which reduces the comfort of driving experience. (Fischer, et al., 2015)



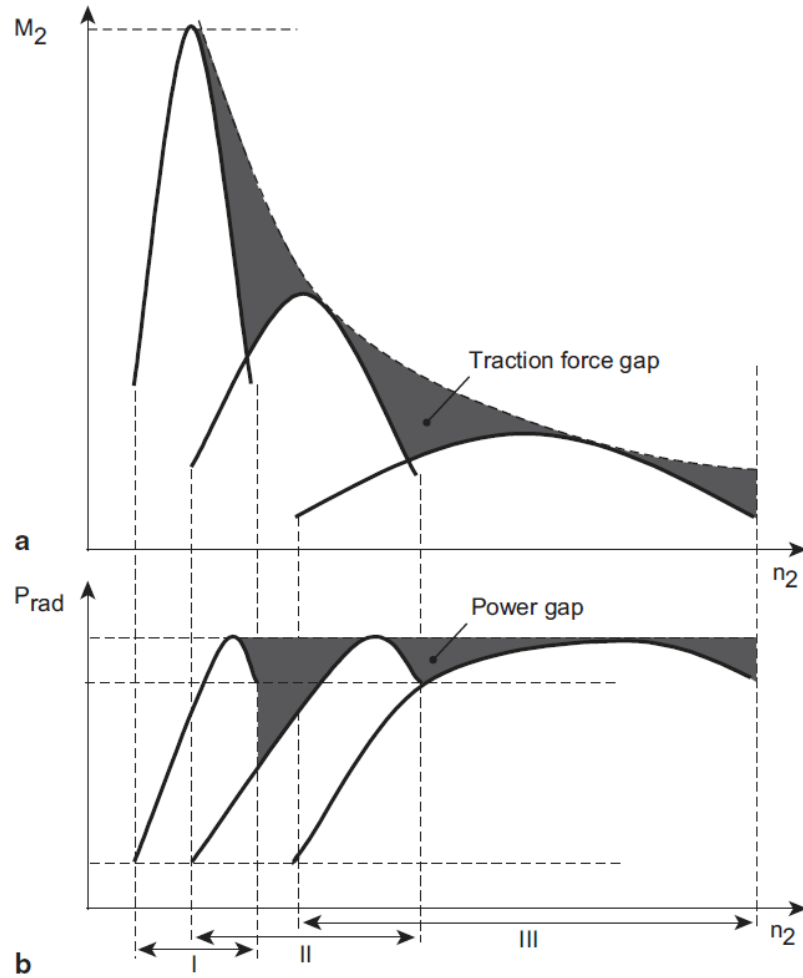


Figure 2.8 a) Traction force gap b) Power gap (Fischer, et al., 2015)

Top speed achievement is a predefined requirement prior to project start, Figure 2.9 depicts the 3 possible gear ratio selection points which could be utilized. Two design possibilities are available with their pros and cons, in order to satisfy maximum speed requirement.

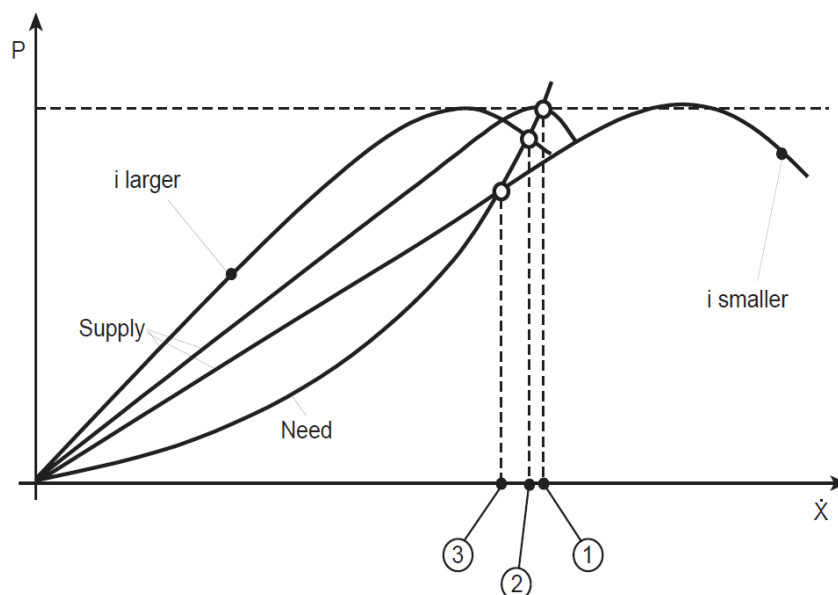


Figure 2.9 Designs to achieve maximum speed (Fischer, et al., 2015)

## 2.2 Fatigue Theory

Failures on metallic materials occurs from two situations, one is from static loadings and the second type of failure is occurred from variable loadings. Since the main aim of this thesis is the fatigue investigation on the layshaft, fatigue science will be mentioned in detail and will be benefited by current studies and state of art literature.



Figure 2.10 Failure of a construction truck transmission layshaft

### 2.2.1 History of Fatigue Theory

Fatigue behaviour of the structures is relatively a new topic when we compare it with material science and design of statically loaded structures. Even though it has a vital importance in material and design failure, first research on fatigue was conducted in first half of 19<sup>th</sup> century and moreover it was initiated by accidents. First systematic approach on metal fatigue was generated by a German engineer Wilhelm August Julius Albert on iron chains in Mining industry. His idea which that the fatigue is associated with the load and the number of load cycles instead of accidental overloads, supports the basics of fatigue theory currently accepted.

Materials are subjected to fatigue failures under the aspects of fatigue phenomena listed below. Fatigue crack nucleation and crack growth are beginning phase of the fatigue failure incident. The others, variable loading, uniaxial, multiaxial loading, corrosion, fretting or creep are the cause of the fatigue failures.

- Fatigue crack nucleation
- Fatigue crack growth
- Variable amplitude loading
- Uniaxial or multiaxial loading
- Corrosion fatigue
- Fretting fatigue
- Creep fatigue under isothermal or thermo-mechanical condition

According to International Organization for Standardization in 1964; the term fatigue is described as the changes in material properties in metals caused by periodically loadings with cyclic stress or strain. Mostly, this term refers to changes which results damage and failure.

Fatigue phenomena occurs under cyclic load with mean stress and it basically has stages. Which means, it does not occur suddenly with an applied stress. A fatigue failure metal structure under cyclic loading experiences some unusual stages which are the initiated fatigue phenomena, see Table 2.2. Fatigue failure requires a crack initiation, crack growth and sudden



abrupt fracture at latest stage. Due to these steps a fatigue failed component contains an initiation point which is around the surface and polished beach marks and sudden fracture following these indications.

Table 2.2 Fatigue Phases

Crack Initiation		Crack Propagation	
Fatigue Damage of Microstructure	Formation of technical crack	Stable macro-crack propagation	Instable propagation with subsequent abrupt rupture
Without micro cracks	With micro cracks		

Fatigue strength explains two terms:

- Fatigue behaviour.
- Structural durability.

Fatigue behaviour mostly means fatigue strength under repeated periodic cyclic loading under free of environmental influences. Structural durability on the other hand is fatigue strength under stochastic or aperiodic deterministic load-time histories. It means, additionally, component design regarding fatigue life with real load – time data under environmental effects.

Almost %60 – 70 of the accidents caused by fatigue failed metallic components and the half of them are manufacturing defects. Design engineers mostly considers the yielding point of materials for their designs, however under cyclic loadings, components fail far below of their tensile strengths. In practice, tests and real load conditions revealed that crankshafts are failed under  $0.2R_m$  strength. In other words fatigue behaviour of crankshaft.

Investigation of fatigue failure on rotary shafts is important, which are under effects of push/pull – bending and torsion forces so these are the external forces should be mainly considered.

In the 19<sup>th</sup> century, fatigue science started manifesting itself, and it became an interesting area to research. Scientists, throughout this century had conducted remarkable investigations and made fatigue phenomena an understandable mechanism for the rest of the world. The leading researchers in this area with respective research areas in 19<sup>th</sup> century are listed below:

Wilhelm August Julius Albert published first article on fatigue - Repeated Loads in 1829.

Jean-Victor Poncelet in 1839 officially used fatigue term in a mechanical academic book.

William John Macquorn Rankine was the first engineer recognized the failures of railways in 1840s was caused by crack initiation and its growth especially right after Versailles train crash occurred in 1842.

August Wöhler was a railway as Rankine, he made the first systematic investigation on metal fatigue in 1860. His name still remembered by naming stress-cycle curve as Wöhler Curve.

Johann Bauschinger is known his work on cyclic deformation in 1886.

John Goodman developed a theory which is easy to use for all practical purposes with the data of Wöhler Curve in 1890.

Ewing, J.A. & Humfrey, J.C revealed micro crystalline development of a crack tip after many reversal cyclic loads in 1903. (Socie, 2002)

In 20<sup>th</sup> century fatigue was still an intriguing area to study on and this century created its well-known researches.

A. A. Griffith studied surface finish and scratches' effect on fracture mechanics in 1920.

M. A. Miner proposed under repeated loads cumulative damage occurs due to the absorbed net energy by specimen in 1945.

L. F. Coffin & S. S. Manson both scientists explained the fatigue crack growth depending on plastic strains in 1954.

P. C. Paris published methods for prediction the crack growth rate in 1961.

R. E. Peterson worked on strain-life Method and stress concentrations in 1963.

Tatsuo Endo & M. Matsuishi revealed a simple method called cycle rain flow counting method to simplify complex loadings and apply miner's rule for assessment in 1967.

Component durability in engineering in 21<sup>st</sup> century is a trend topic area for industry leading companies. The main purpose is establishing reliable methods and models to take into account of fatigue behaviour of the materials for component design. This challenge is overcome by in-situation monitoring of components for estimation of the product's service life. This approach gives opportunity to engineers to design their products with adequate features, sufficient material usage and prevents overdesigned products which is redundant for the end user.

Starting from the 1980s to 2000s with the help of software developments, fatigue investigation is moved in to computer aided simulation world. Finite element and multi body simulations are really helped design engineers to take into account the fatigue phenomena in their design criteria.

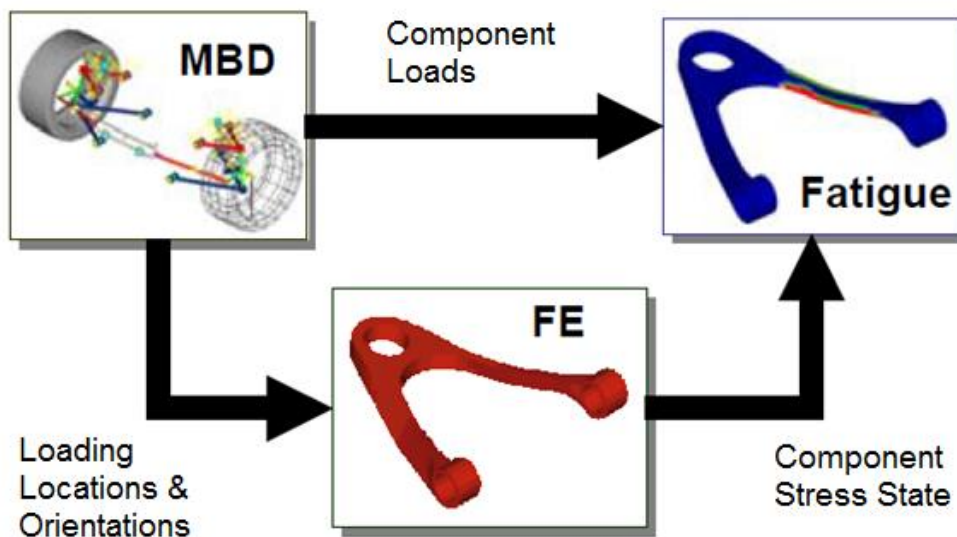


Figure 2.11 Simulation based fatigue investigation (Socie, 2002)

Increased digital prototyping with less testing has become a goal for the 21st century fatigue design. Therefore, It should not be ignored that computer simulations on stress or fatigue investigations still requires material based tests to define material models into the simulation. In other words the best product design still needs the testing step to guarantee the component service life.

### 2.2.2 Fatigue Failure Phases

Fatigue process includes phases to be occurred for a component failure. These are mostly accepted as in order of crack nucleation, short crack growth in elastic plastic stress field, long crack growth and final fracture. Crack nucleation starts at the highest stress concentration sites on persistent slip bands. After the crack nucleation, crack growth stage takes place in finite length. This phase referred as stage I and mostly affected by grain size, grain orientation, stress level which is mostly depended material's microstructure. This phase followed by long crack propagation named as Stage II, crack in this phase propagates in the direction of maximum shear stress which is less affected by material's micro structure, since the crack length is much larger than the material grain size. (Lee, et al., 2005)

Slip band formation

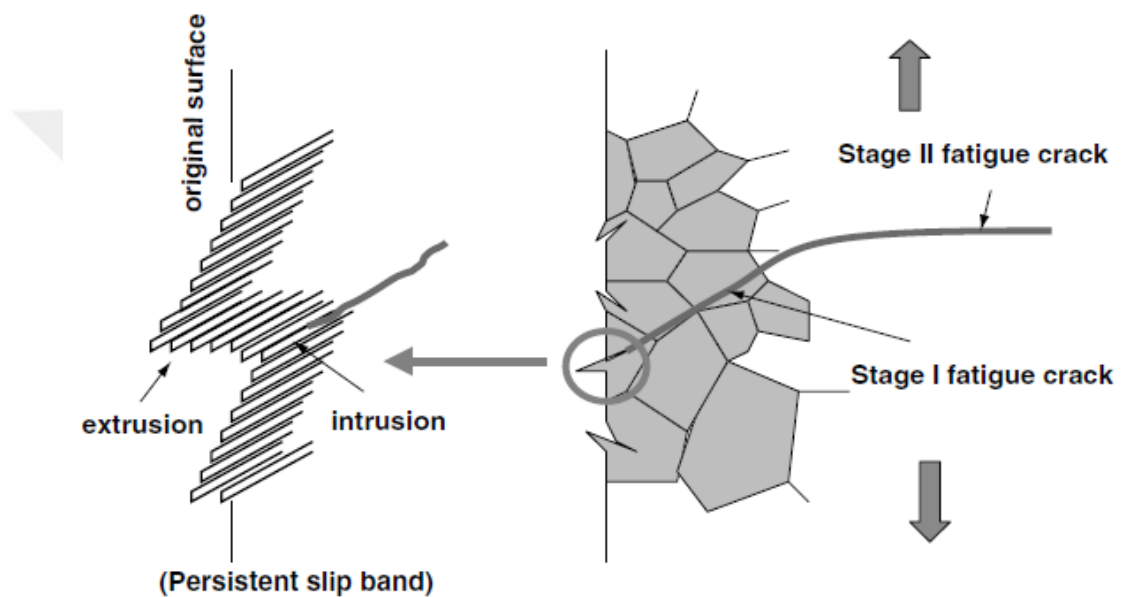


Figure 2.12 Slip band formation under cyclic loading (Lee, et al., 2005)

Stable crack propagation to the technical crack which is assumed as 1mm or until fracture is accepted as stage two.

In first phase cyclic softening and cyclic hardening occurs, thereafter in phase 2, due to the cyclic loading micro crack formations occurs on surface. In phase 3, continuous macro crack propagations observed. In phase 4 sudden fracture occurs on remaining cross section.

Fracture surface can give so many information about the fracture incident. For example it shows where the crack started reveals its velocity and progress along with fracture area. Critical crack size and fracture toughness.

### 2.2.3 Mean Stress Effect

There are several empirical curves which is used to estimate the mean stress effect on fatigue life.

- a. Soderberg equation (1930, USA)

$$\frac{\sigma_a}{\sigma'_e} + \frac{\sigma_m}{\sigma'_y} = 1$$

Equation 2.5

b. Goodman (1899, England)

$$\frac{\sigma_a}{\sigma'_e} + \frac{\sigma_m}{\sigma_u} = 1$$

Equation 2.6

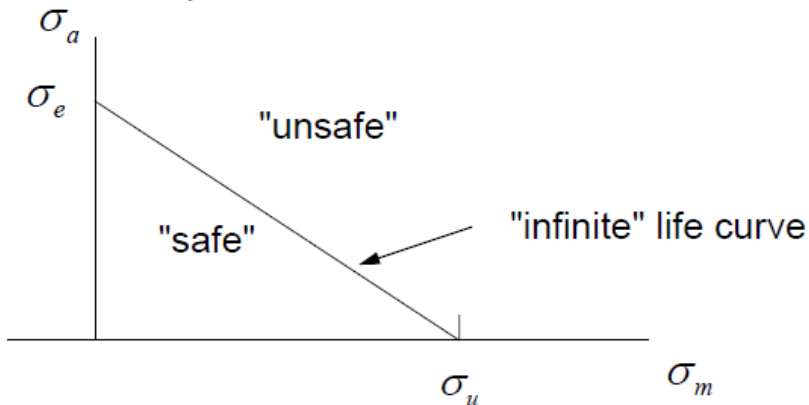


Figure 2.13 Alternating and mean stress combination according to Goodman

The space on the right hand side for the combinations of alternating and mean stresses are described as not safe region however if it is deemed to attain a infinite life, it is better to design the component which should experience the alternating and mean stresses in combination at left hand side of the infinite line of Goodman.

c. Gerber (1874, Germany)

$$\frac{\sigma_a}{\sigma'_e} + \left(\frac{\sigma_m}{\sigma_u}\right)^2 = 1$$

Equation 2.7

d. Morrow (1960, USA)

$$\frac{\sigma_a}{\sigma'_e} + \frac{\sigma_m}{\sigma_f} = 1$$

Equation 2.8

Here below the stresses with indices are listed.

$\sigma_y$ : Yield Stress

$\sigma_u$ : Ultimate Stress

$\sigma_f$ : True Fracture Stress

$\sigma'_e$ : Effective Alternating Stress

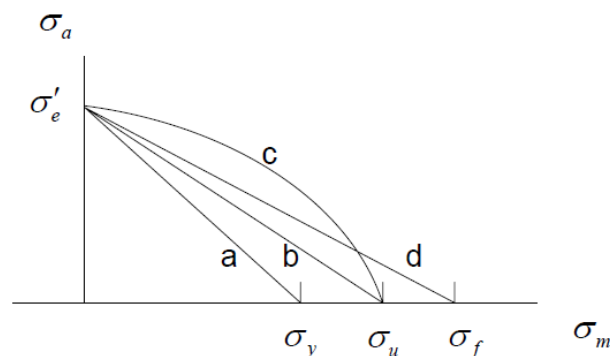


Figure 2.14 a) Soderberg, b) Goodman, c) Gerber and d) Morrow approaches

In order to take into account of mean stress effect, these equations mostly represents the best material model. For ductile materials Gerber parabola, Goodman line for brittle and Soderberg equation is low ductile materials are mostly preferred.

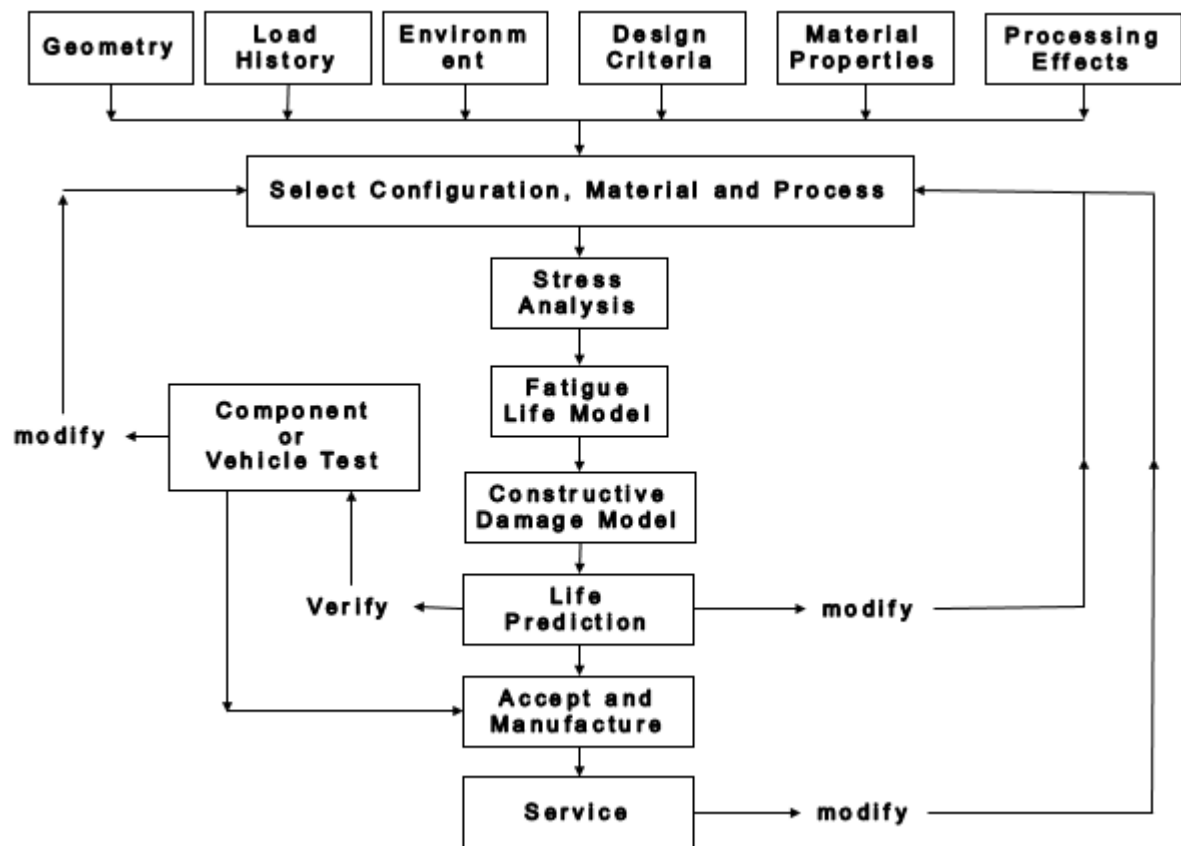


Figure 2.15 Fatigue design flow chart (Fatemi, et al., 2001)

#### 2.2.4 Fatigue Life Models in Fatigue Design

- **S-N Stress - Life method**  
Relates nominal stresses to local fatigue strengths for notched and unnotched members
- **$\epsilon$ -N Strain - Life method**  
Investigation of local strain around a notch is related to smooth specimen strain controlled fatigue behaviour.
- **Fatigue crack growth method**  
Utilized to obtain the number of cycles for a crack to be grown from a defined length to another length.
- **Two stage method**  
The two stage method is a combination of second and third methods to evaluate fatigue and crack nucleation and growth. Strain life model used to obtain the life span to formation of macro crack than then the third step helps to reveal integration of the fatigue crack growth rate equation for remaining life. (Fatemi, et al., 2001)

#### 2.2.5 Fatigue Design Criteria

There are several design criteria available and assimilated by engineers by consciously or unconsciously considering fatigue of failure while in the design stage of components. These

---

design criteria are listed below and each of them has their usage mainly depending on the application. (Fatemi, et al., 2001)

1. Infinite life design
2. Safe life design
3. Fail safe design
4. Damage tolerant design

A structure or a component can be designed with in different conditions. For example the target could be infinite life for vital structures in most cases. The infinite life is considered when designs are made for human oriented life threatening structures. Exemplification of these are steel bridges, constructions like skyscrapers and so on. From Automobiles to house goods the infinite life was the design criteria. However recently this approach is evolved from infinite life to damage tolerance design.

#### **2.2.5.1 Infinite Life Design**

Infinite life design basically means unlimited safety for a design. In mechanical approach, local stresses must be kept below yield strength and elastic limit of material more safely below fatigue limit. As we mentioned before vital components like life threatening components, locally critical components at low maintenance areas etc. Despite the reality of excessive cost of over durable parts which is a drawback for global competitiveness, and higher weight contribution to structure it is still a main choice in most of the applications. (Fatemi, et al., 2001)

#### **2.2.5.2 Safe Life Design**

Design consideration for a predicted life is named as safe life design. Current industries are mainly benefiting this design approach and aiming to manufacture products with a definite life value to prevent, excessive material usage and to be competitive in the market. As we assume designing a laptop housing with excessive durability is going to make the product over weighted and hinder its main purpose of mobility design for computers. Most common machine element for safe life design is bearing, therefore bearing selection is a design limitation or requires replacement after its fulfilled mileage. (Fatemi, n.d.)

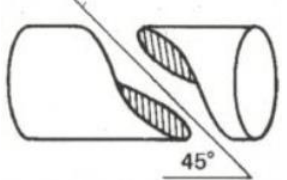
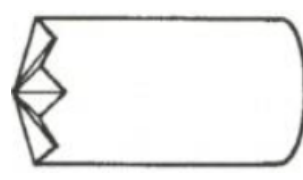


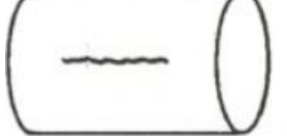
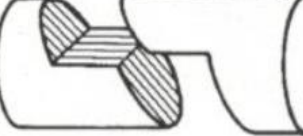
#### **2.2.5.3 Fail Safe Design**

In fail safe design approach, there is tolerance for failed component. Fatigue cracks could occur in this type, but it gives sufficient time for detection and replacement prior to complete system failure. This type of systems requires regular inspections to detect crack occurred components and its replacement. (Fatemi, n.d.)

#### **2.2.5.4 Damage Tolerant Design**

Damage tolerant design is required by U.S. Air Force. Damage tolerant design is sound similar to fail safe design but it is an evolved version. In other words the cracks will eventually occur but still in design step these failures are forecasted by fracture analysis and mechanical tests. These prior investigation for future crack determination allows designers to control the possible damage of the in process crack formation. Crack detection by non-destructive testing of component, crack growth behaviour of the selected material for the design and residual stresses are important parameters to be controlled for a proper damage tolerant design. (Fatemi, n.d.)

Table 2.3 Occurred fatigue fracture at torsional load (Fatemi, et al., 2001)

Failure Modes		
Tensile		
Transverse Shear		
Longitudinal Shear		

Microscopic fatigue cracks usually nucleate and grow in direction of maximum shear planes, nevertheless macroscopic fatigue crack growing direction occurs in plane of maximum tensile or it can be occurred in maximum shear stress plane when the torsional or multiaxial loading scenarios.

### 2.2.6 Generation and Standard Load – Time Histories for Fatigue Investigation

Determination of the load cycle either by statistical method based on engineering experience or directly obtaining it with time is an important step. Assuming the intended product will experience the worst loading situation leads to over engineering which is not physical in current industrial world order.

### 2.2.7 Fatigue Stress Life (S-N) Approach

Loading Type

- Constant Amplitude, Proportional Loading
- Constant Amplitude, Non-Proportional Loading
- Non-Constant Amplitude, Proportional Loading
- Non-Constant Amplitude, Non-Proportional Loading

In a simple cyclic loading, there are formulations available which help us to characterize the loading condition. Using the equations below, load, moment, torque, strain, deflection and stress intensity could be calculated. (Fatemi, et al., 2001)

The cyclic stress range:

$$\Delta S = S_{\max} - S_{\min} \quad \text{Equation 2.9}$$

The cyclic mean stress:

$$\sigma_m = \frac{\sigma_{\max} + \sigma_{\min}}{2} \quad \text{Equation 2.10}$$

The cyclic stress amplitude:

$$\sigma_a = \frac{\Delta \sigma}{2} \quad \text{Equation 2.11}$$

The cyclic stress ratio:

$$R = \frac{\sigma_{min}}{\sigma_{max}} \quad \text{Equation 2.12}$$

Fully reversed loading:

$$(\sigma_m = 0 \text{ and } R = -1) \quad \text{Equation 2.13}$$

Zero based loading situation:

$$\sigma_m = \left(\frac{\sigma_{max}}{2}, R = 0\right) \quad \text{Equation 2.14}$$

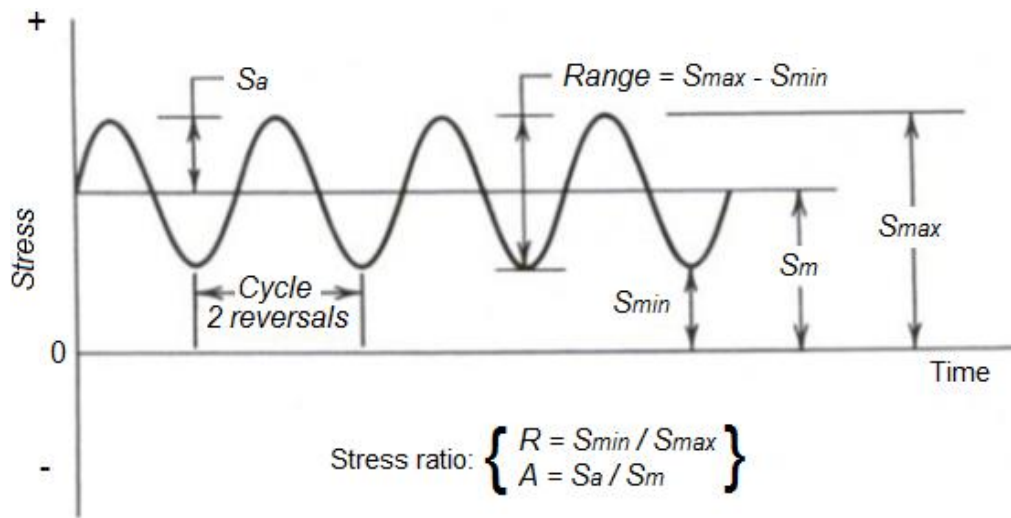


Figure 2.16 Constant amplitude loading

In fatigue simulation and testing the correlation between minimum stress and maximum stresses are represented by R values. The R value which equals to -1 is fully reversed loading condition in other words  $S_{min} = S_{max}$ . In the condition of  $S_{min} = 0$  called pulsating tension loading. These two loading situations do not reflect the real life scenarios but mostly preferred for standard fatigue test of materials.

### 2.2.8 Damage Accumulation Theories

Palmgren-Miners rule, the name of the rule credited to scientist Palmgren and Miner. Basically this rule assumes a component can endure a certain amount of damages which is indicated as D, and every damage occurrence indicated as  $D_i$  ( $i=1, \dots, n$ ), in total of n different loading stresses. As a next step all the occurred damages added up to check whether the accumulated damage on the structure achieved to the structure's endurance limit or not.

Linear damage accumulation:

$$\sum_{i=1}^n \frac{D_i}{D} = 1 \quad \text{Equation 2.15}$$

Equation 2.15 is the mathematical representation of the cumulative damage rule which indicates summation of fractional damage, when this equation reaches to 1 means failure. This equation claims for alternating stress  $\sigma_1$  occurs  $n_1$  cycle and  $\sigma_n$  alternating stress occurs  $n_n$



cycle. Consequently, with the help of material S-N diagram, alternating stresses and corresponding cycles one can easily estimate the number of cycles until failure. Equation 2.16 helps to work out fractional damage level for investigated alternating stresses.

Fractional damage summation:

$$\sum_{i=1}^N \frac{n_i}{N_i} = 1 \quad \text{Equation 2.16}$$

The drawback of application Palmgren-Miner rule is elimination of the sequence effect of the applied stresses. For example to explain the sequence effect in a simple way, a structure's durability to endure alternating stresses  $\sigma_1, n_1$  and  $\sigma_2, n_2$  which are different magnitudes and cycles, is different. In other words stress application sequence has a major impact on fatigue theory.

If stress application sequence is from high to low magnitudes, Palmgren-Miner rule's reliability is questionable and stress application sequence from low to high this rule is reliable but includes higher safety factor. The most applicable usage of this rule has reliability on random loading histories.

The sequence and the interaction of stress events have influence on fatigue life prediction. Mostly low loads has influence on crack nucleation and high loads triggers crack growth. In this point many proposals are raised to improve linear damage theory named as nonlinear damage theories. These theories propose nonlinear relation such as Equation 2.17.  $a_i$  in this equation is a factor representing load level as distinct from Equation 2.16. (Stephens, et al., 2001)

Nonlinear damage accumulation:

$$D = \sum \left( \frac{n_i}{N_{fi}} \right)^{a_i} \quad \text{Equation 2.17}$$

Due to nonlinearity a cycle ratio (Figure 2.17) of 0.6 on linear rule corresponds to 0.6 damage fraction, however it refers different damage fraction values on  $\Delta S_1$ ,  $\Delta S_2$  and  $\Delta S_3$ . Despite the reality of the nonlinear approach allows us to come up more precise assumptions, linear model is still widely accepted and used among engineers (Stephens, et al., 2001)

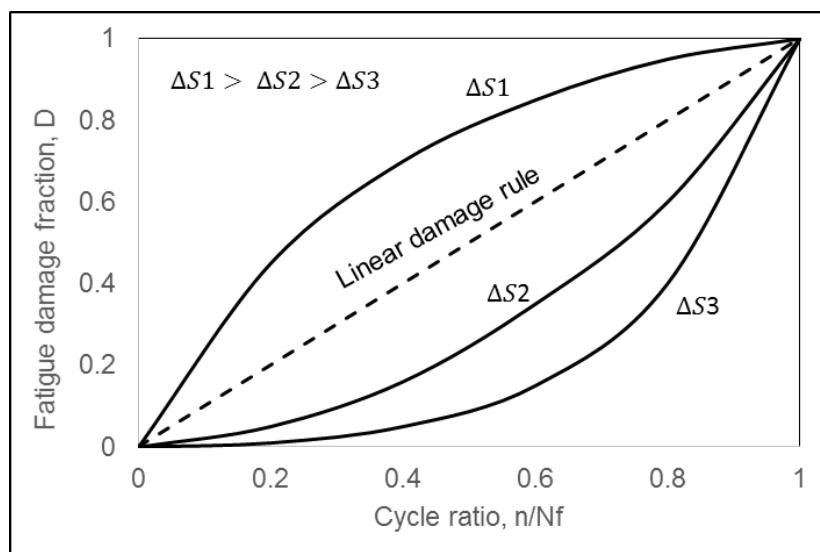


Figure 2.17 Linear vs. nonlinear damage fraction (Stephens, et al., 2001)

### 2.2.9 Fatigue Limit Testing & S-N Curve Generation

From 6 to 12 specimens for preliminary and research and development purposes are enough for stress cycle curve generation is enough however it is recommended to test from 12 to 24 specimens for design reliability tests. (Lee, et al., 2005)

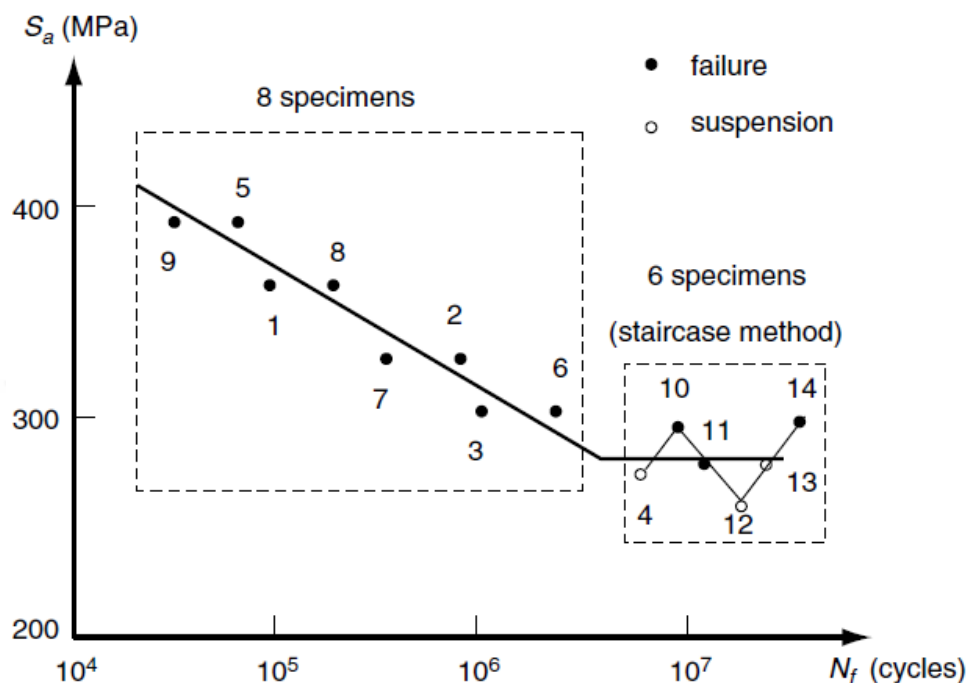


Figure 2.18 S-N testing with small sample batch (Lee, et al., 2005)

Fatigue testing under torsional or bending loads are not performed for shorter lives ( $10^3 - 10^4$  cycles or less) in order to not to lead plastic deformations while testing.

### 2.2.10 Post Investigation of Fatigue Failed Surface

The failed component's surface contains so many information, it is easy to identify the failure is either as a result of cyclic loading or monotonic loading. As a post failure analysis, examining the fractured surface can be done by a naked eye, small magnifying glass or could be an electron microscope to have a better insight of the fracture cause.

### 2.2.11 Using FEMFAT Post FEA for Fatigue Life Estimation

Today's highly competitive world, product development, faces high pressure for testing time. For component tests, less time allocated before introducing the product to the market. For this reason, simulations takes more important roles for the product development process due to the lack of enough testing. Of course, to be able to trust on a simulation result, requires a trustworthy software package like FEMFAT.

There are three ways of choice for material generation for fatigue analysis.

- The first material generation method referred to FKM "*Forschungskuratorium Maschinenbau*". It is a material generation approximation developed by ECS.
- The second material generation method takes reference TGL "*Die Technischen Normen, Gütevorschriften und Lieferbedingungen*". It is a material generation approximation developed by ECS.

- The last material generation method is defining the all required material parameters by the user. This method will give the best approximation results when the material characterization is well done by engineer.

FEMFAT offers several modules for loaded components, selection of one of these has advantages and disadvantages one on other.

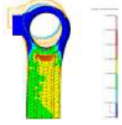
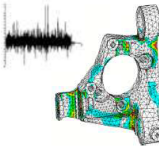
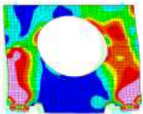
Module	When to use	Examples	What to Import
<ul style="list-style-type: none"> <li>• BASIC</li> </ul> 	<ul style="list-style-type: none"> <li>• Direction of principle stresses are constant</li> <li>• 2 Load Conditions</li> </ul>	<ul style="list-style-type: none"> <li>• Con rod with the two dominating load cases ignition and inertial force</li> <li>• Engine bulkhead and bearing cap (assembly and ignition)</li> <li>• Shafts with torque history (only one channel)</li> </ul>	<ul style="list-style-type: none"> <li>• Two stress results, which can be:</li> <li>• Upper and lower stress or</li> <li>• Amplitude and mean stress</li> <li>• Load spectra if necessary</li> </ul>
<ul style="list-style-type: none"> <li>• CHANNEL MAX</li> </ul> 	<ul style="list-style-type: none"> <li>• Direction of Principle Stresses are permanently altering</li> <li>• Direction and location of forces and boundary conditions are constant</li> <li>• Existing Load Histories</li> <li>• More than one channel, which are generally not in phase</li> </ul>	<ul style="list-style-type: none"> <li>• Chassis parts like: Knuckles, subframes, H-Arms,...</li> <li>• Body in White</li> <li>• Crankshaft with modal approach</li> </ul>	<ul style="list-style-type: none"> <li>• One stress result for each channel (e.g. for unit load)</li> <li>• One load history for each channel</li> </ul>
<ul style="list-style-type: none"> <li>• TRANS MAX</li> </ul> 	<ul style="list-style-type: none"> <li>• Load application point and boundary conditions are altering with time</li> <li>• Sequence of stress results</li> </ul>	<ul style="list-style-type: none"> <li>• Engine bulkhead and bearing cap or crankshaft with stress result each n crankangle</li> </ul>	<ul style="list-style-type: none"> <li>• Sequence of stress results</li> </ul>

Figure 2.19 FEMFAT modules (Gaier, 2010)

### 2.2.12 Current Fatigue Related Researches

(Kandreegula, et al., 2016) practiced a methodology to assess the fatigue behaviour and improve stress concentration factor of crank shaft's web fillets and its optimization by utilizing CAE analysis and post process the results with Femfat fatigue software.

(Marini & Ismail, 2011) examined received and heat treated aluminium (T6) 6061 alloys as both solid and thin walled hollow specimen with servo-hydraulic axial monotonic torsion test to see the effects of heat treatment and shape of the structure on fatigue behaviour.

(Göksenli & Eryurek, 2009) conducted a systematic approach to investigate fatigue failure occurred on elevator drive shaft operating under torsional bending which was in operation over 30 years and the failure reason was faulty design or manufacturing at keyway radius.

(R.A.Gujar & S.V.Bhaskar, 2013) studied fatigue behaviour of a multi cross-sectional inertia dynamometer shaft under cyclic loading and used distortion energy theory for failure theory, then the work results were compared to ensure both results mutually proved.

(Tovo, et al., 2014) approached the fatigue theory experimentally. They uncovered a new experimentally obtained multiaxial fatigue data for cast irons and compared their results with available literature data. They performed the experiments with specimens from real components and tested them with uniaxial, biaxial and torsional and tensile loading combinations.

(Chapetti & Guerrero, 2013) researched on notch size effect  $k_f$  and notch sensitivity  $k_t$  on HCF resistance, and proposed a new simple approach while dealing with the notch effects on mathematical model representation of fatigue. They compared the proposed model accuracy with the experimental data presented by (Frost, 1959) and (Tanaka & Akinawa, 1987). The outcome of this approach showed a close and satisfying results with the experimental data.

(Ural, et al., 2009)

(Genel & Demirkol, 1998) researched on of AISI 8620 material's fatigue behaviour of 10 mm diameter specimen with 0.73 and 1.00 mm hardening depth.



## 2.3 Choice of Material & Its Characterization

Material selection is an important step to be excelled in machine design. Machine design requires material knowledge for high quality products in the market. A designer must estimate the materials behaviour under real life condition, like mechanical behaviour, corrosion resistance especially the designed part is under atmospheric condition. %50 of the component design is done by material selection, heat treatment to enhance the mechanical resistance, geometric dimensioning and tolerance. Mechanical design is like cooking in the kitchen, first you have to know the materials and their behaviour under operating physical condition, just like knowing the food ingredients and their tastes when you compose them.

For particular machine design areas like gears shafts there are intended materials like case hardening steels. However, if a designer have no idea of material selection, it is advisable to use material selection intended software like CES. Dr. Thankachan and Prushothaman from UCAM PVT LTD utilized this software in design of gearbox pedestal and verified the design with material specification on commercial FEA software. (Cambridge Engineering Material Selection tool). (Thankachan & Purushothaman, 2014).

### 2.3.1 Tensile Test

Tensile testing is the most common material testing method for steels which provides most of the required material strength data for design. In Figure 2.20 a characteristic tensile test specimen is represented. This specimen could be either a solid bar or a sheet metal for both design usage. As in the all material testing procedure, tensile testing and the specimen used are standardized as well. Prior to a tensile test, specimen diameter  $d_0$  and gauge length  $l_0$  must be recorded to measure elongation. After the measurement procedure test specimen is mounted to testing machine and the tension force loaded slowly and elongation at gauge length measured while until the fracture occurs. (Budynas, 2006)

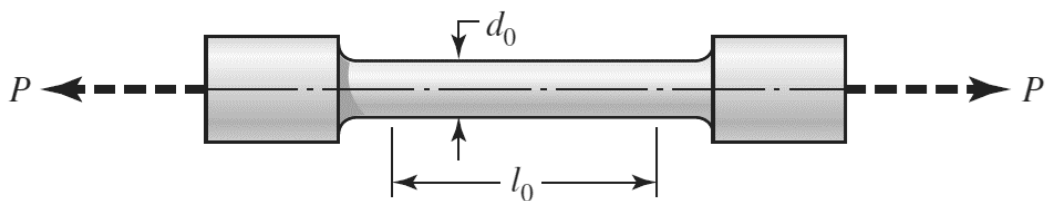


Figure 2.20 Tensile test specimen (Budynas, 2006)

For its simplicity and geometry independent property the force-elongation data converted to stress – strain data to represent only material properties which must be independent from its geometry. See Equation 2.18 for stress calculation and Equation 2.19 for strain calculation.

Stress in tensile test:

$$A_0 = \frac{1}{4} \pi d_0^2 \rightarrow \sigma = \frac{P}{A_0} \quad \text{Equation 2.18}$$

Stress and strain calculation is necessary after tensile testing of material to be able to draw characteristic material stress-strain diagram.

Strain in tensile test:

$$\varepsilon = \frac{l - l_0}{l_0} \quad \text{Equation 2.19}$$

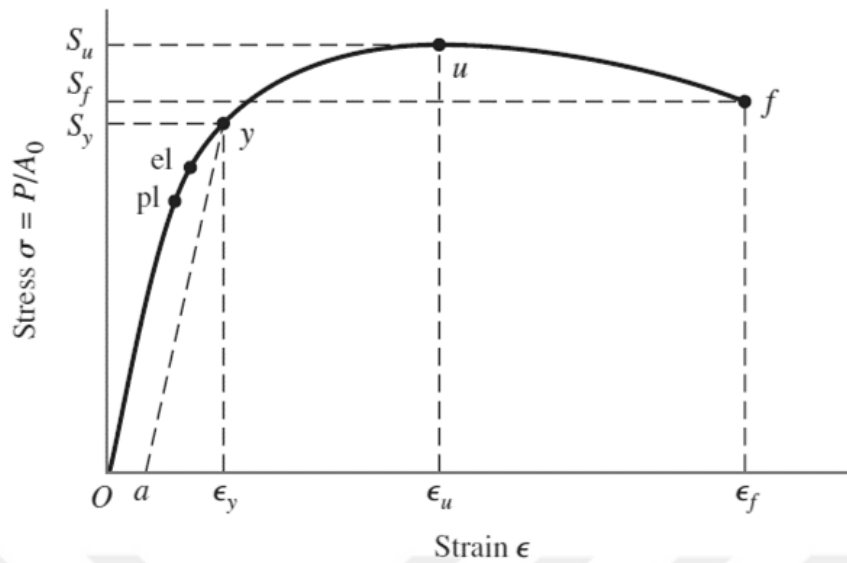
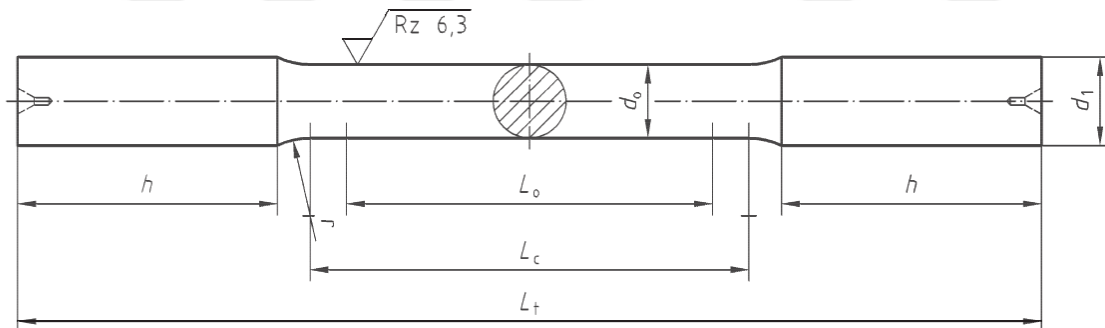


Figure 2.21 Tensile strength representation of materials (Budynas, 2006)

Tensile testing of metallic materials is performed under standard testing condition with standardized test pieces. Tensile testing of metallic materials has a designation “BS EN ISO 6892-1-2016” describes how tensile testing is performed by drawing the sample’s size borders. DIN 50125:2016-04 on the other hand is describing more specifically about the standardized tensile test specimen and how to prepare them. In other words ISO 6892 draws the borders for tensile testing and DIN 50125 defines the standard shape of the specimen.



#### Key

$d_0$	test piece diameter	$L_0$	original gauge length ( $L_0 = 5 d_0$ )
$d_1$	diameter of gripped ends ( $\geq 1,2 d_0$ )	$L_c$	parallel length ( $L_c \geq L_0 + d_0$ )
$h$	length of gripped ends	$L_t$	total length of test piece

Figure 2.22 Example of Type-A test specimen per DIN 50125

### 2.3.2 Material Fatigue Testing

Fatigue testing is performed by scientific and commercial purposes. Scientific side performs these tests to understand material behaviour with repeated loading by considering the parameters of surface roughness, test piece size, heat treatment etc. Main concern for industry side however, to make sure a product’s reliability behaviour and performance under real life situation. Different from the other testing methodologies, fatigue test requires more effort and time. These parameters inherently bring in more cost when it comes to testing step.

Mostly the main purpose of fatigue testing is comparison of fatigue performance in metals, and the correlation between model and the real component. Following concerns are aim of the testing.

- Data extraction from intended material.
- Correlation creation between numerical model and material.
- Investigation of manufacturing techniques' effect on behaviour.
- Investigation of surface finish and heat treatment effect.
- Investigation of environmental effect, corrosion etc.
- Investigation of crack nucleation and its propagation.

Fatigue testing aim puts constraints on the test procedure to be performed. For example material selection is the main concern but, depending on the area of the research, testing specimen should reflect the real component's physical attributes as much as possible. Fatigue test oriented parts should be processed as in real life product in order to have a good sight of test results. Applied loading history, surface quality, heat treatment, surface hardness, ambient temperature, ambient itself etc. (Schijve, 2001)

Fatigue testing of materials are standardized with international agreements and the standards such as BS ISO 1143, DIN 50113 and ASTM E08 standards. ASTM committee E-09 on fatigue and ASTM committee E-24 on fracture combined together to form the committee E-08 on fatigue and fracture.

### 2.3.2.1 Fatigue Test Machines

Fatigue testing is done with load specific testing machines to simulate torsion, bending, tension and compression. These load conditions can be applied independently or in combined situations to represent multiaxial fatigue test if the machine is capable of performing this scenario. The traditional testing machines can only apply constant amplitude loading. With the modern advance in technology the closed loop servo hydraulic testing machines, variable amplitude loading testing is also possible. Figure 2.23 and Figure 2.24 are used to represent rotating bending situation. These two machines basically carry out the bending loading, however the distinct superiority of the rotating pure bending machine is being capable of enforcing the uniform bending over the complete test specimen see Figure 2.25. Axial loaded fatigue test machine is the most common test machine which is capable of applying both mean and alternating amplitude loads. (Fatemi, et al., 2001)

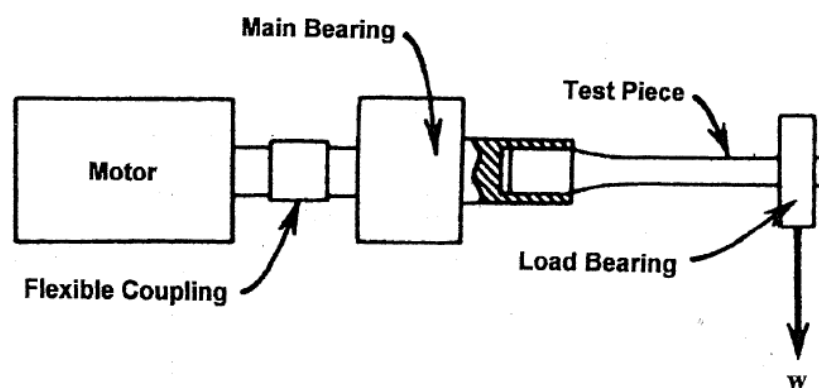


Figure 2.23 Cantilever rotating bending

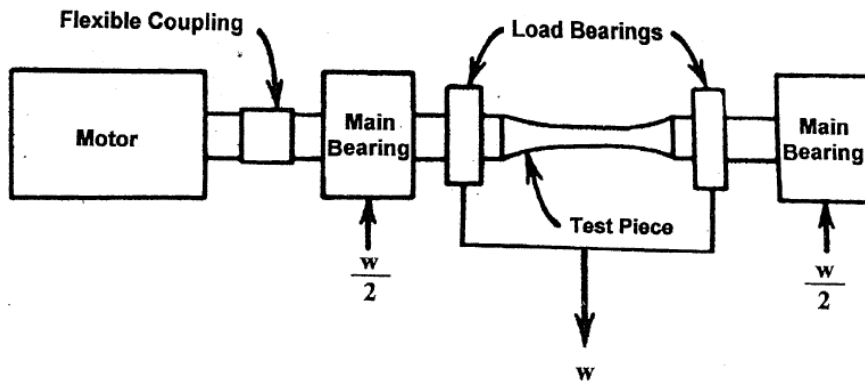


Figure 2.24 Rotating pure bending

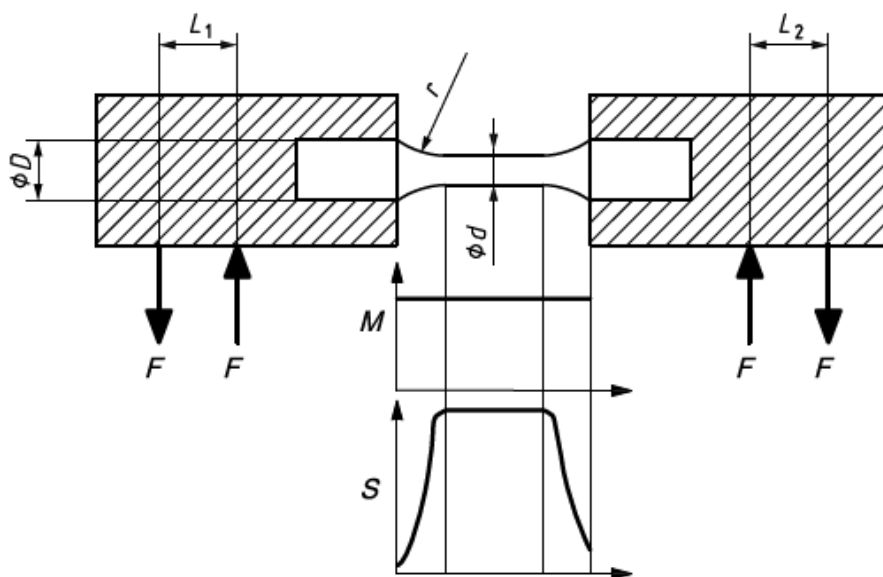


Figure 2.25 Four point bending with parallel specimen (BS ISO 1143:, 2010)

**D:** diameter, **M:** Bending moment, **d:** diameter of specimen where maximum stress occurs, **F:** applied force, **L<sub>1</sub>-L<sub>2</sub>:** force arm lengths, **r:** radius, **S:** stress



### 2.3.2.2 Specimen

BS ISO 1143 focuses on rotating bar bending test procedure, test machine and the specimen to be used in test (BS ISO 1143:, 2010). Fatigue specimen should be round cross section for this particular test. According to the standard, it could be in three different shapes.

It could be, cylindrical, with tangentially blending fillets at one or both ends, tapered or hour-glass-type specimen.

In test condition it is important to pay attention for some materials, to prevent excessive heating of the specimen by combining of high stress and high speed. According to the standard test frequency should be between 15 to 200 Hz to avoid abnormal vibration and the self-heating of the material.

The test is continued until failure of test piece or by reaching the required number of cycles (eg.  $10^7$   $10^8$ ) cycles. If failure occurs outside of the specimen gauge, the test result must be considered as invalid and shall be repeated.

The gauge portion of the specimen is very important. This portion represents a volume section the studied material. A special attention must be paid while preparing the gauge part of the specimens. Tolerances on the specimen restricted as follows and general dimensions must conform Table 2.4.

Table 2.4 Recommended dimensions for test specimen per (BS ISO 1143:, 2010)

Parameter	Dimension
The recommended d values (mm)	6 – 7,5 – 9
Transition radius (from parallel section to grip end)	$r \geq 3d$
Each specimen measured diameter accuracy	0.01 mm
Parallelism tolerance for parallel test section	0.025 mm

The following figure shows the general dimensioning and tolerancing of rotating bar fatigue test specimen. This test specimen require a careful preparation especially surface roughness quality in order to minimize the surface quality effect on fatigue data both on gauge length and the radius of transition area.

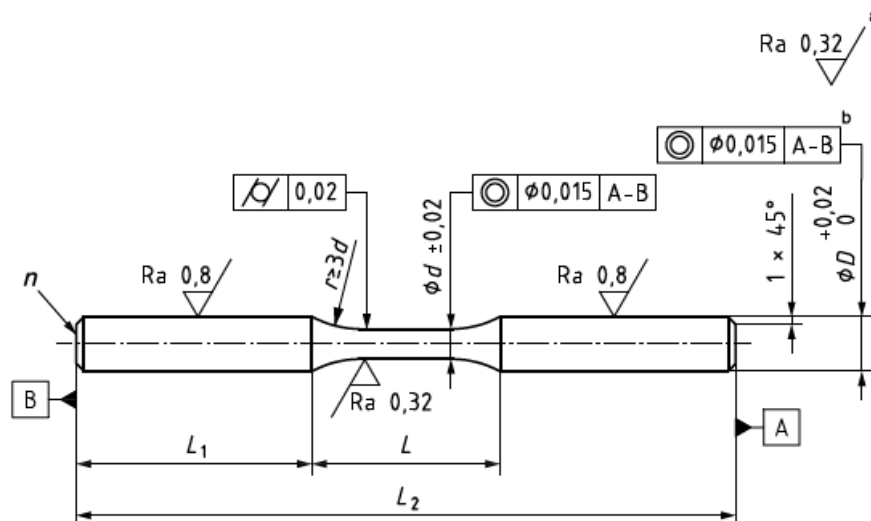


Figure 2.26 Cylindrical smooth specimen as per (BS ISO 1143:, 2010)

**n:** specimen number, **a:** others, **b:** two tops

## 2.4 Shaft Hub Connections

Manufacturing of shaft with gears on it as one piece is not a logic solution due to the cross section differences in diameter which requires a heavy material removal on section. So to come up with a solution to design the layshaft component with appropriate coupling with gears to allow torque transmission to another gear and shaft, there are several solutions available. Commonly used solution is placing a keyway slot, press fitting two components by choosing the adequate tolerance mate, providing the necessary friction by tightening with bolt and nut, placing splines all the way around or sometimes conical coupling and etc.

### 2.4.1 Keyway Connection

Key element is standardized machine torque transmitting element and its dimensions are provided in following standards:

- ANSI B17
- DIN 6885
- ISO/R 773

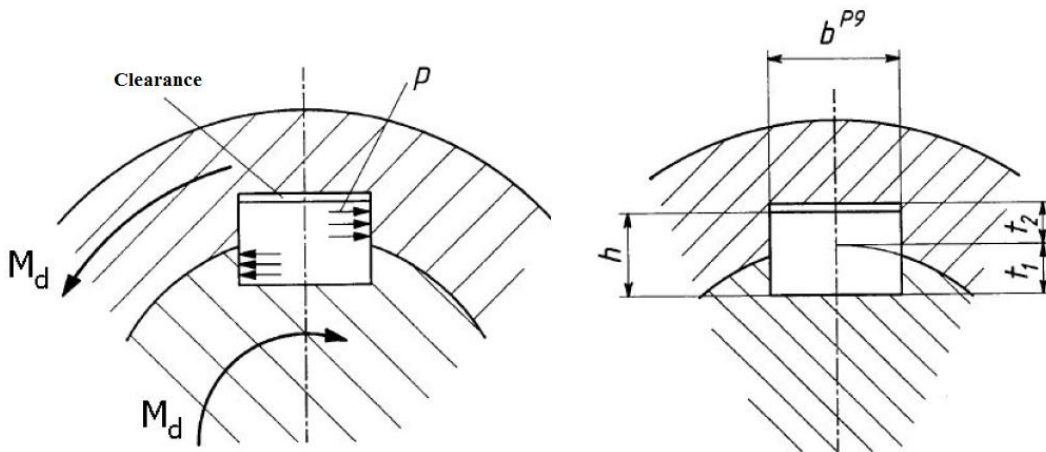


Figure 2.27 Key element for torque transmission (Temiz, n.d.)

Although the aim to use this machine element basically transmitting the desired torque, however it must be failed to prevent the system failure when excessive torque tries to flow through this element. It could be named as safety connection. (Budynas & Nisbett, 2011)

Principle design consideration includes 3 major approaches when deciding the size of key to be used. (Budynas & Nisbett, 2011) These main calculations are:

Keyway connection, deformation of the shaft wall material:

$$P_{shaft} = \frac{2M_d}{dt_1l} \leq P_{shaft, safety} \quad \text{Equation 2.20}$$

Keyway connection, deformation of the hub wall material:

$$P_{Hub} = \frac{2M_d}{dt_2l} \leq P_{hub, safety} \quad \text{Equation 2.21}$$

Keyway connection, shearing of key itself between hub and shaft walls:

$$\tau_{shear} = \frac{2M_d}{dbl} \leq \tau_{shear, safety} \quad \text{Equation 2.22}$$

### 2.4.2 Interference Fit Connection

This shaft – hub connection is easy to manufacture, however difficult to control the coupling parameters. The two connected components, shaft and hub diameters are defined with tolerance values which makes the shaft external diameter slightly bigger than hub bore diameter, and hub bore diameter slightly lower than the shaft diameter. This dimension difference when two parts are assembled, creates a pressure between two surfaces and this pressure with friction coefficient between surfaces creates a friction force against rotating force. In other words this friction is used to transmit torque from shaft to gears. As it mentioned keyway connections, tolerance values and press fit strength could be controlled to allow desired torque to transfer and prevent the system from excessive torque by slipping. See Figure 2.28 for diameter arrangement by tolerance. (Budynas & Nisbett, 2011)

As it is seen almost every mechanical components and systems, interference fit was standardized with the code DIN 7190 which controls shaft and hub assembly tolerances, required temperature for assembly, connection safety calculations etc.

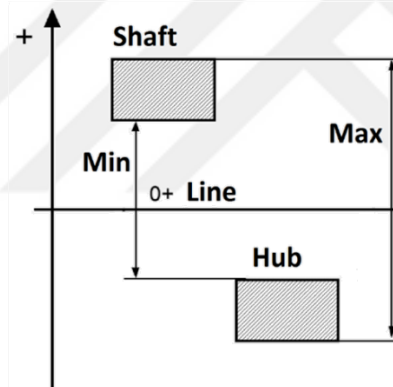


Figure 2.28 Press fit shaft and hub size with tolerance (Temiz, n.d.)

Press fit normally achieved either with tolerances, or pressure could be created by tightening bore diameter over shaft or conical fitting by creating pressure with axial tightening. Figure 2.29 shows a conical press fit controlled by a nut to create frictional force between conical shaft and hub surfaces. This type of assembly is a good approach when well calculated because assembly and disassembly is easy for aftermarket maintenance.

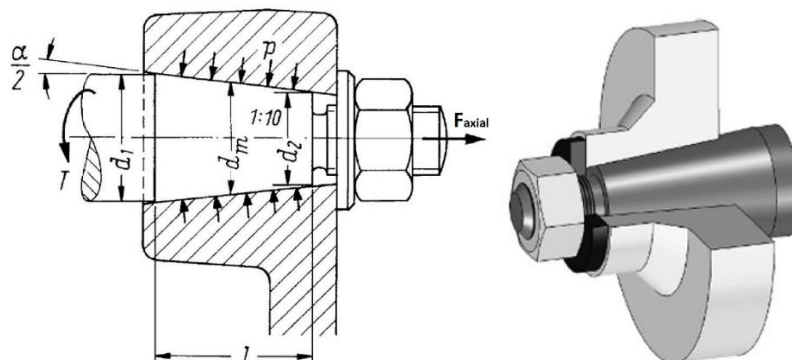


Figure 2.29 Conical press fit connection (Temiz, n.d.)

Another type of connection to allow torque flow is bolt tightened shaft hub assemblies. In this type of connections, hub itself should be designed with a slit to allow radius shrinkage when tightening the bolts. After assembling the components, uneven stress gradient occurs over shaft surface. See Figure 2.30 for occurred stress. The occurred stress is depend on the pre-loading applied to the bolts and can be controlled and achieved by only with the bolt strength.

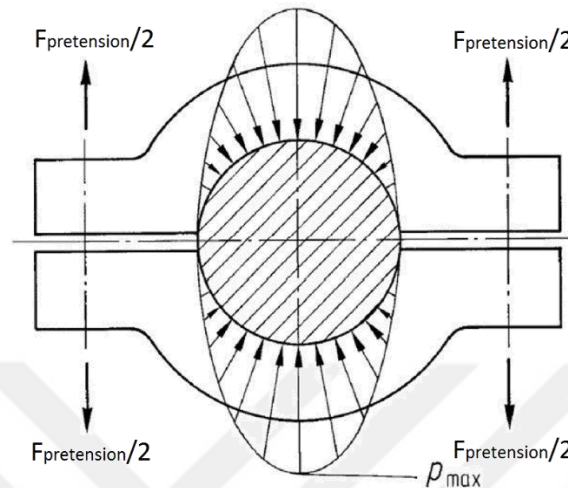


Figure 2.30 Bolt preloaded shaft – hub connection (Temiz, n.d.)

The surface pressure when interference fit applied can be analytically calculated with the Lamé equation (1983) (Klebanov, et al., 2007). This calculation method is more accurate with some assumptions. In this thesis we will benefit of using FEM in order to calculate the pressure occurs on the surface.

IF contact pressure:

$$P = \frac{E\delta}{2d^3} \frac{(d^2 - d_1^2)(d_2^2 - d^2)}{d_2^2 - d_1^2} \text{MPa} \quad \text{Equation 2.23}$$

**E** is the modulus of elasticity (MPa) Making assumption of two structures have same elasticity. **d1** and **d2** connection diameters see Figure 2.31,  $\delta$  is rated interference which could be calculated from Equation 2.24.

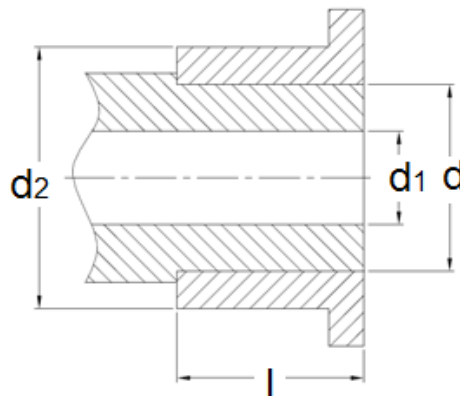


Figure 2.31 IF parameters (Klebanov, et al., 2007)

For example taking into account of the connection is infinitely long and the coupling hub-shaft is precisely round cylinders. This calculation method takes into account of surface roughness

as well. According to this rule, the occurred pressure at the mating surfaces smashes the 60% of the sum of the roughness height (Rz).

IF rated interference formula:

$$\delta = (d_S - d_H) - 1.2(R_{ZS} - R_{ZH}) \quad \text{Equation 2.24}$$

Shaft outer diameter is  $d_S$  and hub inner diameter is  $d_H$ . Shaft and hub roughness height of surfaces are  $R_{ZS}$  and  $R_{ZH}$  respectively.

### 2.4.3 Splined Connection

Splined connections are internationally standardized and the parameters when selecting a connection are the length of the splines, teeth number and the spline modulus. The durability of the connection is depends on the length calculation of the spline profile.

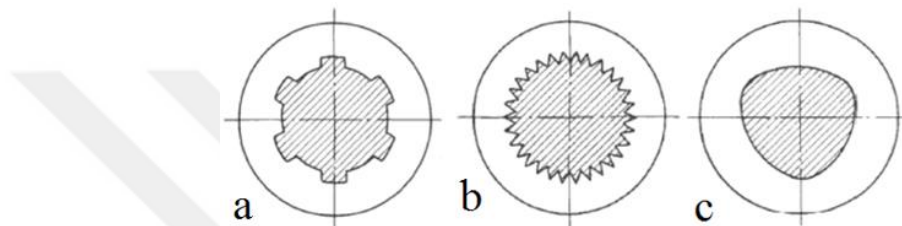


Figure 2.32 Shaft - hub connections a) DIN5480 spline, b)DIN5481 c)DIN32711

In Figure 2.32 some of the geometrically centred coupling types can be seen. These type connections are also standardized by international norms. Amongst of them type a DIN 5480 is the most commonly used spline in power transmission applications. Spline calculation is kind of similar compared to keyway applications. The critical consideration is, calculation of tooth to tooth compression interaction. The occurred stress here must be calculated and controlled. Equation 2.25 is used to calculate the effective pressure occurred on tooth wall of splines. (Temiz, n.d.)

Spline tooth wall stress:

$$P_{Wall\ pressure} \approx \frac{F_t}{h.l.i.k} \quad \text{Equation 2.25}$$

$P_{wall-pressure}$ : Side wall pressure occurred on tooth flank

$F_t$ : Tangent force due to transmitted torque  $F_t = M_d / r_m$ ;  $r_m = 0,25(d_2 + d_3)$

$h$ : Tooth height  $0,5(d_3 - d_2)$

$l$ : Length of spline

$i$ : Number of tooth

$k$ : Coefficient of load carriage capacity, for inner diameter centred is 0,75, for profile centred assemblies 0,9.

## 2.5 Key Aspects of FE Modelling

In order to properly design fail free products, synthesis, analysis and testing steps must be included. Only performing fatigue testing alone is not a decent way of design procedure for fatigue investigation, because only product testing is oriented for product durability determination, which does not represent product development. Since a proper material model and numerical fatigue model requires to be correlated by decent fatigue testing. Therefore, when considering product development and fatigue free design. Testing and numerical models are indispensable cooperated partners. Scientists and engineers should always keep the logic of representing the real world situation both in testing and in simulations. This gives more confidence in results.

For further fatigue analysis stress analysis should be performed by FEA software which is a preparation for fatigue durability analysis. FEA analysis requires a pre-processing step which could be both by done using Hypermesh user interface or any other pre-processing software like Abaqus/CAE. While establishing a model it must be kept in mind the model should be constructed for the intended simulation solver.

### 2.5.1 Deciding Element Type for the Analysis

Element type selection depends on several parameters,

- Geometry, size and shape
- Type of analysis
- Project allocated time

First of all, one must define the geometry's specification according to 1D, 2D or 3D, because it is allowed to create elements and represent the model with using only one type of these elements. For example, long shaft, rod, beam, column, bolts, pin joints, etc. could be modelled with 1D elements. In general, when one of the dimensions is very large in comparison to the other two of them, it is easy to utilize 1D elements. If two of the dimensions are very large when comparing to the third one, 2D meshing is advised. Basically the mid-surface is extracted and mesh creation is performed on this surface, thickness is defined as a parameter. For example, sheet metals are modelled with 2D elements. When three of the dimensions has comparable length, it is appropriate to use 3D elements. Such as power train components, casings, engine blocks, shafts, gears, etc. (Altair Engineering, Inc., 2015)

According to Altair, for structural and fatigue analysis investigations, quad (2D), hex (3D) elements are recommended over tria (2D), tetra and penta (3D). For the purpose of crash and nonlinear analysis, brick elements are advised over tetrahedrons and meshing should performed following flow lines. (Altair Engineering, Inc., 2015)

Ideally if there is no urgency for the project report the most appropriate approach is performing good mesh quality, capable element selection for all the components. However in industry time is important. Automatic, batch matching methods are preferred, 3D tetra meshing preferred over 3D hexa elements. For assembly meshing, only the investigated component meshed appropriately and the other assembly components are coarse meshed or represented by 1D elements by beams, springs, or concentrated mass. (Altair Engineering, Inc., 2015)

In Abaqus manual, it is stated that the second-order elements provide higher accuracy in Abaqus/Standard than first-order elements. Especially, if there is no severe element distortion occurs, which means for "smooth" problems could be modelled more precisely by second order

usage. The second order elements have ability of capturing stress concentrations more effectively and better for modelling geometric features. Abaqus also recommends to use these elements in bending dominant problems. (Dassault Systemes, 2006)

In Figure 2.33 it is shown on the left the first order tetrahedral 4 noded elements so called first order tetrahedral. On the left it is shown the 10 noded tetrahedral element, in abaqus terminology it is called as second order tetrahedral element which is recommended by Dassault Systemes to utilize for bending dominant problems. However the big burden is using the 10 noded element instead of three noded one brings more than two times computation cost. This is an engineering optimization problem instead of using fine C3D4 better to use coarser C3D10 to have better results. Also it is advised not to use first order elements in stress analysis problems. These elements are described as overly stiff and have slow convergence.

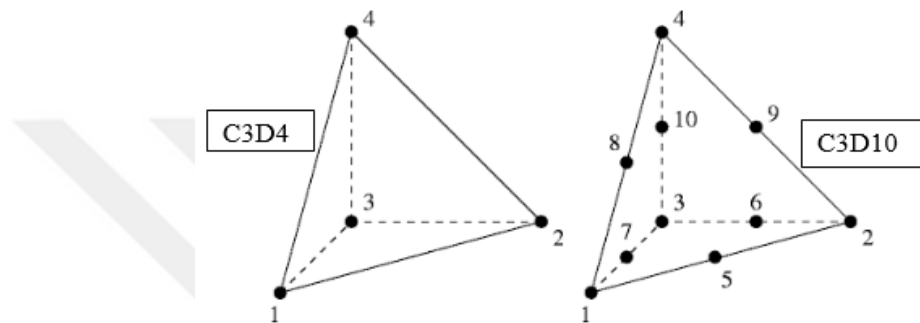


Figure 2.33 First and second order tetrahedral elements

It basically recommends when the user decided to use tetrahedral mesh for the complex geometries. It advises to use the second-order elements C3D10 for the problems in Abaqus/Standard or C3D10M in Abaqus/Explicit models, or it is advised to use the modified tetrahedral element C3D10M in Abaqus/Standard in analyses if there is large amounts of plastic deformation occurs.

A brief study was done and presented in 2011 in local Abaqus User's meeting in UK which was concentrated on the result differences between first order and second order tetrahedral elements in different element sizes from course to fine and revealed the accuracy of the results when using quadratic second order elements instead of linear first order elements. (Dassault Systemes, 2011)

Contact definition is commonly required in FE modelling. It is always recommended to model a mechanical part or the part that be investigated under FEA should be modelled as much close as to its real working condition. For example if two gears are mating they should be modelled as contacted parts and there should be contact defined with an adequate frictional coefficient. Small sliding contact is defined for the contact occurred between mating gear tooth.

Once the contact defined in FEA simulation it becomes a nonlinear problem so that the FEA setup should also include the nonlinearity activated within the simulation. Within Hypermesh contact creating could be performed by contact manager. Basically a contact includes 2 mating surfaces. One is called as master surface and the other mating one is called as slave surface. For a defined contact in Optistruct, prior to analysis run, master and slave surfaces should be already in contact situation in other words user should avoid a clearance between contact surfaces to have them work.

Optistruct has the ability of parallel calculation utilizing the cpus, available on the computer. Of course the owned licenses should allow this parallel processing. The company has 50 HyperWorks units which is enough to run the simulations in 8 cpus.

The basic mechanical interactions like frictional coefficient between contacts, interference fit applications, thermal expansion, bolt pretension, gravity are all can be modelled in FEA softwares.

### 2.5.2 Validating The Accuracy of the Results

As it is known by the professionals and the academics Finite Element Analysis is making approximation for the physical condition that occurs on intended component or product. The results obtained from FEA could represent the real condition with a margin of error. This error could be %5 to %90 depending on the accuracy of the constructed FEA model. Before proceeding making estimations with the results of the simulation, it is always recommended to perform experimental correlation. (Altair Engineering, Inc., 2015)

Table 2.5 FEA accuracy check

<b>Computational accuracy</b>	<b>Correlation with actual testing</b>
1. Strain energy norm, residuals	1. Stress comparison
2. Reaction forces and moments	2. Natural freq. comparison
3. Convergence test	3. Dynamic resp. comparison
4. Average and unaverage stress diff.	4. Temp. and press. dist. comp.

Visually checking the analysis results could give a feedback on the simulation, for example sudden change on the stress distribution means there is refined local mesh required in order to capture correct stress values. In worst case %15 deviation between analysis and test results could be considered as good result. (Altair Engineering, Inc., 2015)



### 3 8+1 Manual Transmission Preliminary Design

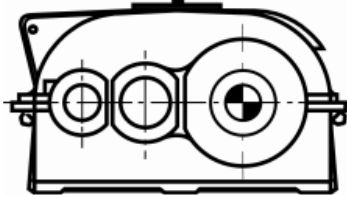
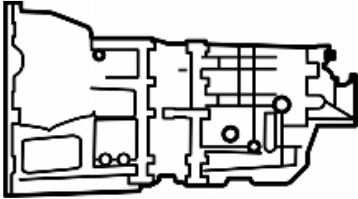
#### 3.1 Concept and Benchmarking

8+1 refers to a transmission with 8 forward and 1 reverse gear speeds. A simple description for transmission task stated by (Naunheimer, et al., 2011) as “Vehicle transmission adapts the power output to the power requirement by converting torque and rotational speed. The power requirement at the drive wheels is determined by driving resistance.” From this phrase it could be easily understood between the two boundary conditions, engine and driving resistance, transmission is a crucial system and it had to be optimized for best traction and power output.

Transmission design has several design concerns when it comes to its application area. For example, service life, power interruption, specific power, fuel consumption, transport capacity, ease of operation, etc. are important requirements on design stages.

Unique transmission design for each engine means perfectly compatible powertrain system. However, it is not feasible to design a transmission to each engine project, and most of the power train Tier companies try to put a product on a market which satisfies its target ICE engines with efficiency compromise.

Table 3.1 Industrial vs. automobile transmission (Naunheimer, et al., 2011)

Transmission	Number of forward speed	Overall gear ratio	Power (kW)	Input Torque (Nm)	Mass (kg)	Specific Power (kW/kg)
<b>Industrial</b> 	1	12.5	330	2100	680	0.48 %100
<b>Passenger Car (MT)</b> 	6	4.2 5.1	294	500	46	6.39 %1300

Unlike the industrial transmissions, automotive transmissions, specifically includes compelling challenges of the design requirements mentioned above like reliably, high specific power road safety and ease of operation are the key design interests.

As it is a market requirement like for all the commercial products, transmission development should follow the same steps. There must be a market survey, required benchmarking of competitors and planning of market goals where to position the intended product, for example which cars are in scope and which are not. These unknowns should be well clarified prior to kick off a transmission development project.

8+1 MT project started with internal demand of the company. First the company was interested in to design a unique off-road multi-purpose vehicle which has a great market share in both




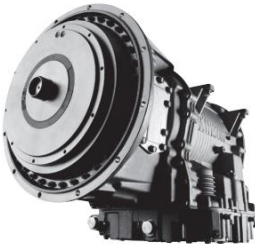
international and Turkish market. There was already a newly developed 6 cylinder diesel engine and the company decided to develop its own transmission to unveil first national vehicle with national power train unit.



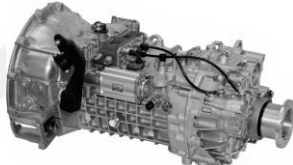


As in the all automotive development projects, predefined competitive vehicles and their transmissions systems were closely examined.





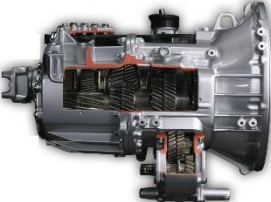
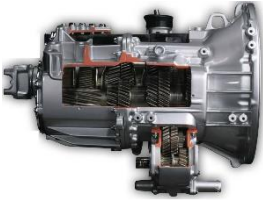
Starting with the categorization of different staged transmission types, after an extended benchmark, 8+1 transmission was decided to have two staged transmission architecture, which has input shaft with coaxial main shaft and one layshaft.

As a next step, gear ratio calculations and their optimization, transmission layout extraction were performed. The general design concept was finalized by comparison of hill climbing, final drive, acceleration attributes of the intended vehicle. These mentioned design phases were for general concept design. Further detailed development on component base were performed after the rough conceptual design by utilizing KissSys and KissSoft machine element softwares.

Table 3.2 Benchmarked transmissions for manual 8+1 transmission

Transmission	Type	Photo	Forward Gear	Reverse Gear
<b>GM Hydra-Matic 4L80E</b>	<b>Automatic</b>		Gear 1: 2,48 Gear 2: 1,48 Gear 3: 1,00 Gear 4: 0,75	Gear 1: 2,07
<b>Allison 1000SP</b>	<b>Automatic</b>		Gear 1: 3,10 Gear 2: 1,81 Gear 3: 1,41 Gear 4: 1,00 Gear 5: 0,712 Gear 6: 0,614	Gear 1: 4,49
<b>Allison 2500SP</b>	<b>Automatic</b>		Gear 1: 3,51 Gear 2: 1,90 Gear 3: 1,44 Gear 4: 1,00 Gear 5: 0,74 Gear 6: 0,64	Gear 1: 5,09
<b>Allison 3000SP</b>	<b>Automatic</b>		Gear 1: 3,49 Gear 2: 1,86 Gear 3: 1,41 Gear 4: 1,00 Gear 5: 0,75 Gear 6: 0,65	Gear 1: 5,03

<b>ZF Ecomid 9S 1110 TD</b>	<b>Manual</b>		Gear 1 : 8,83 Gear 2 : 6,28 Gear 3 : 4,64 Gear 4 : 3,48 Gear 5 : 2,54 Gear 6 : 1,81 Gear 7 : 1,34 Gear 8 : 1,00	Gear 1: 12,04
<b>ZF Ecomid 9S 1110 TO</b>	<b>Manual</b>		Gear 1 : 6,58 Gear 2 : 4,68 Gear 3 : 3,48 Gear 4 : 2,62 Gear 5 : 1,89 Gear 6 : 1,35 Gear 7 : 1,00 Gear 8 : 0,75	Gear 1: 8,97
<b>ZF Ecomid 9S 1310 TO</b>	<b>Manual</b>		Gear 1 : 6,58 Gear 2 : 4,68 Gear 3 : 3,48 Gear 4 : 2,62 Gear 5 : 1,89 Gear 6 : 1,35 Gear 7 : 1,00 Gear 8 : 0,75	Gear 1: 8,97
<b>ZF Ecomid 9S 109</b>	<b>Manual</b>		Gear 1 : 6,779 Gear 2 : 4,776 Gear 3 : 3,529 Gear 4 : 2,611 Gear 5 : 1,921 Gear 6 : 1,353 Gear 7 : 1,00 Gear 8 : 0,740	Gear 1: 9,436
<b>ZF Ecomid 9S 75 DD</b>	<b>Manual</b>		Gear 1 : 8,913 Gear 2 : 6,497 Gear 3 : 5,313 Gear 4 : 3,500 Gear 5 : 2,547 Gear 6 : 1,856 Gear 7 : 1,518 Gear 8 : 1,000	Gear 1: 11,74

<b>MB G140-8</b>	<b>Automated</b>		Gear 1 : 9,296 Gear 2 : 5,837 Gear 3 : 3,673 Gear 4 : 2,306 Gear 5 : 1,593 Gear 6 : 1,252 Gear 7 : 1,000 Gear 8 : 0,786	Gear 1: 8,538 Gear 2 : 5,361
<b>ZF 6 AS 1110 BO</b> <b>ZF As Tronic</b> <b>lite bus</b>	<b>Automated</b>		Gear 1 : 6,42 Gear 2 : 3,42 Gear 3 : 2,02 Gear 4 : 1,32 Gear 5 : 1,00 Gear 6 : 0,74	Gear 1: 5,76
<b>MBT520-6DA</b>	<b>Automated</b>		Gear 1 : 9,20 Gear 2 : 5,23 Gear 3 : 3,14 Gear 4 : 2,03 Gear 5 : 1,37 Gear 6 : 1,00	Gear 1: 8,65
<b>MBT660-6OA</b>	<b>Automated</b>		Gear 1 : 6,70 Gear 2 : 3,81 Gear 3 : 2,29 Gear 4 : 1,48 Gear 5 : 1,00 Gear 6 : 1,73	Gear 1: 6,29
<b>MB T520S-6D</b>	<b>Manual</b>		Gear 1 : 9,20 Gear 2 : 5,23 Gear 3 : 3,14 Gear 4 : 2,03 Gear 5 : 1,37 Gear 6 : 1,00	Gear 1: 8,65
<b>MB T660S-6O</b>	<b>Manual</b>		Gear 1 : 6,70 Gear 2 : 3,81 Gear 3 : 2,29 Gear 4 : 1,48 Gear 5 : 1,00 Gear 6 : 1,73	Gear 1: 6,29

### 3.2 Gear Count & Ratio Determination

Determining the gear count for the transmission is a trade-off between engine – transmission efficiency and driver comfort. In other words increasing speed stages allows for transmission to scan engine's sweet spot on rotational speed – torque map however it urges the driver shift more frequently to obtain desired vehicle speed and causes the transmission to be more heavier owing to more meshed gear pairs. (Fischer, et al., 2015)

The first gear ratio determination is a requirement defined prior to intended vehicles. For the first gear, vehicle's launch and its climbing, slip condition between tire and road should be considered. Top gear ratio is another vehicle requirement as well and it is a vehicle specification demanded from the engine – transmission unit. The main parameter for its definition is the final desired speed of the vehicle. The top gear also creates another category for the vehicle transmissions as direct drive and overdrive.

The gear ratio is mostly represented with  $i$ , angular velocity with  $\omega$ , revolution with  $n$  symbols. A simple gear ratio calculation is seen in Equation 3.1.

Gear ratio formula:

$$i = \frac{\omega_1}{\omega_2} = \frac{n_1}{n_2} \quad \text{Equation 3.1}$$

The first and the last gear ratio determination provides the ratio spread of the transmission in Equation 3.2.

In this equation  $n_s$  subscript indicates the number of gears. Deciding number of gears advantages and disadvantages are already mentioned in this section. Therefore like in every engineering design, here the optimization process must be performed. Today's passenger vehicles could have up to 6 gears in manual transmissions and 5 geared design is the most common option. Truck's manual transmissions could have up to 18 gears and 12 geared designs for AMT Truck is commonly used. (Fischer, et al., 2015)

Transmission ratio spread formula:

$$\varphi_s = i_1 / i_{n_s} \quad \text{(Fischer, et al., 2015)} \quad \text{Equation 3.2}$$

$i_1$ : first gear and  $i_{n_s}$ : last gear

The next step in this regard is determination of intermediate gear ratios. There are two types of strategies commonly accepted for determination of gear ratios, (Fischer, et al., 2015) which are:

- Geometric gear ratio design
- Constant progression gear ratio design

Basically both approaches are used to define the gear ratios of the two adjacent gears. The first approach proposes the constant change of the output speed at defined input which means constant ratio steps for each shift. The second approach is a progression for acceleration event. For example while acceleration, shifting always takes place at the same engine speed, which means between shift events, velocity increase is constant.

Geometric gear ratio step formula:

$$\varphi = \sqrt[n_s - 1]{\varphi_s} = \text{constant} \tag{Equation 3.3}$$

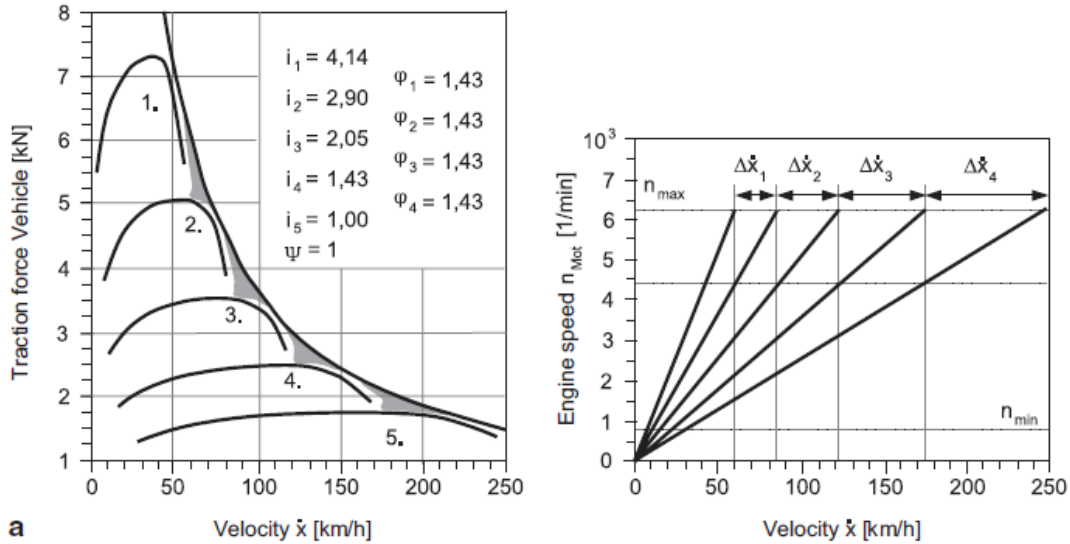


Figure 3.1 a) Geometric gear ratio design (Fischer, et al., 2015)

Constant progression gear ratio calculation has constant relationship with adjacent gear ratio.  $\Psi$  is progression factor defined in design. If this factor selected as 1, the design becomes geometric gear ratio.

Constant progression gear ratio formula:

$$\psi = \varphi_k / \varphi_{k+1} = \text{constant} \tag{Equation 3.4}$$

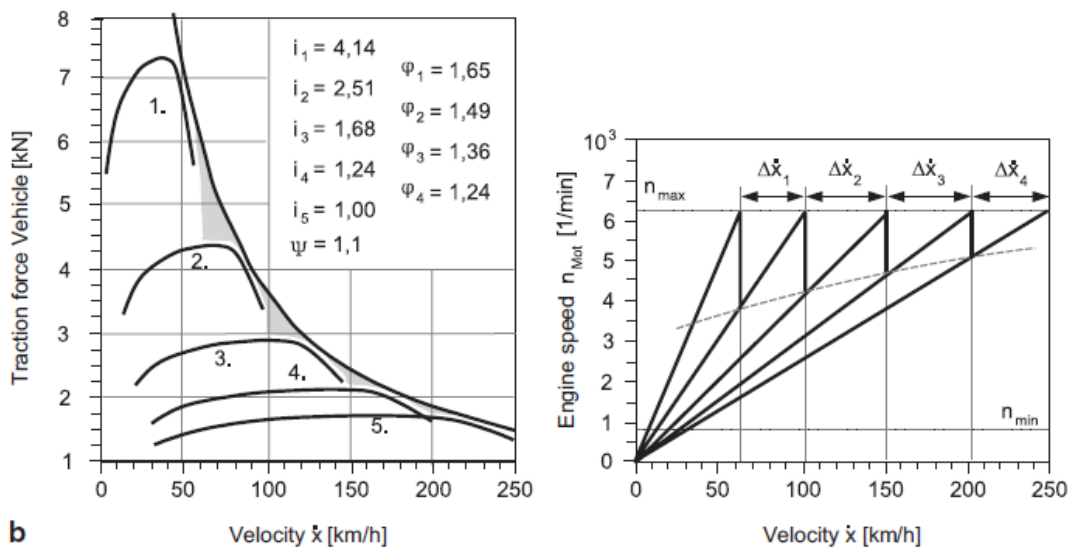


Figure 3.2 b) Progressive gear ratio design (Fischer, et al., 2015)

In Figure 3.1 and Figure 3.2, the differences between geometric and progressive gear ratio design can be seen easily.

Geometric gear ratio design approach is accepted to determine 8+1 manual transmission and further calculations are done with this approach.

Intermediate gear ratio determination:

$$\phi = \frac{i_{n-1}}{i_n} \leq \frac{n_{max}}{n(\tau_{max})} \quad \text{(Naunheimer, et al., 2011)} \quad \text{Equation 3.5}$$

$n_{max}$  maximum engine speed of ICE, ( $n_{\tau_{max}}$ ) engine speed at maximum torque, ( $n-1$ ) next lower gear.

For the gear ratio determination, the step must be well designed to enable next gear engagement while the engine is in maximum torque in the range of maximum engine speed.

This transmission will be mounted to 6 cylinder diesel engine which produces 273kW power, maximum torque @ 1700rpm, and maximum achievable rotational speed is 2400rpm. By the help of Equation 3.5. Gear ratio step is calculated as 1.417 to operate the engine at its sweet spot see Figure 3.3.

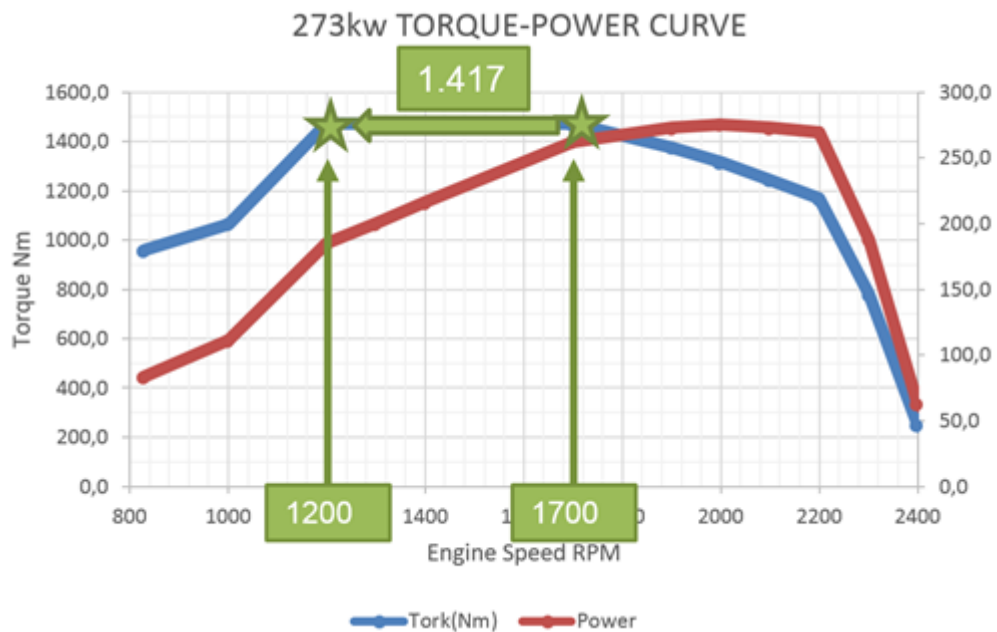


Figure 3.3 Gear ratio to scan engine's effective torque range

As a result transmission gear ratios are calculated as in table below and transmission layout can be seen in Figure 3.4.

Table 3.3 8+1 Transmission gear ratios

<b>1. Gear ratio</b>	8,854
<b>2. Gear ratio</b>	5,971
<b>3. Gear ratio</b>	4,194
<b>4. Gear ratio</b>	2,982
<b>5. Gear ratio</b>	2,111
<b>6. Gear ratio</b>	1,424
<b>7. Gear ratio</b>	1,000
<b>8. Gear ratio</b>	0,711
<b>Reverse Gear ratio</b>	9,319



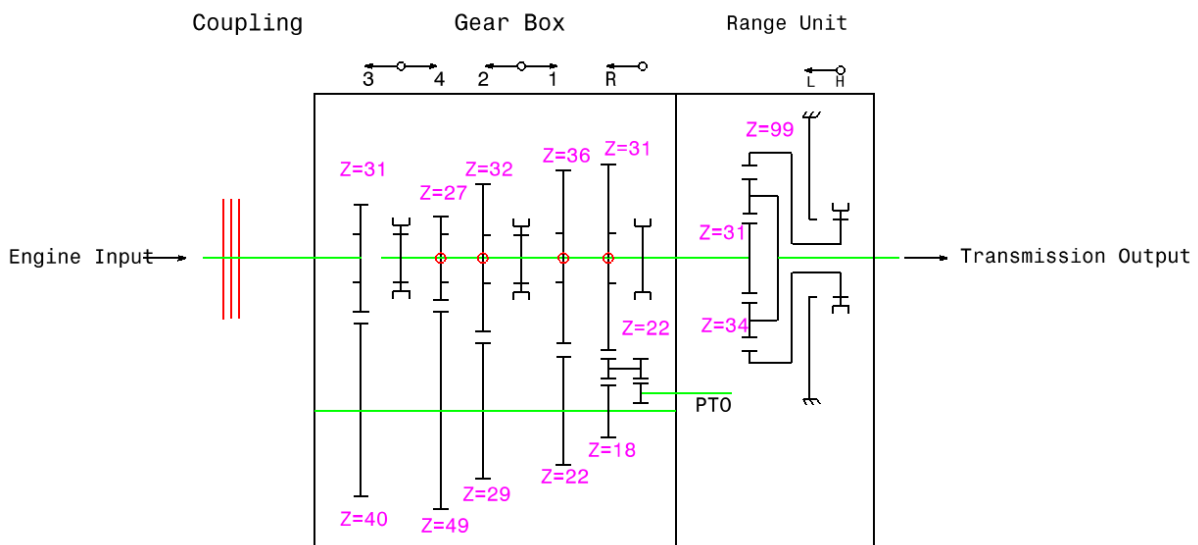


Figure 3.4 The manual 8+1 transmission layout

Once the efficient transmission ratios are defined, 3D illustration and rough sizing of the transmission torque transmitting element are modelled by utilizing machine element software Kiss-Sys. The main aim of the rough modelling is to check durability of gears, shafts, bearings and dimensional packaging at first impression. See Figure 3.5 for a preliminary design of 8+1 MT.

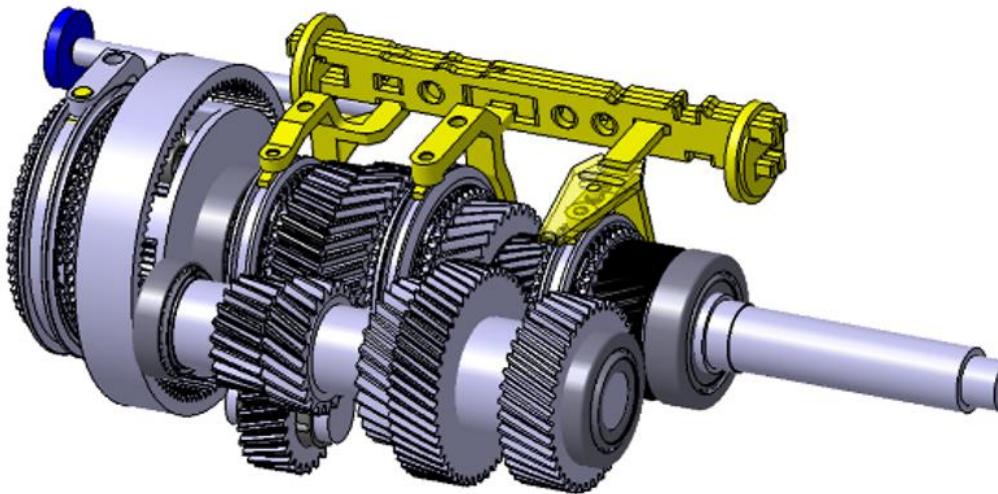


Figure 3.5 8+1 MT 3D rough sizing using KissSys, courtesy of the Company



## 4 Layshaft Design Alternatives

Layshaft itself is the main topic of this thesis, and from the benchmark investigations we faced with three different design options for establishing the connection with the gears assembled on it. The splined and the one with keyways are the solutions for old type transmissions. However the general trend is the interference fit assembly of the layshaft and its gears. The main transmission manufacturers (Mercedes, ZF, Scania etc.) are following this option.

The first design option for the layshaft is the keyway throughout its gear carrying side, see Figure 4.1.



Figure 4.1 Keyway slotted layshaft, the manufacturer is unknown

The Figure 4.2 show the variety of transmission shafts, in the foreground one is the coarse splined shaft which was popular choice of design by German manufacturers. One of the layshaft design for 8+1 transmission is splined connection, see Figure 4.4.



Figure 4.2 Various shaft designs in mechanic workshop

Another choice of design is as seen in Figure 4.3 is interference fit with gears. In this particular design there are several parameters to be concerned. In Figure 4.3 there is a replaced component in a heavy truck transmission mechanic. The reason of replacement is due to overload of the truck and badly engine – transmission integration. Basically the transmission assembly should safely transmit the maximum torque generated by the engine. The failure is slipping of layshaft from its interference fitted gears.



Figure 4.3 Interference fitted gears and flat surface layshaft (ZF)

The interference fit parameters such as, interference design tolerance is the main factor, being able to transmit the design torque between gears and the shaft. Additionally surface roughness of the assembled surfaces in relation with friction coefficient, also diameter tolerances which is going to be supplied by the manufacturer within a range. So that the interference value between gears and the layshaft will be carefully calculated by considering the probability of the lowest interference situation which could be occurred within the design tolerances and also temperature changes while in operation.

#### 4.1 Splined layshaft CAD design

The splined geometry for the layshaft was considered as the main solution for the assembly. Due to the fact that there was no successful reference work done within the company before for highly critical parts, especially torque transmitting machine element connections.

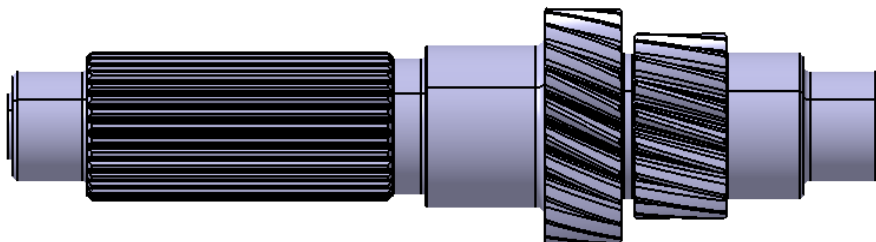


Figure 4.4 DIN 5480 splined layshaft

The splined connection for the layshaft assembly is chosen according to DIN5480 splined connection standard.

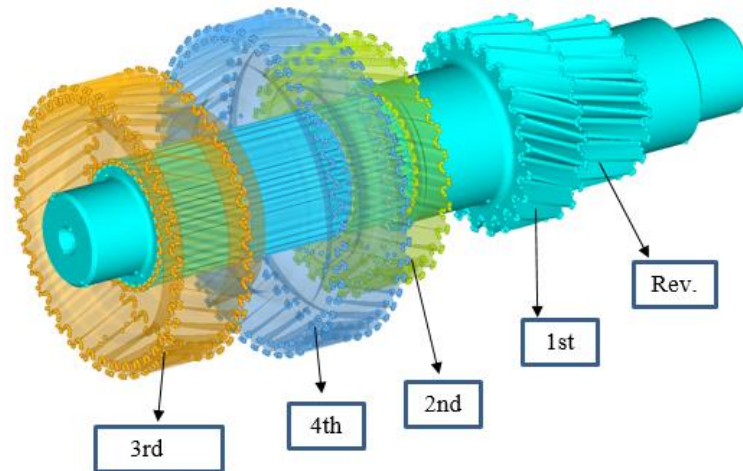


Figure 4.5 Splined layshaft assembly with gears

The torque “1250Nm” value transmitted from the input shaft is done via the third gear coupling between input and layshafts. The occurred torque value is 1613Nm on layshaft splines in worst case if the efficiency is considered which is around 0,96 per gear coupling, the resulted torque could be assumed as 1548,5Nm and just to stay in the safe zone spline calculations were done by considering the max. torque value excluding efficiency ratio.

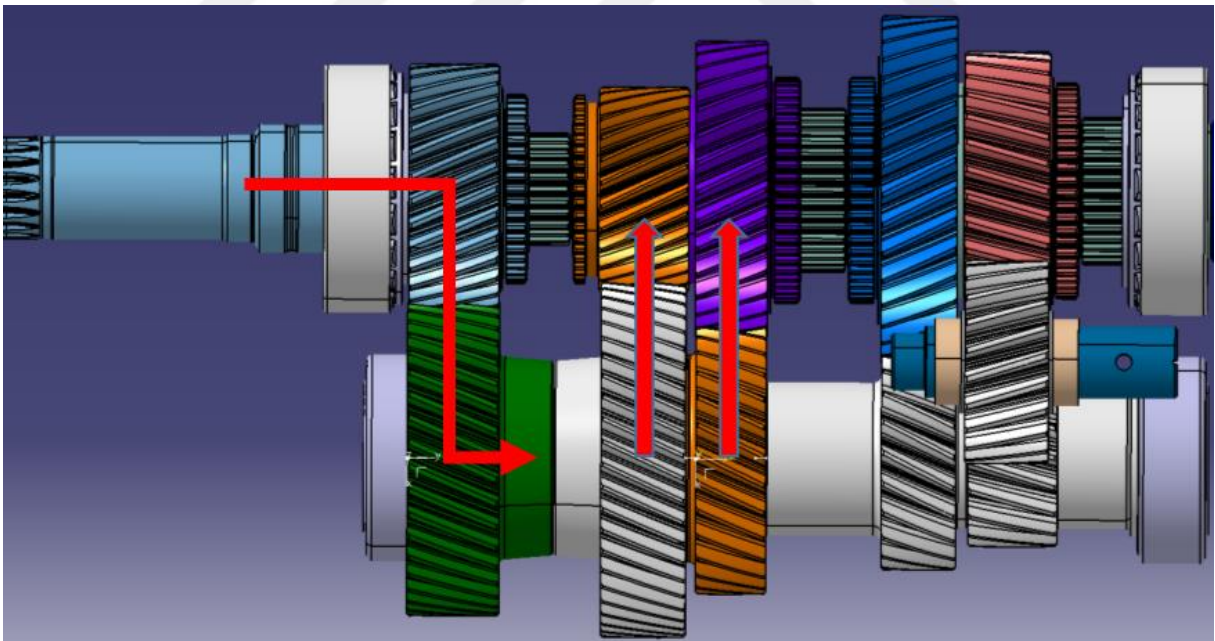


Figure 4.6 Torque transmission on layshaft splined connections.

As input parameter, transmitted torque, shaft and hub material, Niemann/Winter stress calculation methodology, face width of the intended connection were defined to the software and as the result Kisoft offers applicable spline module, tooth and safety of this coupling. As an initial design these parameters are accepted for splined connections.

For the face width consideration of the splined connection the minimum face width of the gear assembled on it is considered which has a value of 39 mm. For this length by considering the

other parameters the safety of the connection design is obtained as 9,5 which is in the quite high safe zone. Niemann/Winter calculation method is used with application factor of 1.75 for the safety calculation. 20NiCrMo2-2 selected as base material. See Figure 4.7 for the calculation screenshot of this connection.

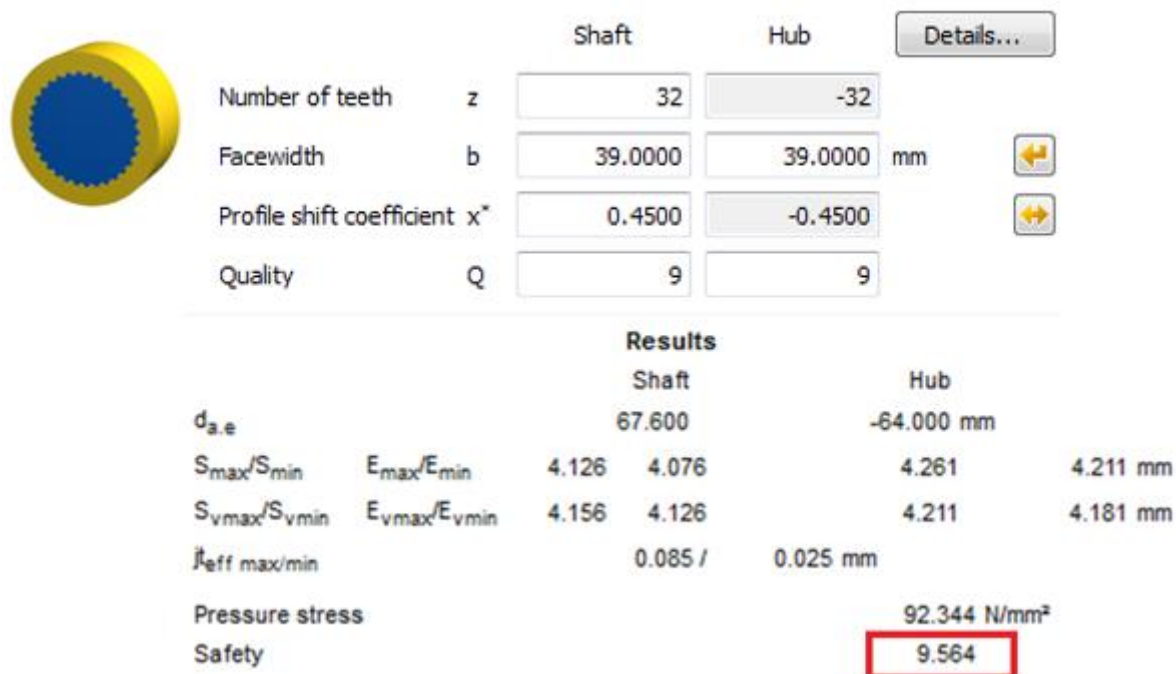


Figure 4.7 Spline safety calculation for the shortest face width

Splined connections can either be interference fit or clearance fit. Our calculations are done for the clearance fit assembly. 9H tolerance was defined for gear hubs and 9f clearance is defined for the layshaft spline in accordance with Kisoft database. Layshaft spline is defined as DIN5480 W68x2x30x32x9f, gear hub splines designation according to DIN5480 is N68x2x30x32x9H.

As it was mentioned in splined connection chapter, this connection could be interference fit or clearance fit

## 4.2 Interference Fit Layshaft CAD Design

Interference fit is the simplest way for manufacturing the components. It relieves all the burden of chip removal for splines which are shaped by broaching or any other shape connected geometries. This type of connection only uses the principle of two phenomenon already available. The one is the friction coefficient between two surfaces and the other is the material expansion with the temperature increase. The parts must be enough thick walled in order to withstand the higher pressure created due to the interference phenomenon. Main advantage is after machining the flat boring and the outer diameters the gears and the shaft is ready for assemble. The most importantly it is the cheapest solution to put them together.



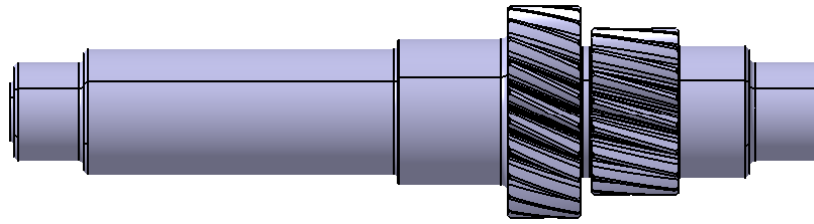


Figure 4.8 Smooth interference fit layshaft design

The disadvantage of the interference fit is disassembly. Assembly is easy because heating up the gear bore and enough cooling for the shaft will allow easily the connection. On the other hand dismantling is become problematic. Owing to micro slippage under continuous duty mating surfaces change and the friction coefficient is increasing. This helps the connection to create more frictional coupling under torque transmitting.

Layshaft carries three gears and torque on the shaft is identical for each gears. Therefore required interference fit calculation should be performed for the gear with lowest face width which is second gear with 38 mm press fit length. Shaft radius is 31 mm.

The shear force on the connection:

$$\text{Shear Force @ IF connection} = \frac{\text{Torque}}{r} = \frac{1613Nm}{0.031m} = 52032.3 N$$

Safety value is defined as 1.5 for this connection. The minimum frictional surface should be greater than this shearing force. Connection diameter is 62 mm, face width is 38 mm, and 0.15 taken as generic friction coefficient between two steel surfaces. By this approach the required connection pressure on the connection can be calculated as follows:

$$P = \frac{\text{Shear Force} \times \text{Safety}}{\pi \times d \times l \times f} = \frac{52032.3 N \times 1.5}{\mu \times 62 mm \times 38 mm \times 0.15} = 70.3 MPa$$

Here in the formulation above,  $f$  designates the friction coefficient,  $P$  is the pressure occurred on surface,  $d$  is the connection diameter and the  $l$  is the length of the coupling.

After calculating the required connection pressure, next step is utilization of Equation 2.24 to calculate rated interference. For this formula,  $d_1$  considered zero since the shaft is solid without centered hole.  $d_2$  is taken as 120 mm in diameter to represent the outer diameter of the hub. Young's modulus of the joined component is 210 GPa. By simply putting the knowns in the equation, rated interference calculated as follows.

$$70.3 MPa = \frac{210000MPa \times \delta (62^2 - 0^2)(120^2 - 62^2)}{2 \times 62^3 (120^2 - 0^2)} MPa$$

$$\delta = 0.0566 mm \text{ (rated interference)}$$

By the help of Equation 2.23 from rated interference, the required interference can be calculated by eliminating the effect of surface roughness. For the shaft outer roughness as taken 3,2 Rz and the inner surface of the hub 12.5 Rz as design input.

$$0.0566 mm = (d_S - d_H) - 1.2(0.0032 mm - 0.0125 mm)$$

$$(d_S - d_H) = 0.045 mm$$

The interference value is calculated as 0.045 mm as minimum interference value in order to create adequate pressure for the contact.



Figure 4.9 Interference fit layshaft model with gear hub

A FEA model created (Figure 4.9) to simulate connection pressure for 0.0225 mm radial interference. Node to surface contact is defined between two surfaces with 0.15 COF. This is a nonlinear model due to defined contact.

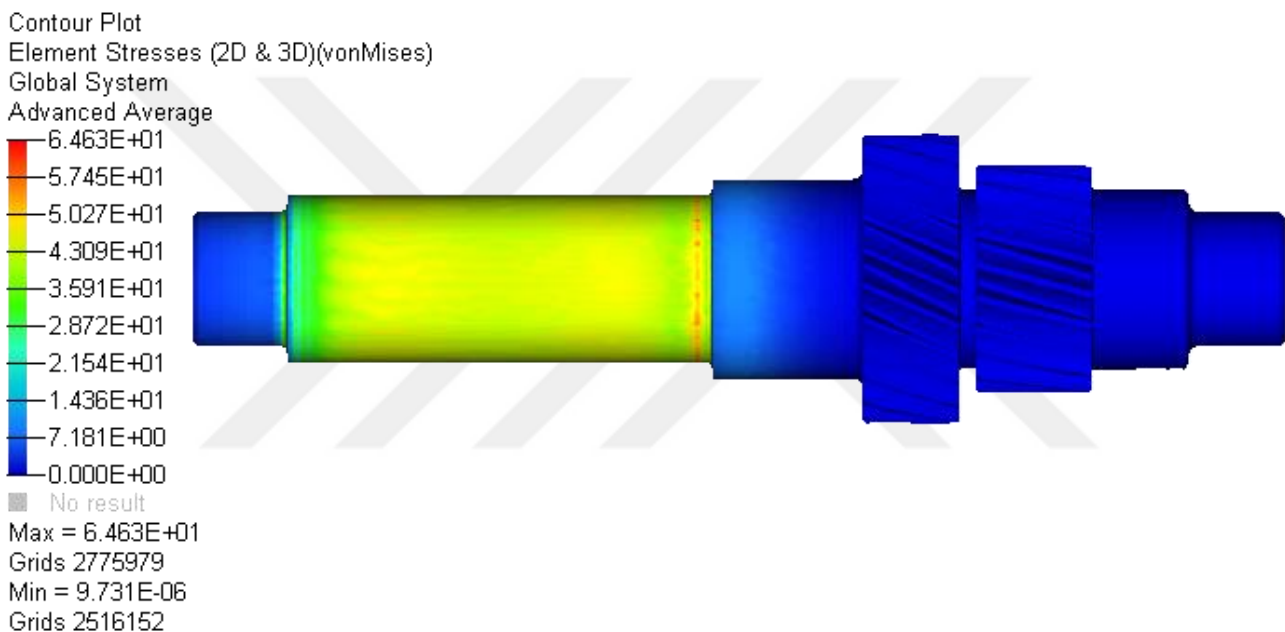


Figure 4.10 IF FEA stress result

Simulation results supports the calculated interference value for creating required pressure on the surface. The approximated stress level with analytical calculation results, promotes this FEA model to be used in further FEA calculation.

The next step is interpreting the IF design alternative for manufacturing of the component. 45 $\mu$ m interference should be the minimum interference value. Therefore to indicate a standard diameter tolerance on 2D drawings, ISO 286-2 standard tolerances for shaft and hub were referenced. For diameter of 62 mm shaft tolerance of n5 (+33/+20) and hub tolerance of P6 (-26/-45) were defined. According to this tolerance range, minimum interference would be 46  $\mu$ m and maximum interference value 78  $\mu$ m which will provide sufficient coupling for the components.

## 5 Material Selection

Technical components require a guaranteed sufficient lifetime with full functionality and economical manufacturing process is a consideration as well. Material properties such as wear, erosion and corrosion resistance, ability to withstand static and cyclic dynamic service loads and manufacturability are key parameters.

Material selection for the layshaft of 8+1 manual transmission which is a torsional stressed cylindrical shaft, under bending forces due to the meshed gears is a comprehensive decision to make. It also carries the 3 additional gears and fixed by two endpoints.

First of all, working conditions, gear meshes between main and layshaft, production methodology and the expected lifespan of the component comes into play.

In terms of fatigue failure, some material characteristics have good crack nucleation resistance, some are resistant to micro crack growth and some are resistant to macro crack growth. Finding the material specification which is in optimum resistant to all three is difficult to find. Therefore material selection must be done by the importance of the occurred fatigue process in the structure.

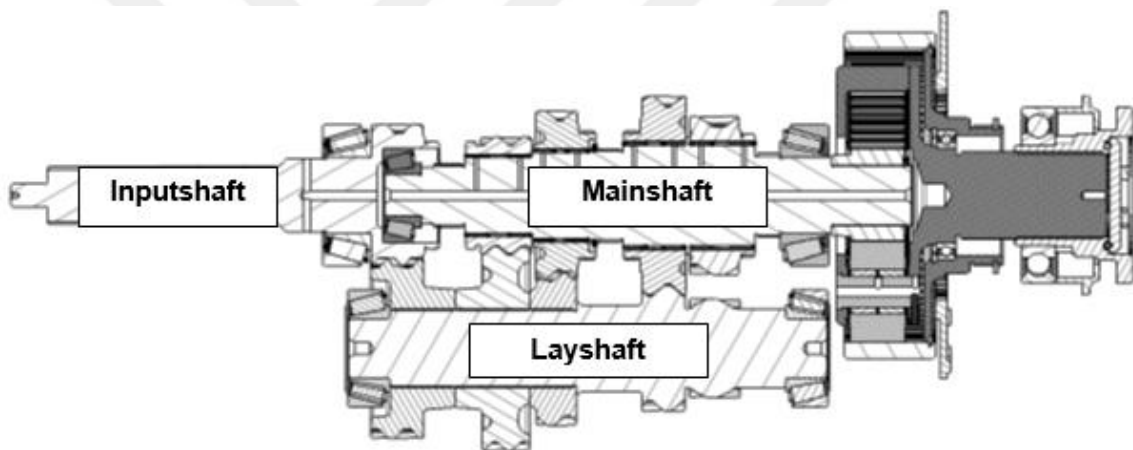


Figure 5.1 Section view of 8+1 MT gear train (courtesy of the company)

The design intended shaft is within the transmission casing and completely in oil sump while the vehicle is not moving and again in motion it is subjected to oil splash. This means corrosion phenomena is not the consideration for the material of the component. Another important parameter is the component will be assembled in a ground vehicle so the weight is a major parameter to be considered in comparison with the strength of candidate material. The material must be ductile to endure the unbalanced and time varying loading conditions, on the other hand it must be surface hardened to allow gear contact and commonly available material. Therefore our common area of interest is focused on alloyed steels.

The second criteria is engine output and transmission input torque is 1250 Nm. It is simply calculated to obtain maximum torque transmitted through the layshaft with Equation 5.1. Calculation reveals the maximum torque which is the layshaft is going to experience is 1613 Nm. (Efficiency counted as one)

Torque calculation on layshaft:

$$M_{lay} = i_1 \times M_{inp} \times \eta \quad \text{Equation 5.1}$$

Continuing to the durability concern, the shaft includes reverse and first gears as one piece, and to accommodate the other gears the rest of the shaft, machined to obtain all the way splined geometry for the first design alternative which is heavily subjected to machining operation. The investigated second layshaft design is going to be produced without splines.

Strength for shaft material selection is not major parameter when considering the deflection but the stiffness of material is important. Since steel is the major shaft material and the modulus of elasticity is almost same for all the steel materials, rigidity of shaft is mainly controlled by shaft's geometric decision instead of material selection. On the other hand in order to resist the loading stresses, necessary strength bring us to material selection and heat treatment. (Budynas, 2006)

The last criteria but the most important one is selecting the economical and commonly available workpiece as raw material.

We conducted our design process for the three different candidate material from BS ISO 10084 case hardening steel family. It will be the design choice determining which material is optimal to be used as shaft material.

- Case hardening steel grade 1.7147 (20MnCr5)
- Case hardening steel grade 1.6523 (20NiCrMo2-2)
- Case hardening steel grade 1.6587 (18CrNiMo7-6)

The first material is commonly available case hardening steel alloy grade of 1.7147 and widely used raw material in production of shafts and gears. Its DIN-ISO norm equivalent is 20MnCr5 and the internationally agreed material composition is provided in Table 5.1.

Table 5.1 Composition of steel grade 1.7147 (20MnCr5)

<b>Chemical composition % of grade 20MnCr5 (1.7147): EN 10084-2008</b>								
C	Si	Mn	Ni	P	S	Cr	Mo	B
0.17	max	1.10	-	max	max	1.00	-	-
-	0.40	-	-	0.025	0.035	-	-	-
0.22		1.40				1.30		

Table 5.2 Composition of steel grade 1.6523 (20NiCrMo2-2)

<b>Chemical composition % of grade 20NiCrMo2-2 (1.6523): EN 10084-2008</b>								
C	Si	Mn	Ni	P	S	Cr	Mo	B
0.17	max	0.65	0.4	max	max	0.35	0.15	
-	0.40	-	-	0.025	0.035	-	-	
0.23		0.95	0.7			0.7	0.25	

Table 5.3 Composition of steel grade 1.6587 (18CrNiMo7-6)

<b>Chemical composition % of grade 18CrNiMo7-6 (1.6587): EN 10084-2008</b>								
C	Si	Mn	Ni	P	S	Cr	Mo	B
0.12	0.15	0.4	1.4	max	max	1.5	0.25	
-	-	-	-	0.035	0.035	-	-	
0.18	0.4	0.6	1.7			1.8	0.35	



## 5.1 Material Cost Analysis

Cost analysis of the layshaft is not depended only on material selection. The chip removal process time, manufacturing from solid bar or machining from pre shaped forged material are all affecting the cost of component. Material selection will have a small effect on total cost but still an area to be pursued. Another cost reduction is preferring interference fit connection instead splined connection which will consequently reduce the machining operation.

For the calculation of raw material cost, the local steel manufacturer and supplier provided average investigated steel billet prices as in Table 5.4.

The layshaft is manufactured from  $\varnothing 110$  billets with 415 mm long and its weight is 31 kg and by 2019 planned transmission assembly number is 650. For only layshaft production 20,150 kg raw material is needed. The raw material cost for this component is indicated in Table 5.4.

Table 5.4 Material cost per ton (Asil Çelik San. & Tic. AŞ.)

Steel Grade	Cost Per Ton	Required Raw Material	Total Cost
18CrNiMo7-6	€ 1528	20,150 kg	€ 30,789.20
20MnCr5	€ 1183	20,150 kg	€ 23,837.45
20NiCrMo2-2	€ 1175	20,150 kg	€ 23,676.25

The calculation shows no significant difference between materials 20MnCr5 and 20NiCrMo2-2. However selection of 18CrNiMo7-6 brings %30 more cost instead of choosing other two of the materials.

Other cost aspect is chip removal for splines on the shaft, eliminating this operation by preferring interference connection helps to lessen manufacturing cost of both shaft and the other three gears. For this type connection only turning and grinding operation will be enough to obtain connection face.

## 6 Experimental Investigation

The deficiency of the testing apparatus in the company, tests were conducted in ITU's material laboratory and MATIL AS, independently from the company. Available metal testing devices within the company are listed in Table 6.1.

Experimental investigation was performed only on material basis. Rotating bending fatigue testing was performed in order to simulate the working condition that the intended component experience.

The determined material grades 1.7147, 1.6523 and 1.6587 for shaft design were tested under rotating bending fatigue testing to obtain their Wohler Curves and to have an idea of their comparative behaviour. The extracted S-N date also utilized for the numerical investigation and safety calculations.

Table 6.1 Available testing equipment in the company

Apparatus	Brand-Model-Year	Meas. Range
Universal Tensile & Compression Test	SCHENCK TREBEL Upm 400 1981	max 400 kN
Brinell Hardness Meas. Device max. 3000 kg	WOLPERT DIA TESTOR 3b5 1980	max.3000 kg
Rockwell Hardness Meas. Device	WOLPERT HT-2000 1980	30-60-100-150 kg
Rockwell Superficial Hardness Meas. Device	WOLPERT HT-2002 1980	15-30-45 kg
Vickers Hardness Meas. Device	KARL FRANK Fino test 1984	10 ÷ 10000 gr
Spectrometer	MAGELLAN/BRUKER Q8	-

Due to the busy schedule of the rotating bending testing equipment in ITU, 8 specimens for each material group, in total 24 test specimens were tested.

### 6.1 Chemical Metallurgy

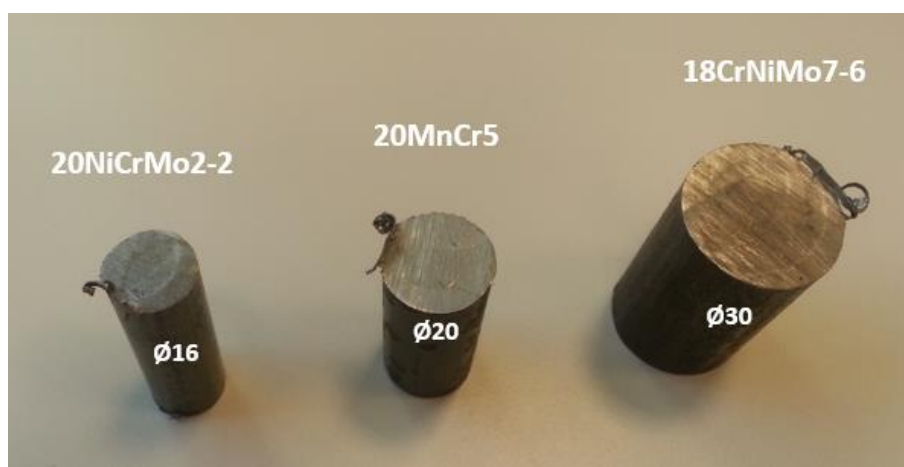


Figure 6.1 Material samples for chemical metallurgy

Layshaft and other gear components are manufactured by Limoz Makina located in Istanbul. Three different raw materials were provided by the company from their steel supplier. Small pieces from each material were cut off and prepared for chemical spectroscopy testing.

Table 6.2 Provided chemical compositions by manufacturer

<b>Provided Chemical composition of 18CrNiMo7-6 Material by Manufacturer</b>									
C	Si	Mn	Ni	P	S	Cr	Mo	Al	Cu
0.17	0.27	0.55	1.45	0.007	0.017	1.65	0.28	0.023	0.17
<b>Provided Chemical composition of 20MnCr5 Material by Manufacturer</b>									
0.20	0.24	1.30	-	0.007	0.010	1.20	-	-	-
<b>Provided Chemical composition of 20NiCrMo2-2 Material by Manufacturer</b>									
0.18	0.21	0.75	0.55	0.007	0.008	0.55	0.20	-	-

The chemical analysis machine Bruker Q8 Magellan is designated as OES “*Optical Emission Spectrometer*”. This instrument is capable to identify iron & steel alloys, Aluminium, Nickel, Magnesium, Tin, Lead, Titanium, Copper, Oxygen and Cobalt elements and their traces.

This method is destructive testing and leaves burn mark on the surface. The arc spark discharge emitted by testing probe to the testing material. Probe spotted location on the material vaporizes and the atoms in this vapour start emitting radiation which is captured by OES. Each atomic elements has their distinct wavelengths and this allow the testing equipment’s software to identify the material content.

Table 6.3 Obtained chemical compositions by spectroscopy

<b>Obtained Chemical composition of 18CrNiMo7-6 Material by company</b>									
C	Si	Mn	Ni	P	S	Cr	Mo	Cu	Fe
0.175	0.267	0.561	1.494	0.006	0.003	1.644	0.289	0.141	95.35
<b>Obtained Chemical composition of 20MnCr5 Material by company</b>									
0.179	0.088	1.301	0.029	0.014	0.027	1.074	0.048	0.002	97.17
<b>Obtained Chemical composition of 20NiCrMo2-2 Material by company</b>									
0.209	0.229	0.866	0.518	0.014	0.023	0.571	0.198	0.253	97.04

This testing device is mostly utilized internal quality control department for incoming material testing.

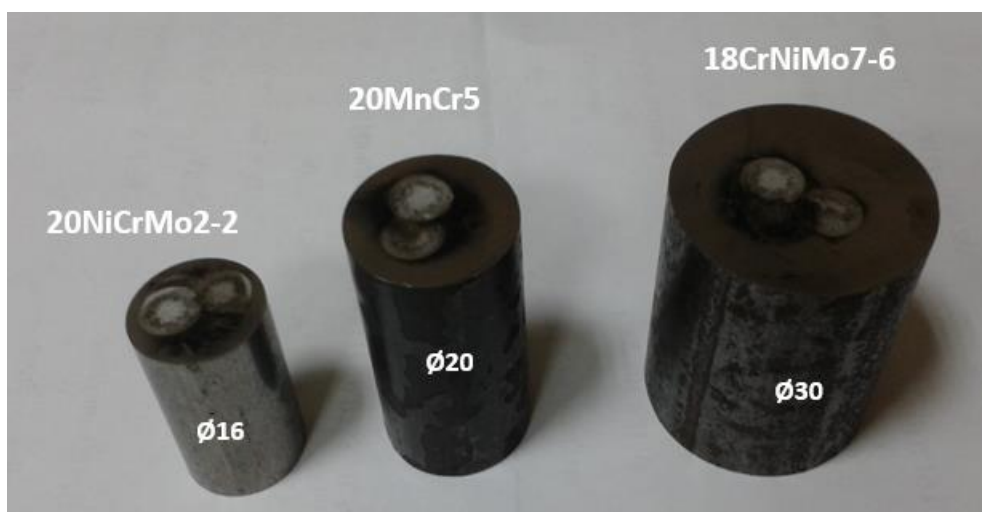


Figure 6.2 Samples after chemical analysis

## 6.2 Tensile Test

The raw materials to prepare test specimens from 18CrNiMo7-6, 20NiCrMo2-2 and 20MnCr5 are supplied by the shaft manufacturer. Geometry of the tensile specimen is defined by considering the available tensile test machine, BS EN ISO 6892-1-2016 and DIN 50125 standards. According to the DIN standard, A type circular cross section which has 6mm diameter and min 30 mm effective gauge length with smooth cylindrical ends workpiece was decided for testing.

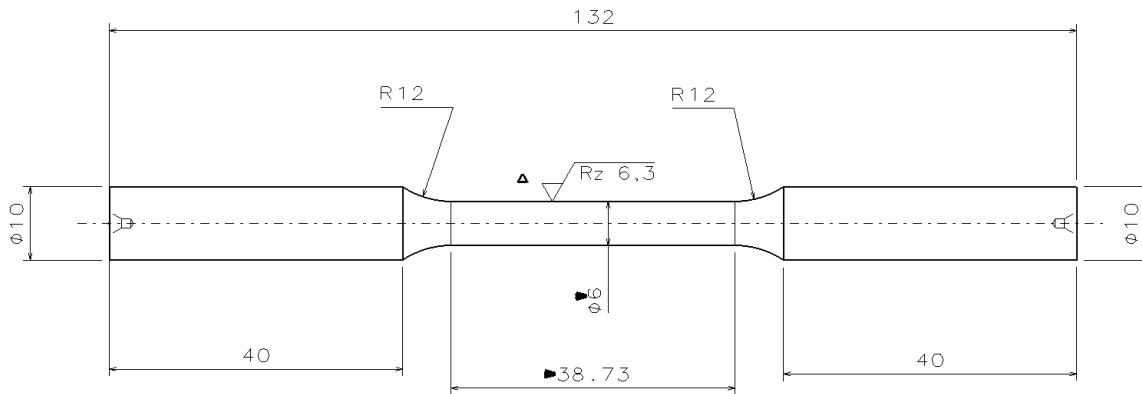


Figure 6.3 Tensile test piece "A 6 × 30" per DIN EN ISO 6892-1

Tensile testing was performed in MATIL AS which is a private company specialized in steel material testing. Tensile testing specimens are prepared adhering to the standards DIN 50125 & DIN EN ISO 6892-1 which are shown in Figure 6.3 and Figure 6.6. For each material group 6 tensile test specimens in total 18 specimens were prepared. For each material group 4 specimens with heat treatment and 2 without heat treatment. Both material condition were tested to have idea of treatment effect and the raw material characteristic. Heat treatment is carburization with 1.2 mm case hardening depth to represent the real component designed for the transmission. After case hardening, tempering process takes place to convert retained austenite on the surface to martensite and helps to increase core toughness.

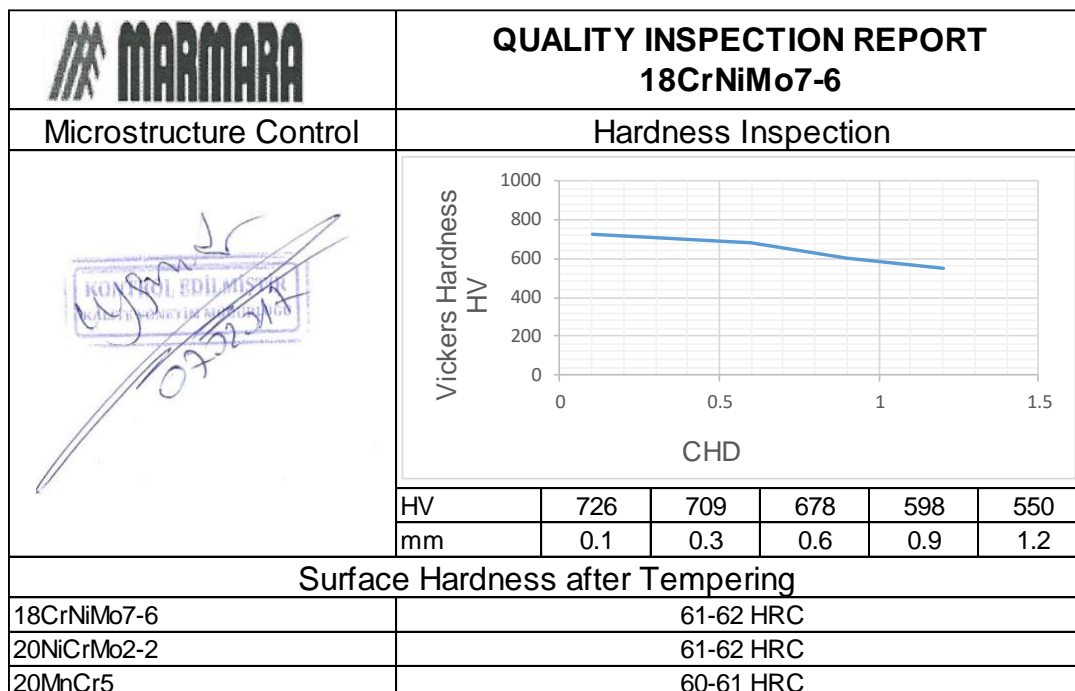


Figure 6.4 Hardness scan inspection report for test specimens

All three type specimens were heat treated in the same company named *Marmara Isil İşlem San.* with the same heat treatment parameters that were defined for layshaft component of transmission. In Figure 6.4 the hardenability and the surface hardness values for specimens were provided by the heat treatment company.

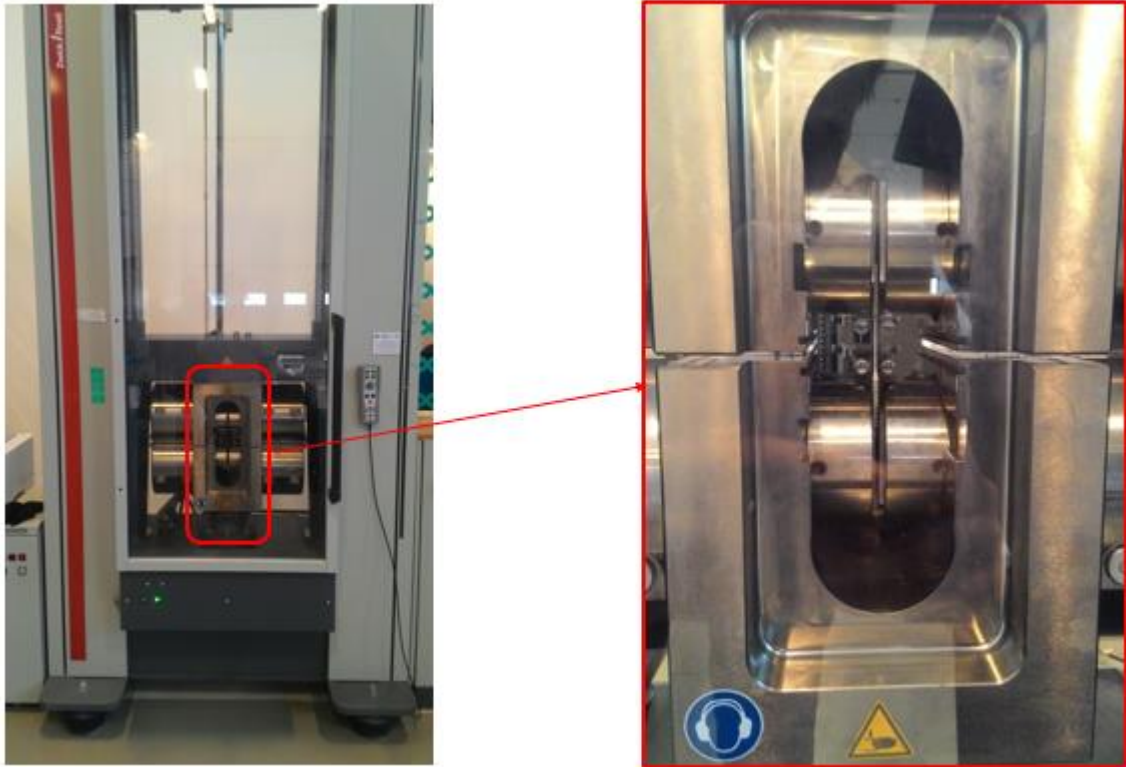


Figure 6.5 Zwick/Roell Z600 600kN tensile test machine with clamped specimen

Figure 6.5 shows the utilized testing machine which is capable of applying up to 600kN tensile force and hydraulic controlled specimen clamping.



Figure 6.6 Manufactured tensile test specimens

12 of case hardened tensile test specimens, 4 from 3 different materials group, test results are tabulated in Table 6.4. In the light of test results we could say that 18CrNiMo7-6 with 1.2 CHD has the highest tensile strength (~1475 MPa average) with reasonable yield (~1180 MPa average). In contrast 20MnCr5 and 20NiCrMo2-2 showed relatively equal tensile strength (~1245 MPa average) and different yield strength as follows, ~1160 MPa for 20MnCr5 and 1233 MPa for 20NiCrMo2-2). The close tensile and yield strengths for 20MnCr5 and 20NiCrMo2-2 shows the fracture almost brittle due to the high case hardening depth value by specimen gauge diameter.

Table 6.4 Heat treated carburized (CHD:1.2 mm) test results

No.	Specimen ID	R <sub>10.5</sub> Mpa	d <sub>0</sub> mm	S <sub>0</sub> mm <sup>2</sup>	R <sub>p0.2</sub> Yield MPa	R <sub>m</sub> Mpa	A <sub>30</sub> %
1	18CrNiMo7-6	952	6.01	28.37	1192.74	1483	0.8
2	18CrNiMo7-6	948	5.95	27.81	1162.98	1455	0.8
3	18CrNiMo7-6	943	5.98	28.09	1177.65	1459	0.8
4	18CrNiMo7-6	956	6.03	28.56	1185.39	1509	0.8
1	20NiCrMo2-2	978	6.02	28.46	1242.37	1249	0.2
2	20NiCrMo2-2	991	5.98	28.09	1218.59	1240	0.2
3	20NiCrMo2-2	986	5.98	28.09	1223.64	1247	0.2
4	20NiCrMo2-2	973	5.97	27.99	1249.47	1253	0.2
1	20MnCr5	978	5.99	28.18	1176.74	1280	0.3
2	20MnCr5	922	5.97	27.99	1157.37	1210	0.3
3	20MnCr5	947	6.02	28.46	1171.19	1241	0.3
4	20MnCr5	954	5.97	27.99	1133.35	1257	0.3

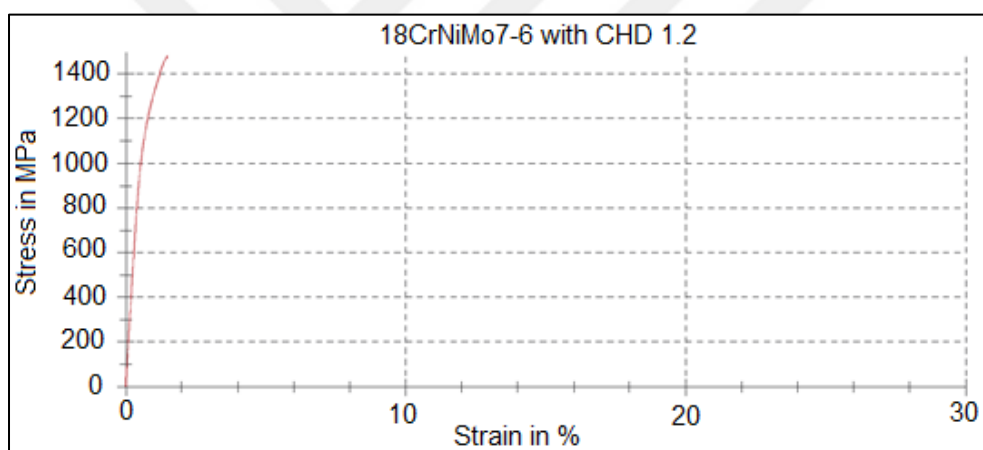


Figure 6.7 Tensile test graph of case hardened 18CrNiMo7-6

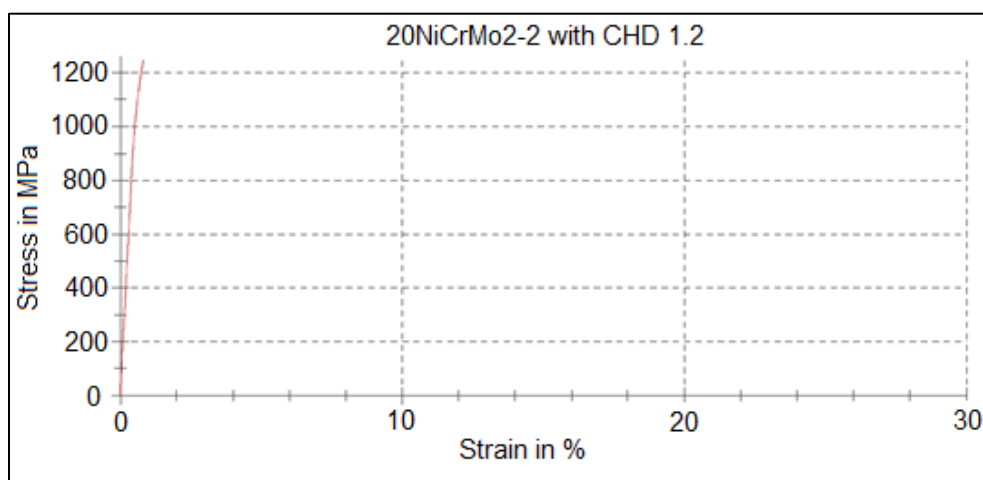


Figure 6.8 Tensile test graph of case hardened 20NiCrMo2-2



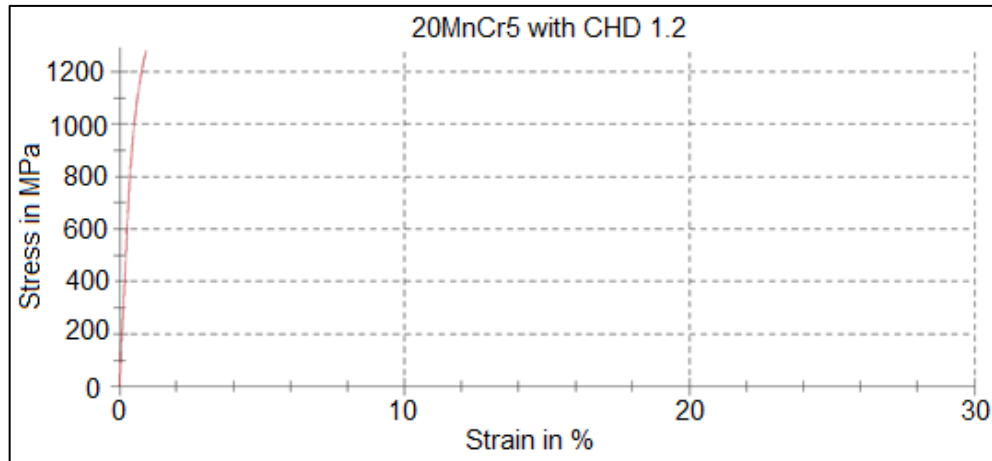


Figure 6.9 Tensile test graph of case hardened 20MnCr5

In order to have idea of the material characteristic of these three materials, some specimens preserved without heat treatment. 2 sets of each material group tested with tensile test to see raw material behaviour. See Table 6.5 for tabulated tensile test results.

Table 6.5 Test specimens without heat treatment

No.	Specimen ID	R <sub>t0.5</sub> Mpa	d <sub>0</sub> mm	S <sub>0</sub> mm <sup>2</sup>	R <sub>p0.2</sub> Yield MPa	R <sub>m</sub> Mpa	A <sub>30</sub> %
1	18CrNiMo7-6	610	5.98	28.09	609.58	725	17.9
2	18CrNiMo7-6	618	6.02	28.46	624.69	732	17.9
1	20NiCrMo2-2	662	5.97	27.99	748.07	816	6.5
2	20NiCrMo2-2	673	5.98	28.09	768.52	837	6.6
1	20MnCr5	474	6.03	28.56	516.41	734	16.7
2	20MnCr5	510	5.97	27.99	557.64	728	16.5

As raw ultimate tensile strength of 18CrNiMo7-6 and 20MnCr5 is almost identical around 730 MPa, 20NiCrMo2-2 has the highest tensile strength around which is around 825 MPa. Yield points for 20NiCrMo2-2, 20MnCr5 and 18CrNiMo7-6 are around 758 MPa, 537 MPa, and 615 MPa respectively. 18CrNiMo7-6 and 20MnCr5 shows the highest elongation before fracture the toughness is high. In contrast 20NiMo2-2 represents half of the elongation of other materials. See Figure 6.13 for comparative tensile test results of both case hardened and raw materials without case hardening.

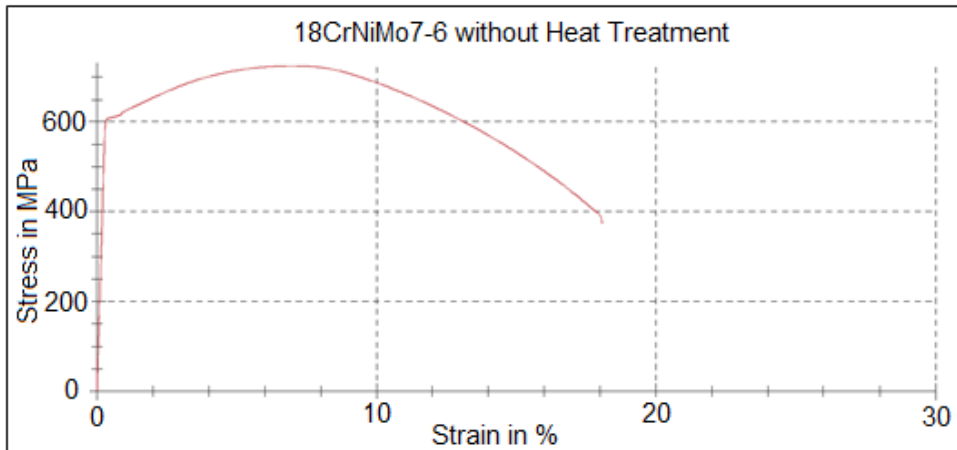


Figure 6.10 Tensile test graph of 18CrNiMo7-6 without CH

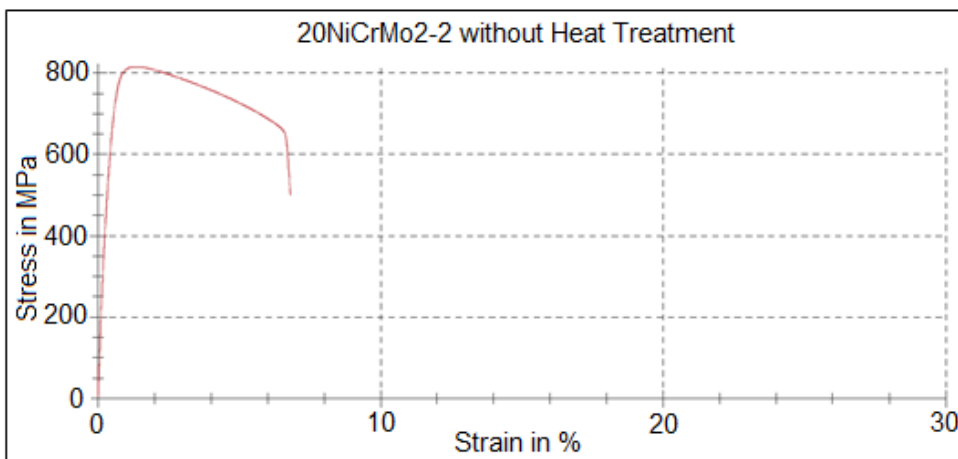


Figure 6.11 Tensile test graph of 20NiCrMo2-2 without CH

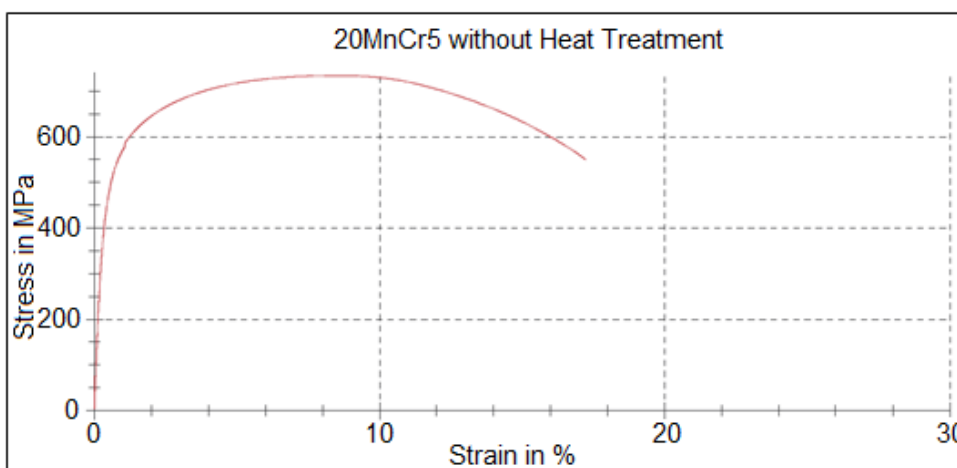


Figure 6.12 Tensile test graph of 20MnCr5 without CH



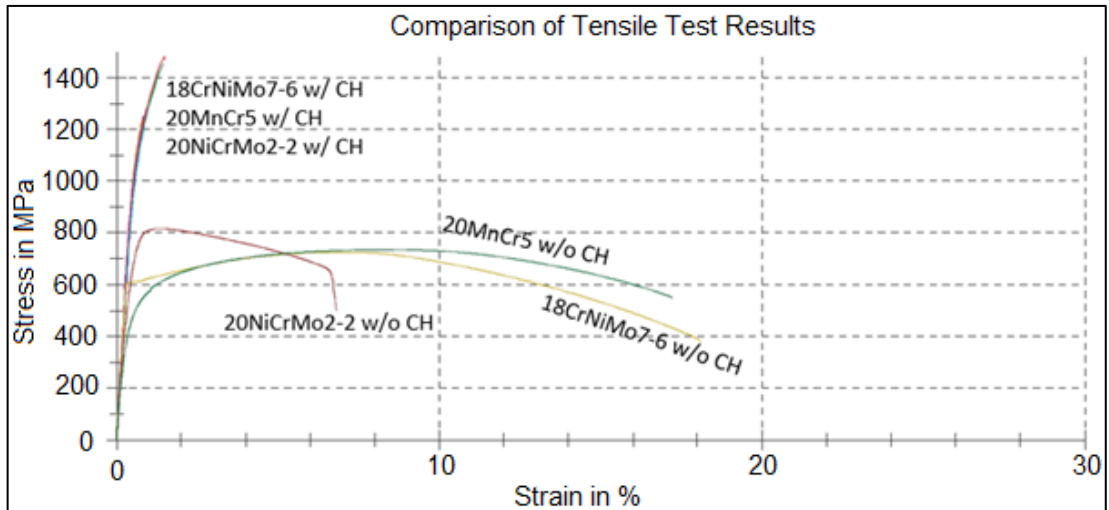


Figure 6.13 All test results are superimposed on one graph



Figure 6.14 Tensile specimens, left to right 18CrNiMo7-6, 20MnCr5, 20NiCrMo2-2



Figure 6.15 Fracture surface left to right 18CrNiMo7-6, 20MnCr5, 20NiCrMo2-2

### 6.3 Rotating Bending Fatigue Testing

Material fatigue testing was performed in ITU Metallurgical and Materials Engineering Department. Layshaft operates under torsion and bending loadings, therefore testing the specimens with this type of fatigue testing machines is optimal for data extraction. Since there is only rotating bending fatigue testing machine available in the laboratory, four point rotating bending test machine was used to test the prepared heat treated specimens.

The test equipment is Walter + Bai 5-200 Nm rotating bending machine see Figure 6.16. There is alternating tension-compression stress occur each time after  $180^\circ$  rotation on the surface of the test specimen. In other words completely reversal stress created on the surface. The stress ratio is -1.

Machine stops the test after breakage of the tested specimen and from a digital indicator located on the control panel, failure cycle can be observed. Or in the case of insufficient loading, the testing machine can be set to stop after certain cycles completed. In our case, we programmed the machine to 7 million cycles, which means if the specimen endures more than this cycle, the machine stops the test.



Figure 6.16 RB Fatigue test bench Walter+Bai AG UBM 5-200 Nm

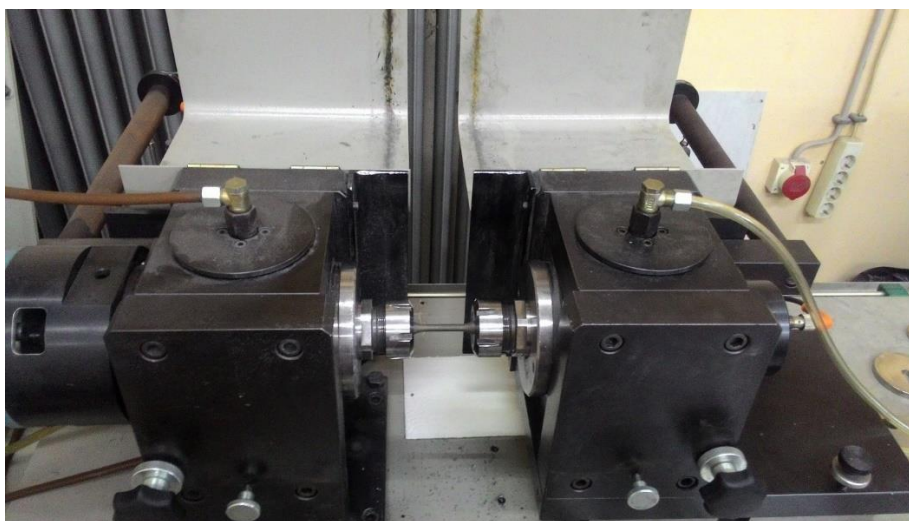


Figure 6.17 A clamped specimen for RB fatigue testing

Test specimen clamped from both ends with  $\varnothing 12$  mm collet clamping. Though, the fatigue testing is performed at 23 °C ambient temperature this machine also allows fatigue testing in elevated temperature. In order to avoid worming up the tested specimen test frequency was set to 50 Hz.

The applied stress is controlled by adding or subtracting weights. There are weight hangers behind of the testing machine on both sides. This structure provides bending stress control over the test see Figure 6.18.



Figure 6.18 Interchangeable weights to create constant bending stress

The weights are metal plates with diverse size and with the help of moment arm Figure 6.19 adequate bending moment could be created over the tested specimen's cross section.

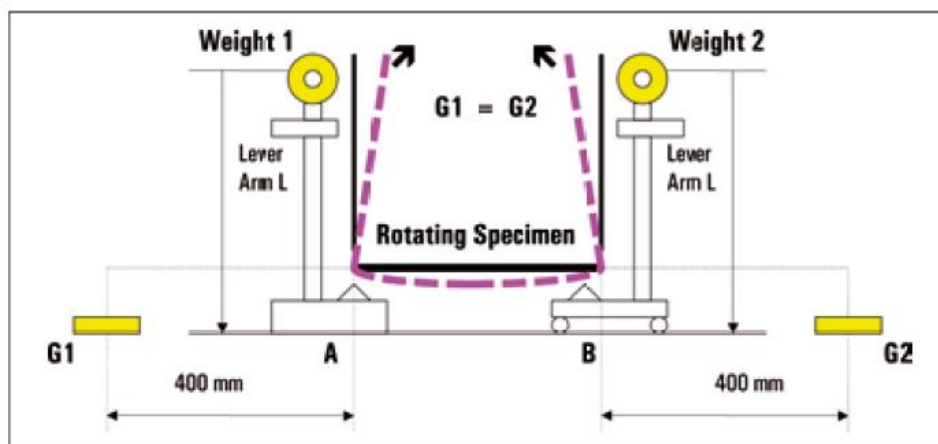


Figure 6.19 Moment arms 400 mm for creating bending moment on specimen

Figure 6.20 shows the designed rotating bending fatigue testing specimen's manufacturing drawing. The values are obtained from the standards. The raw material was in  $\varnothing 18$  mm for 20NiCrMo2-2,  $\varnothing 20$  mm for 20MnCr5 and  $\varnothing 30$  mm for 18CrNiMo7-6. Materials removed to  $\varnothing 12$  mm in clamp and  $\varnothing 6$  mm on the gauge diameter. After machining, specimens are grinded to have smooth surface quality. Specimens are case hardened with 1.2 mm CHD on the surface.

In order to increase the core toughness and eliminate austenite on the surface, tempering process was applied, after case hardening.

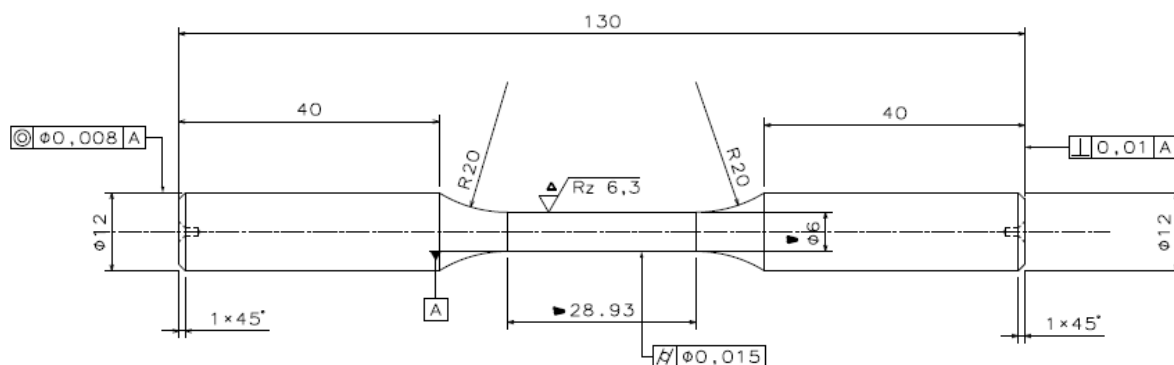


Figure 6.20 Rotating bending fatigue testing sample per (BS ISO 1143:, 2010)



Figure 6.21 Specimens for each material group before heat treatment

Each material group specimens were tested with 50 Hz test setup in the ambient temperature. Test result cycles with respect to applied constant bending moments are tabulated for 20NiCrMo2-2 in Table 6.6, for 20MnCr5 in Table 6.7 and for 18CrNiMo7-6 in Table 6.8. Due to the limited rotating bending specimen and time restriction complete SN curve couldn't be obtained from test, however the results could give us an idea of which material performs better under cyclic load. Besides each material group's RBF result provides approximate endurance limits of the material. For example the average endurance limit of 555MPa for material 20NiCrMo2-2 could be estimated and for materials 18CrNiMo7-6 and 20MnCr5 approximated values for endurance are 780 MPa and 700 MPa respectively.

While performing the RB tests the stop cycle limit is set to 5 million average for material groups 20MnCr5 and 18CrNiMo7-6 this goal is achieved before interrupting the test machine for unbroken specimens. However for the material group 20NiCrMo2-2 the limiting cycle couldn't be achieved due to the busy schedule of the University. Nonetheless, over one million cycle were allowed for the low stressed specimens to run.

Table 6.6 Rotating bending test results for 20NiCrMo2-2 at 50 Hz

Material 20NiCrMo2-2 @ 50 Hz					
No	Load (N)	Bending Moment (Nm)	Max Stress (Mpa)	Cycle	Comment
1	22	11	519	2126708	Not broken
2	25	12.5	589	1111765	Not broken
3	25.5	12.75	601	60629	Broken
4	26	13	613	15279	Broken
5	26	13	613	54723	Broken
6	27	13.5	637	23645	Broken
7	27	13.5	637	36208	Broken
8	30	15	707	26893	Broken

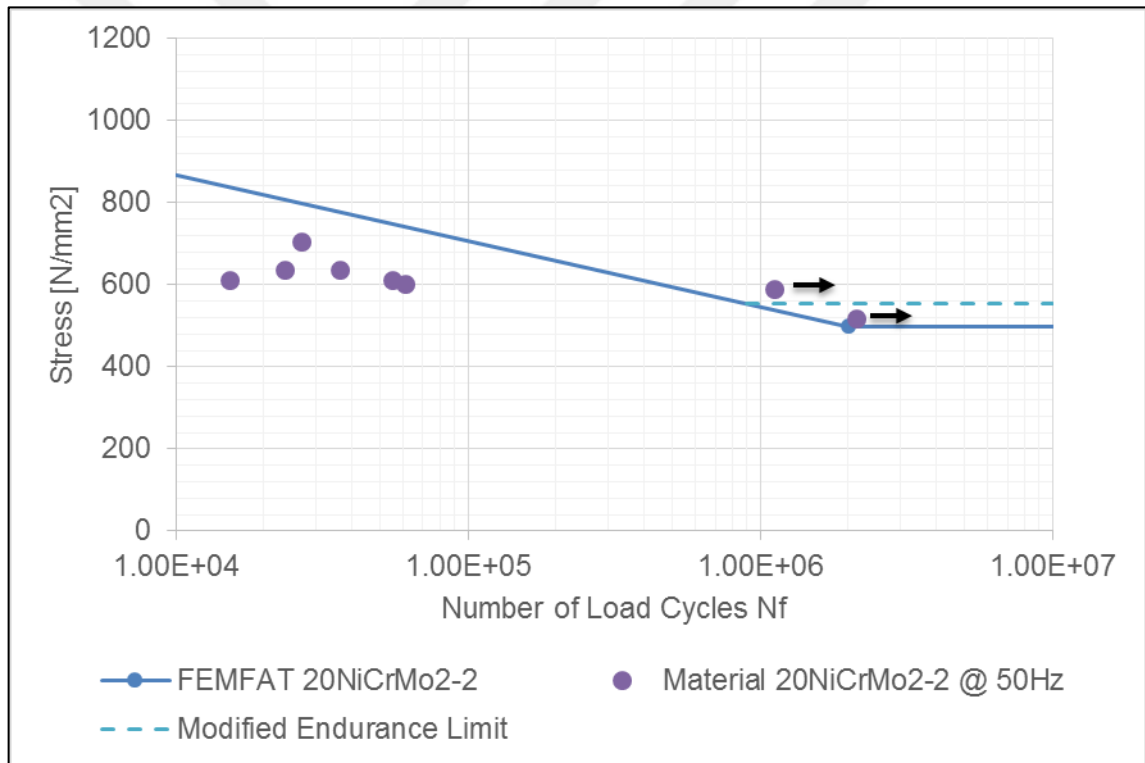


Figure 6.22 20NiCrMo2-2 RB test results with endurance vs. FEMFAT



Table 6.7 Rotating bending test results for 20MnCr5 at 50 Hz

Material 20MnCr5 @ 50Hz					
No	Load (N)	Bending Moment (Nm)	Max Stress (Mpa)	Cycle	Comment
1	26	13	613	2747641	Broken
2	27	13.5	637	5009576	Not broken
3	29	14.5	684	5224868	Not broken
4	32	16	755	7017171	Not broken
5	32.5	16.25	767	7487275	Not broken
6	33	16.5	778	33205	Broken
7	33	16.5	778	28309	Broken
8	35	17.5	825	28627	Broken
9	35	17.5	825	16051	Broken

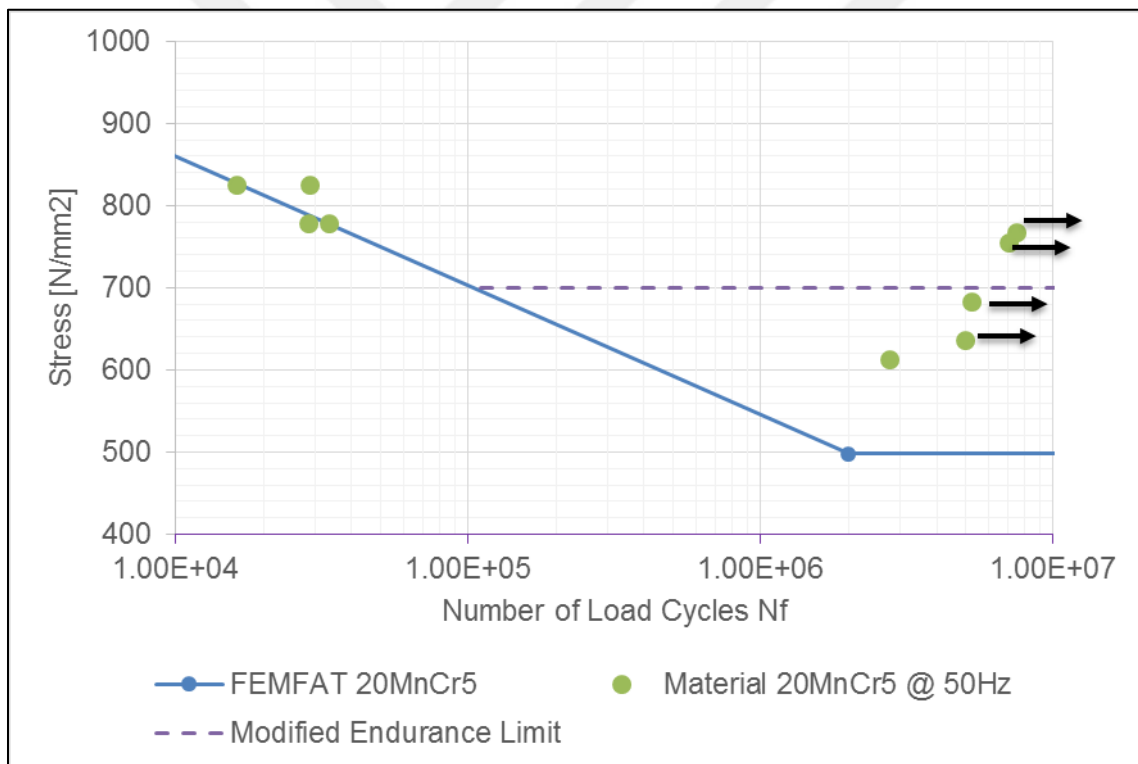


Figure 6.23 20MnCr5 RB test results with endurance vs. FEMFAT

Table 6.8 Rotating bending test results for 18CrNiMo7-6 at 50 Hz

Material 18CrNiMo7-6 @ 50 Hz					
No	Load (N)	Bending Moment (Nm)	Max Stress (Mpa)	Cycle	Comment
1	32	16	755	8264052	Not broken
2	33	16.5	778	8175490	Not broken
3	33.5	16.75	790	7138378	Not broken
4	34	17	802	27798	Broken
5	34	17	802	20608	Broken
6	35	17.5	825	25319	Broken
7	35	17.5	825	81067	Broken
8	38	19	896	66294	Broken

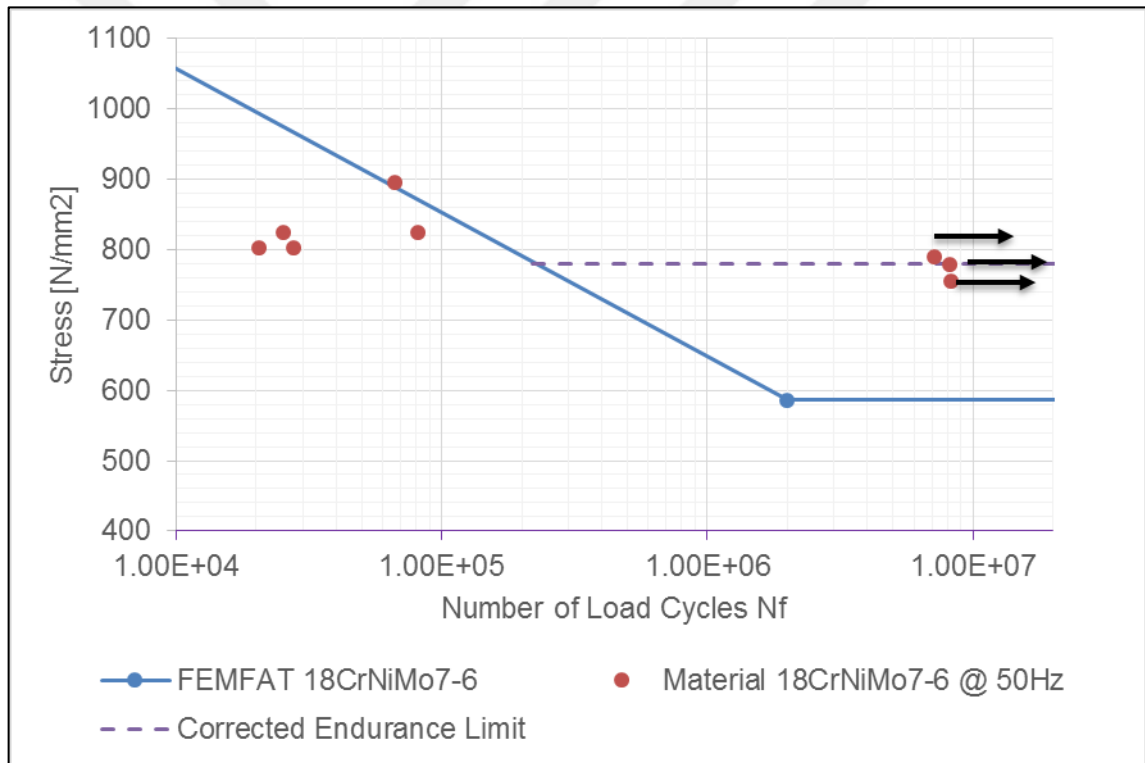


Figure 6.24 18CrNiMo7-6 RB test results with endurance vs. FEMFAT

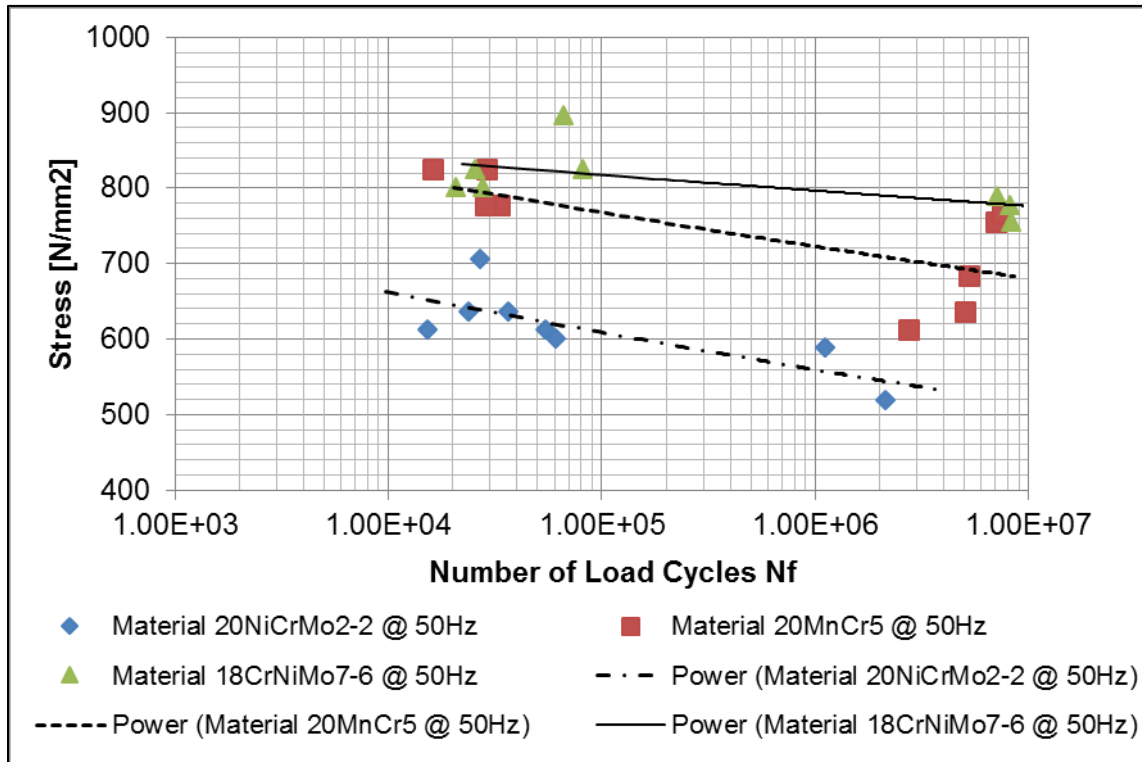


Figure 6.25 RB test result comparison between materials

In Figure 6.25, power lines drawn to represent fatigue vs cycle trend between materials. Green triangles represents 18CrNiMo7-6, red squares for 20MnCr5 and lastly blue diamonds for 20NiCrMo2-2. This figure shows, case hardened 18CrNiMo7-6 has the highest endurance than others and case hardened 20NiCrMo2-2 has the lowest endurance when compared.



## 7 Numerical Modelling

*Test can show what happens, analysis can show why.*

*To make a good decision you need both.*

*(Steven G. Rensinger, Experimental Techniques, 1988)*

### 7.1 Utilized Hardware Specification

The following computer configuration was utilized for the numerical computations.

- Dell Precision T7600 x64 based PC
- MS Windows 7 Professional
- Intel(R) Xeon(R) CPU E5-2687W @ 3.10GHz, 8 Cores, 16 Logical Cores
- 128GB RAM

### 7.2 Commercial Softwares for Analytical Calculation & FEA

There are huge variety of commercial softwares to conduct Finite Element Analysis. Prior to FEA, within the company almost every machine element calculations are performed by utilizing KissSys & KissSoft softwares. HyperWorks software from Altair and Abaqus software from Dassault Systems are already available under the company. Optistruct in Hyperworks and Abaqus Standard FEA solvers are quite enough to perform the stress analysis prior to any commercial fatigue package software. In our case FEMFAT as a post process fatigue investigation software is utilized. Each software in the market used to have some superiority over one another. However, this gap between softwares is almost disappeared owing to easy to access knowledge through current researches by the companies. Utilization of which software for FEA analysis is mostly determined by the companies which they already owns and it is required from a CAE engineer to have adequate knowledge on specific one.

### 7.3 Modelling of Rotating Bending Fatigue Test

First thing is checking mesh convergence. To do this standard RB Bar is meshed with 0,10 mm – 0,25 mm – 0,50 mm – 1 mm – 1,50 mm – 2 mm – 3 mm – 4 mm global mesh sizes in the gauge section.

See Figure 7.1 for mesh density and representation of mesh transition from gauge to clamping partition of the bar.

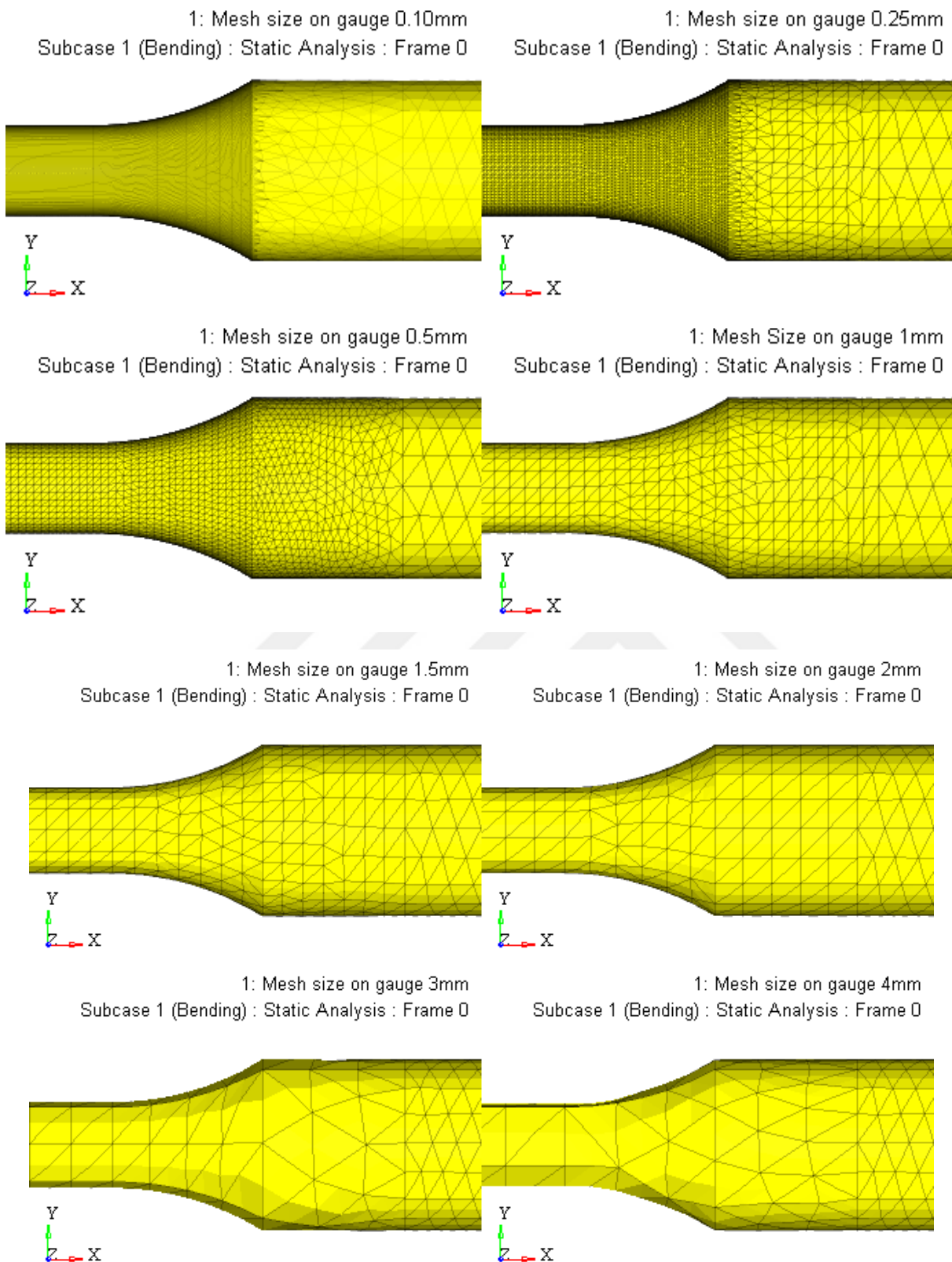


Figure 7.1 Mesh size comparison

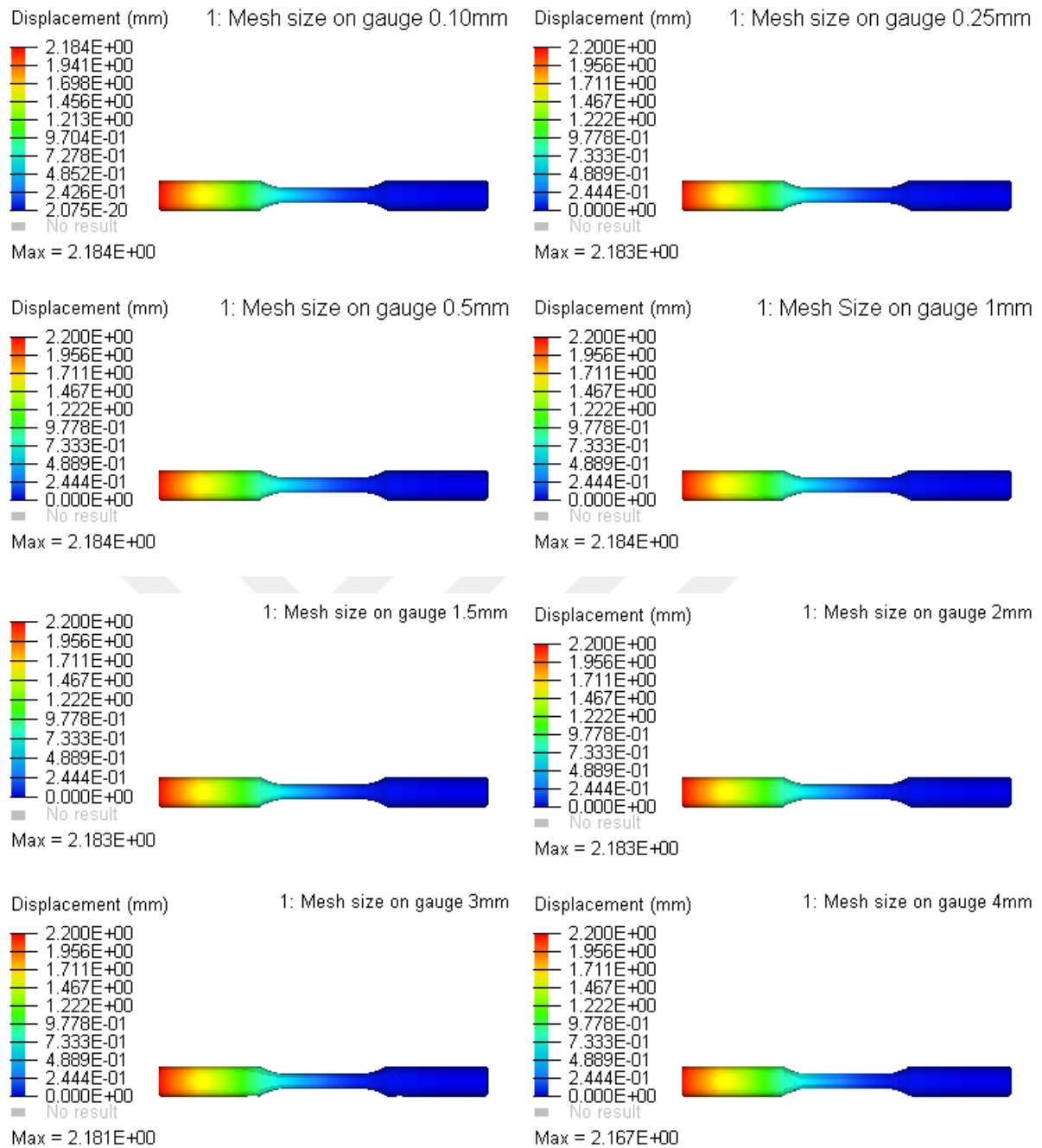


Figure 7.2 Displacement value comparison after 10Nm bending moment

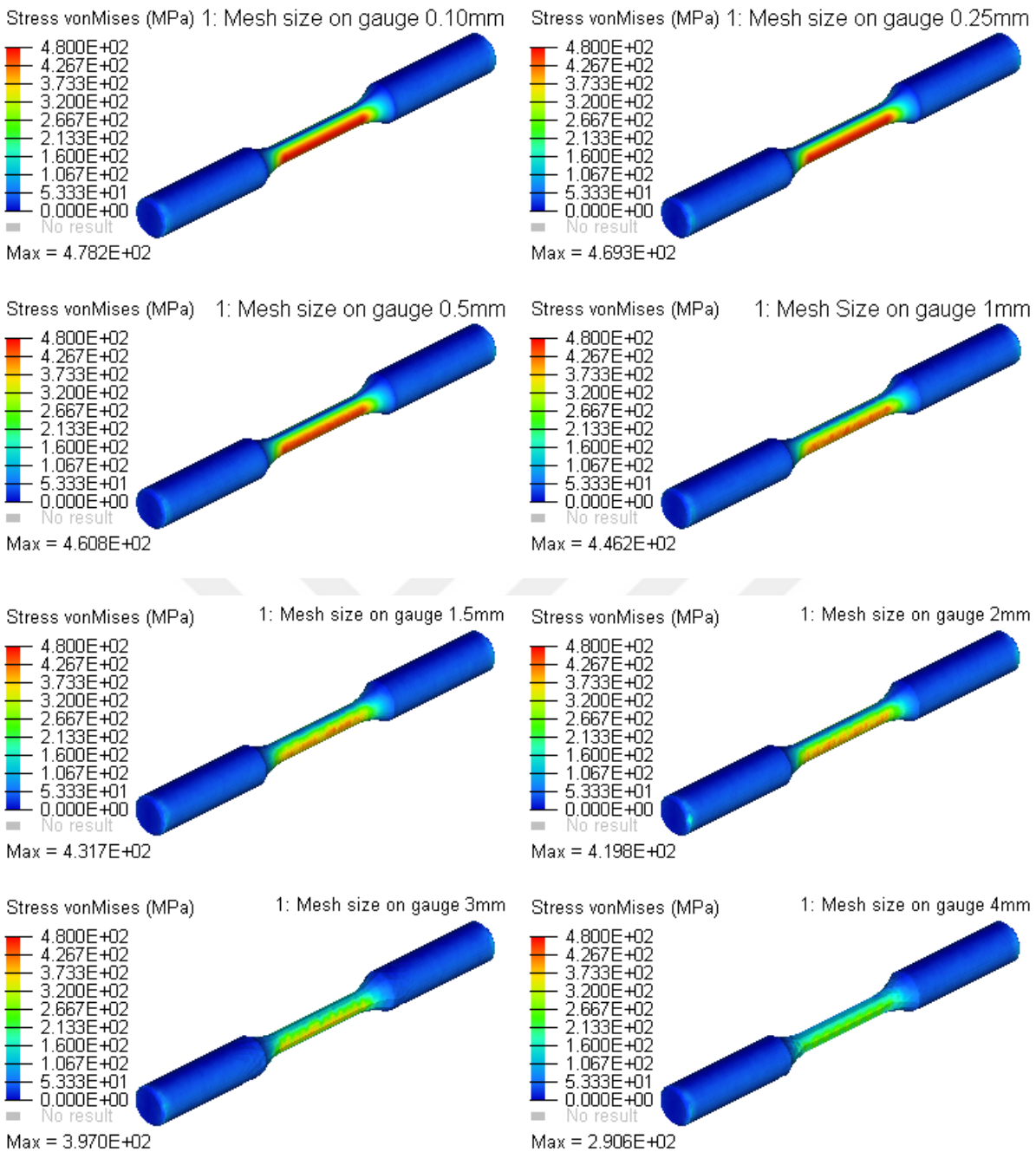


Figure 7.3 Equivalent stress comparison after 10 Nm bending moment

Table 7.1 Mesh information of RBF bar

Mesh size	0.1	0.25	0.5	1	1.5	2	3	4
Element type	tetra10	tetra10	tetra10	tetra10	tetra10	tetra10	tetra10	tetra10
Total element	687,806	227,633	68,848	18,343	14,689	13,350	11,892	5,588
Total run time (min)	20	5.5	1.5	1	1	1	1	1

After several runs of bending simulation with different mesh sizes under 10 Nm bending moment, It is easy to follow the convergence graph on Figure 7.4 It looks like displacement value is converged already. At first glance 0.25 mm mesh sized model is appropriate to use. In order

to evaluate the stress results. Analytical bending stress calculation is made under the section 7.3.1.

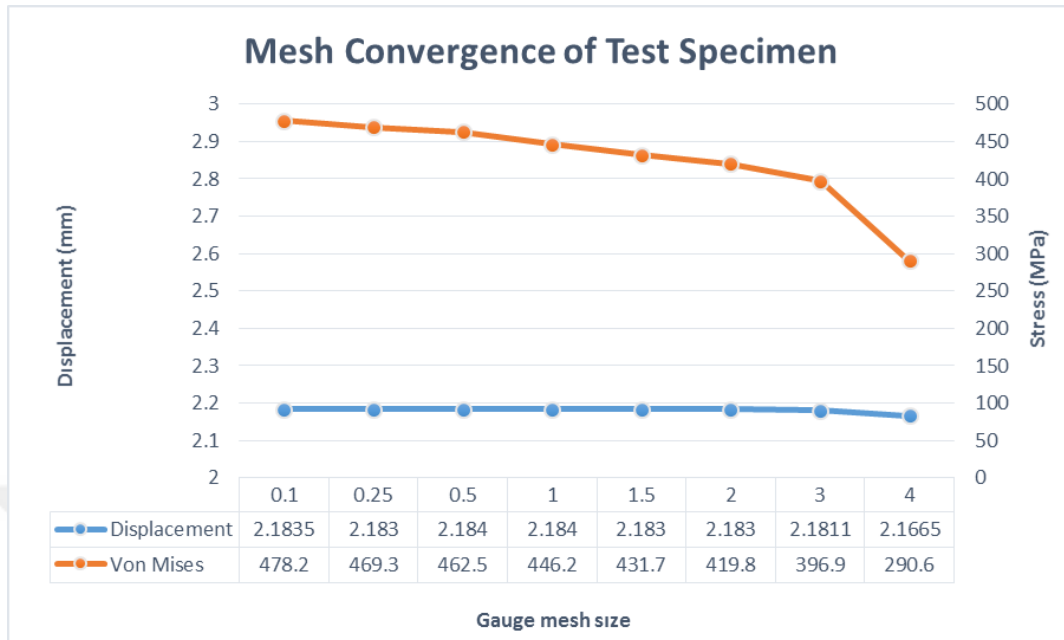


Figure 7.4 Mesh convergence on RB Bar

### 7.3.1 Analytical Calculation of Bending Stress

Bending caused stress on circular round bar calculated as in Equation 7.1.

$$\sigma_{max} = -\frac{M_y}{I} = \frac{32}{\pi d^3} M_y \quad \text{Equation 7.1}$$

$M_y$  is the bending moment and  $I$  is the second area moment about the  $z$  axis. (Budynas & Nisbett, 2011)

$$\sigma_{max} = -\frac{M_y}{I} = \frac{32}{\pi 6^3} 10000 Nmm = 471.8 MPa$$

The closest result to analytical calculation is the model with 0.25 mm mesh size, see Figure 7.3. The FEA obtained max bending stress 469.3 MPa and the analytical result is 471.8 MPa the error is. % 0.5 which is quite accurate result.

$$471.8 - 469.3 = 2.5 MPa$$

$$2.5/471.8 = 0.05 \rightarrow \%0.5 \text{ error}$$

### 7.3.2 FEA and FEMFAT Modelling of Rotating Bending Test

After mesh convergence analysis completed on the 3D rotating bending test specimen, it is decided to proceed with the model with the 0.25 mm mesh size on gauge. In the rotating bending test, component experiences fully reversed loading, in other words, a point on the surface experience the maximum bending stress as tension and after 180 degrees rotation the stress turns to be compression. This can be described as one cycle of the rotating bending test.

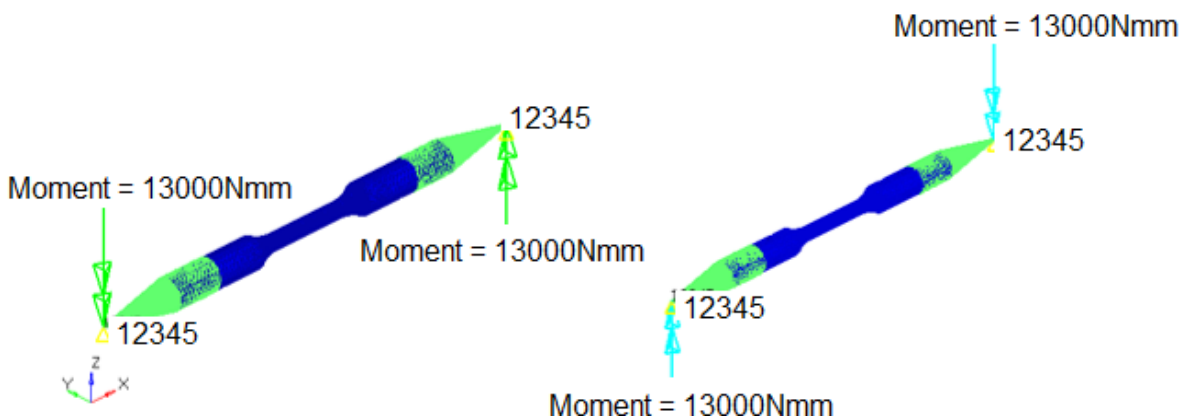


Figure 7.5 Left model: Load case 1, Right model: Load case 2

Two linear static analysis are constructed for both situations with the following FEA parameters.

- Young Modulus: 210 GPa
- Poisson's ratio: 0.3
- Density: 7.85 E-9 tonn/mm<sup>3</sup>
- Full isotropic material model
- 13000 Nmm Bending moment from both ends of the specimen
- Rigid kinematic couplings to represent clamping
- Restriction of clamp movement in x,y,z direction and x and y rotation to prevent rigid body motion. DOF is only allowed rotation in z direction.
- 227633 with 344972 nodes, 2<sup>nd</sup> order tetrahedral elements are used.

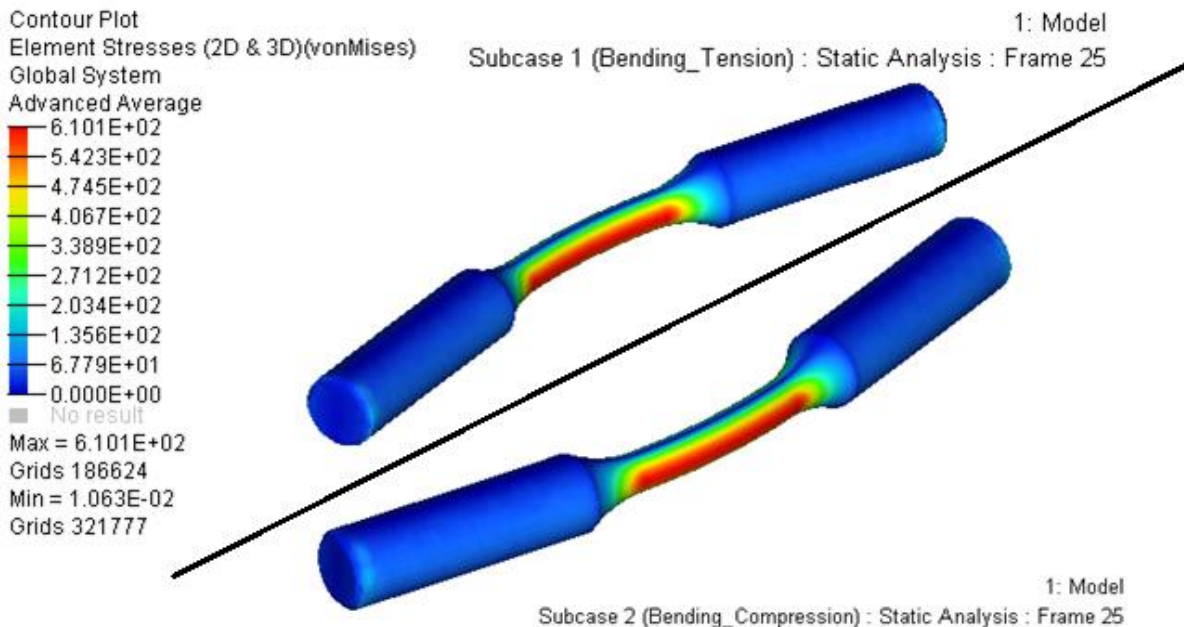


Figure 7.6 Linear static stress analysis results for reversed loading

13Nm bending moment causes 613 MPa maximum bending stress on Ø6 mm round RB fatigue bar. FEA result of the model gives quite approximate solution with 610.1 MPa maximum stress on the surface.

In the next step, these simulation results are used as input for post process FEMFAT fatigue software.

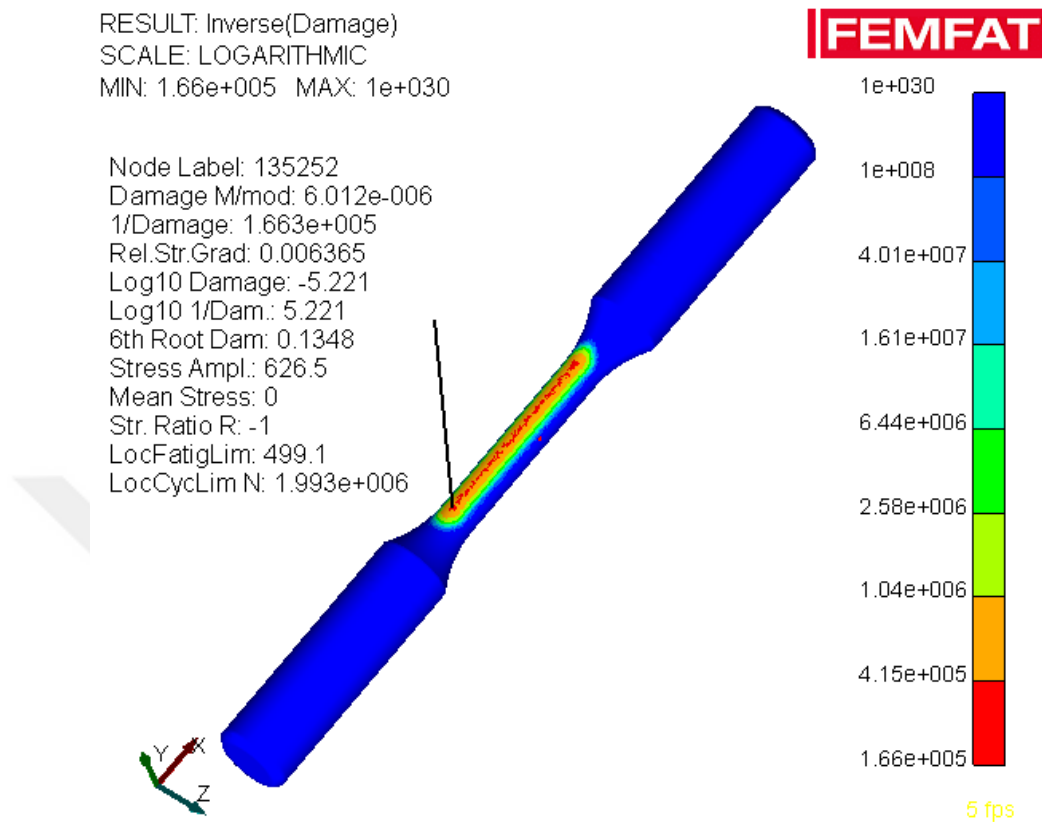


Figure 7.7 FEMFAT result of RBF specimen for 20NiCrMo2-2 material

The result of post fatigue simulation indicates, 13 Nm fully reversed bending moment leads the material to fail after 166300 cycles. When we put a dot for stress amplitude of 613 MPa and corresponding 166300 cycle, it will be obvious to see this point is on the S-N curve of the 20NiCrMo2-2 material Figure 7.8.

With the result of RBT post fatigue investigation, constructed approach and simulation model shows a good correlated approximation for fatigue life estimation. Since the simulation result is on the safe side of the S-N curve the result exhibits a small safety margin as well which is favorable for fatigue life estimation on product development prior to durability tests.



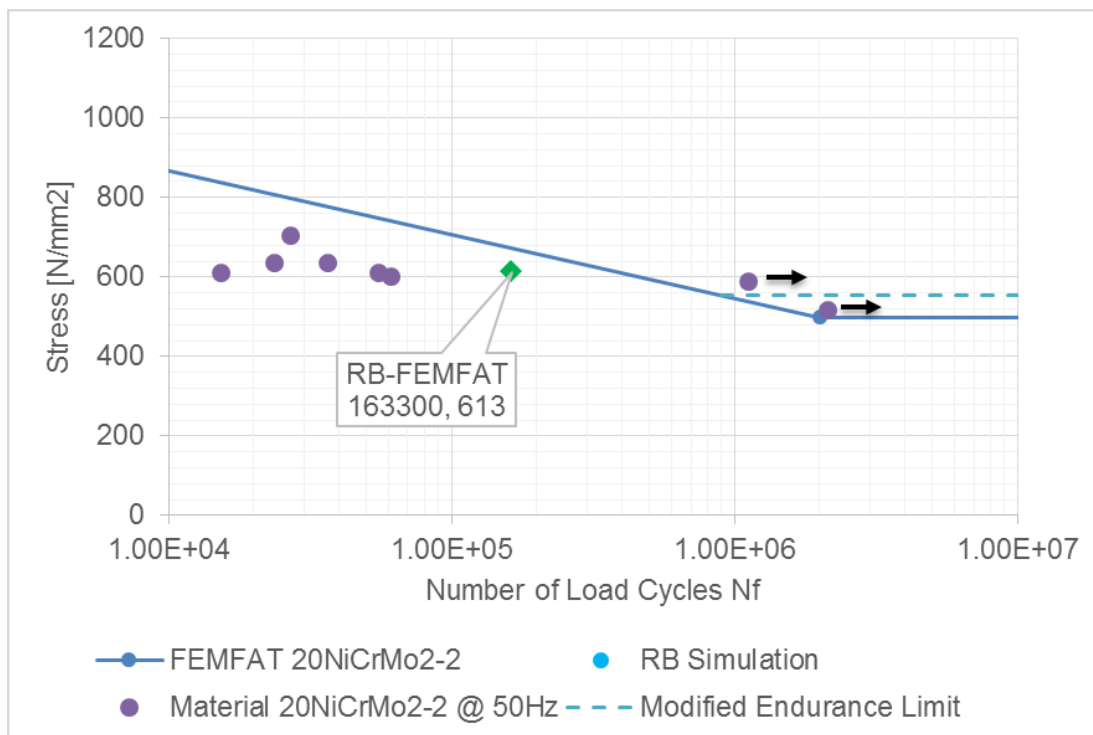


Figure 7.8 FEMFAT RBT with 13 Nm bending moment with 20NiCrMo2-2 SN

#### 7.4 FEA Model for Layshaft Stress Analysis

Both design approaches are modelled by finite element method. In order to make a reasonable comparison and to find out the better design alternative, the two layshaft models were meshed with the same element with approximately same average element size. The splined geometry have 3102864, CTETRA optistruct elements which is so called second order tetra element (tetrahedral) within optistruct solver. 3289092 second order tetra elements created on proposed IF layshaft. The general parameters for analysis as follows.

- Young Modulus: 210 GPa
- Poisson's ratio: 0.3
- Density: 7.85 E-9 ton/mm<sup>3</sup>
- Full isotropic material model
- Rigid kinematic couplings to represent bearings

Apart from the rotating bending FEA analysis, to correctly model of the shaft with gears, contact is defined between engaged components both for gear to gear mesh and for shaft with gears on it. Definition of contact makes the simulation nonlinear and more expensive due to required time allocation.

In mesh construction step, the general afford placed on radius and gear tooth portion of the shaft. These locations are meshed with average 1 mm mesh size and for the core portion of the shaft 4mm mesh size is preferred. Figure 7.9 and Figure 7.10 shows the generated mesh on splined and flat surface layshaft respectively.



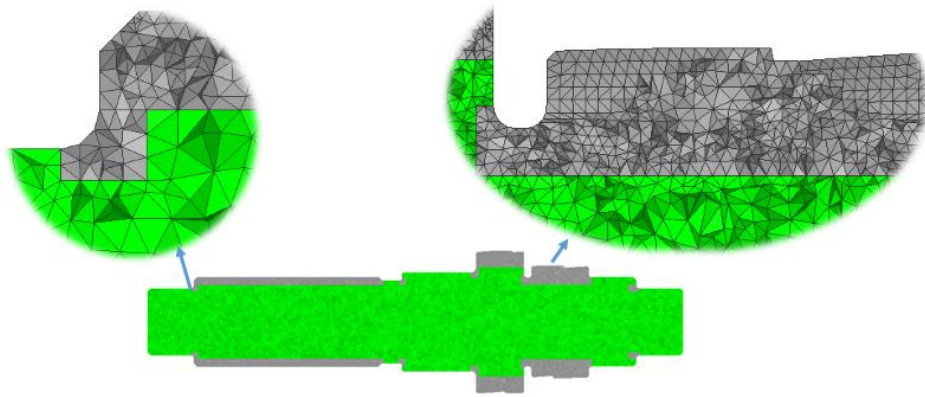


Figure 7.9 CTETRA elements on splined layshaft

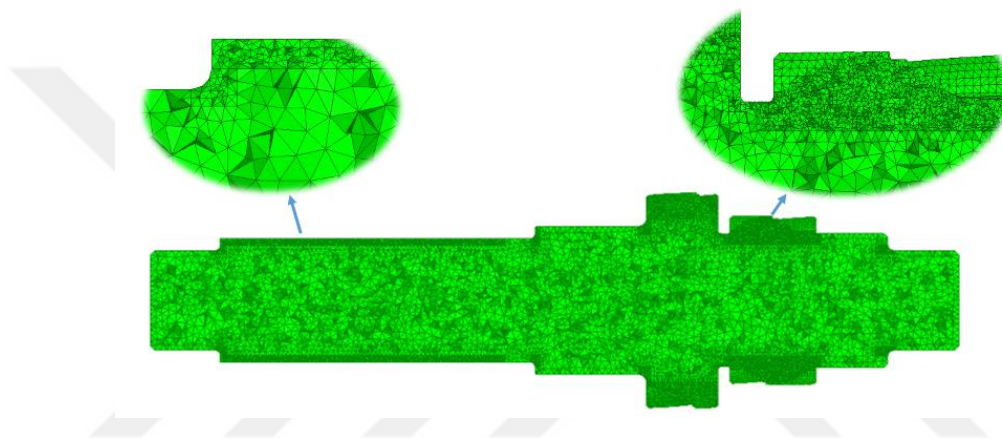


Figure 7.10 CTETRA elements on IF layshaft

#### 7.4.1 Force Extraction of Transmission

Generated torque from engine transferred over input shaft to the transmission via a dry clutch. Here, in Figure 7.11 shafts and sizing can be seen on preliminary design.

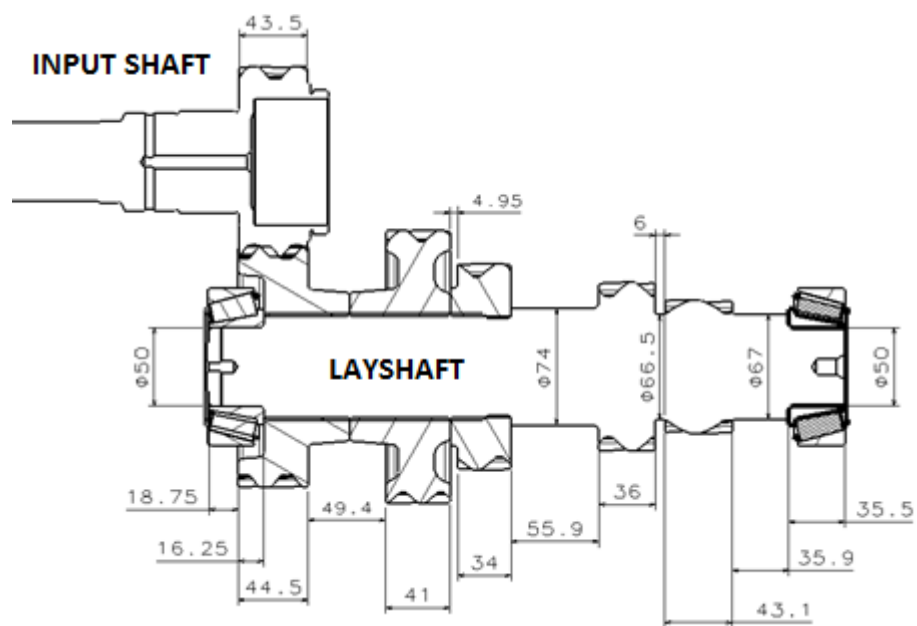


Figure 7.11 Input & Layshaft with rough dimensions

As it is seen, the assembly is accomplished by spline connection and first design and calculations are performed for this connection type. In Figure 7.12 the acted forces on the layshaft is illustrated. Force directions are determined by considering the input rotation of the ICE which is clockwise. From Figure 7.11 applying right hand rule the force direction Figure 7.12 can be obtained.

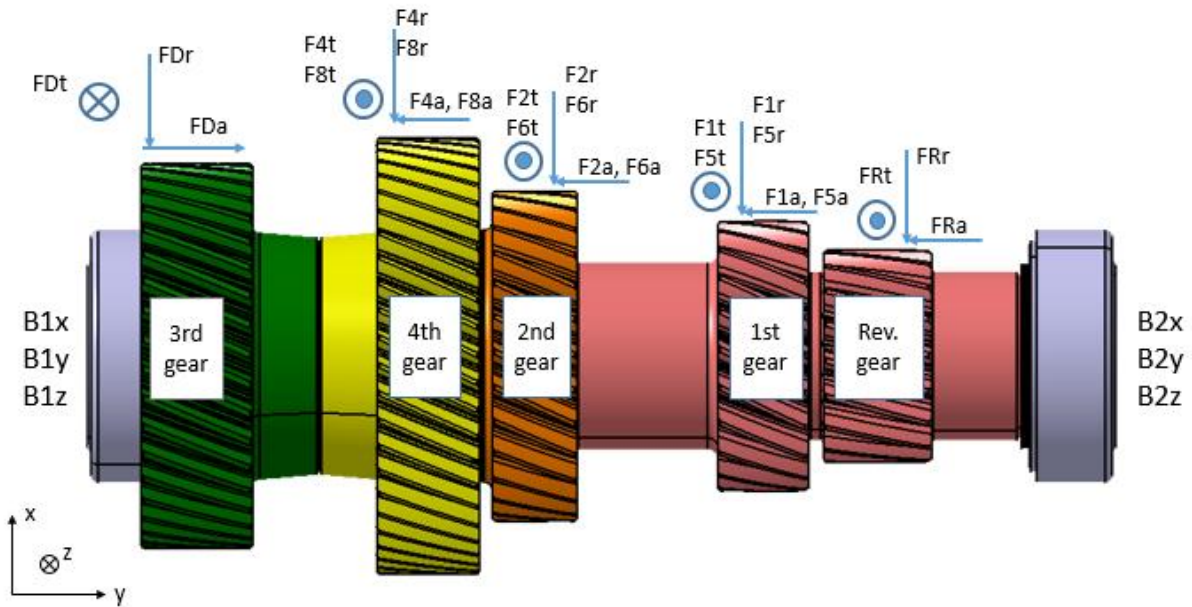


Figure 7.12 Forces on layshaft

With the help of Equation 7.2, Equation 7.3, and Equation 7.4 forces on gear contacts can be calculated. For the gears 4<sup>th</sup> and 8<sup>th</sup>, 2<sup>nd</sup> and 6<sup>th</sup>, and 1<sup>st</sup> and 5<sup>th</sup> occurred contact forces at maximum engine torque is equal. For gears 3<sup>rd</sup> and 7<sup>th</sup> the torque flows directly from input shaft over main shaft which doesn't create a torque flow on layshaft, and layshaft rotates idle for this gear selections. Calculated layshaft forces are tabulated in

Table 7.2.

Gear tangential force:

$$F_t = \frac{M}{r} = \frac{2M}{d} \quad \text{Equation 7.2}$$

Gear radial force:

$$F_R = F_t \times \frac{\operatorname{tg}\varphi}{\cos\beta} \quad \varphi: \text{Pressure angle} \quad \text{Equation 7.3}$$

Gear axial force:

$$F_a = F_t \times \operatorname{tg}\beta \quad \beta: \text{Helix angle} \quad \text{Equation 7.4}$$



Table 7.2 Extracted gear forces for layshaft by active gears

	1st & 5th Gear		2nd & 6th Gear		4th & 8th Gear		Rev. Gear	
<b>Input Moment</b>	1250.000	Nm	1250.000	Nm	1250.000	Nm	1250.000	Nm
<b>FDt (tangential)</b>	21.834	kN	21.834	kN	21.834	kN	21.8337	kN
<b>FDr (radial)</b>	8.6331	kN	8.633	kN	8.633	kN	8.6331	kN
<b>FDa (axial)</b>	9.268	kN	9.268	kN	9.268	kN	9.2678	kN
<b>Moment on Lay</b>	1612.903	Nm	1612.903	Nm	1612.903	Nm	1612.903	Nm
<b>Tangential Force</b>	33.223	kN	26.742	kN	19.400	kN	44.3861	kN
<b>Radial Force</b>	17.0934	kN	13.650	kN	9.903	kN	16.7251	kN
<b>Axial Force</b>	15.492	kN	11.906	kN	8.638	kN	11.8932	kN

## 7.5 CAE Analysis of Layshaft Designs

The 8+1 architecture has a range planetary gear at the final stage before output of gear train assembly, so basically as it is illustrated in Figure 3.5, the torque flow for 5<sup>th</sup>, 6<sup>th</sup>, 7<sup>th</sup> and the 8<sup>th</sup> gears are established over the 1<sup>st</sup>, 2<sup>nd</sup>, 3<sup>rd</sup> and the 4<sup>th</sup> gears. 3<sup>rd</sup> gear engagement is performed directly from the engagement of input and the main shafts. In other words torque flow over layshaft is established only for the 1<sup>st</sup> – 5<sup>th</sup>, 2<sup>nd</sup> – 6<sup>th</sup>, 4<sup>th</sup> – 8<sup>th</sup> and reverse gears.

### 7.5.1 FEA Gear Loading Model

While constructing the model in Figure 7.13 gear forces applied to single point as noted in the figure as gear BC. These nodes are connected directly to the gears on layshaft 3<sup>rd</sup>, 4<sup>th</sup> and 2<sup>nd</sup> and contacted gear meshes 1<sup>st</sup> and reverse gears. The used element is 1D rigid couplings which has no elasticity. The investigated component is layshaft and this rigid element are not connected directly to the layshaft. Gears which are not investigated in this study will take the applied force from these rigid elements and thanks to the defined friction model contact COF is 0.15, the applied force will be transmitted to the investigated component.

The only rigid element in this case which is directly connected to layshaft is bearing connections. This connection type is preferred in order to avoid, bearing mesh creation and contact definition. This allowed to shorten computation time. However, as in every research, this method eliminates the stiffness of bearings and housing wall. Consequently, there must be a limiting border due to the computational cost.

The forces extracted in

Table 7.2 applied to the model from the respected boundary conditions by together with the boundary conditions in Table 7.3. For each gear the axial, radial and tangential forces solved in different FEA jobs to collect each forces effect on the layshaft. Tangential force on layshaft creates torsion, radial force creates bending and axial force creates compression stress.

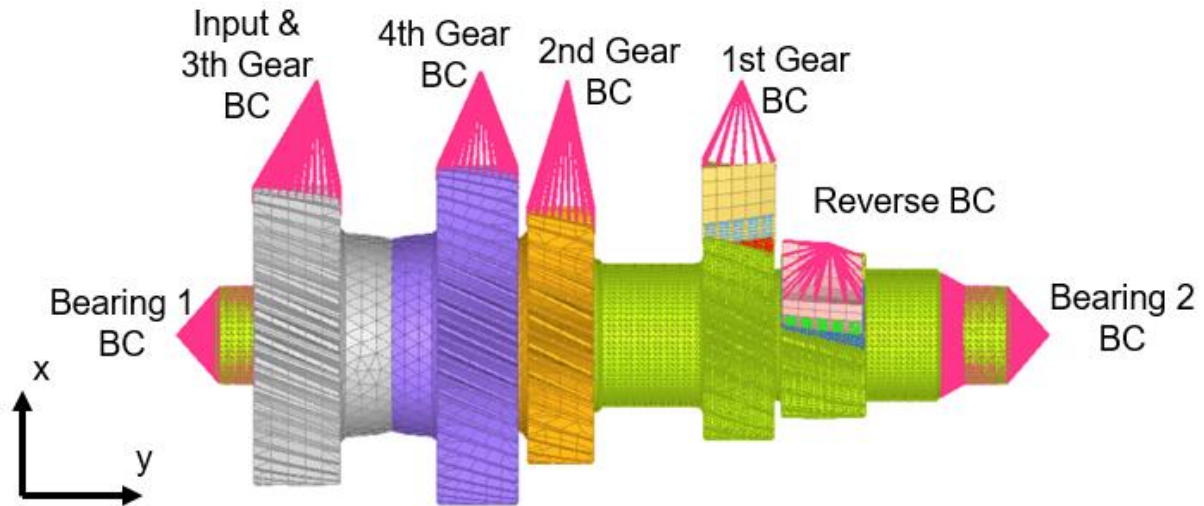


Figure 7.13 Constructed simulation model

Table 7.3 Applied boundary conditions

	Input Torque	Bearing 1	Bearing 2	4 <sup>th</sup> SPC	2 <sup>nd</sup> SPC	1 <sup>st</sup> SPC	Rev SPC
1 <sup>st</sup> & 5 <sup>th</sup> Speed	1250Nm	xyz Trans xz Rot	xz Trans xz Rot	xz Trans xz Rot	xz Trans xz Rot	xyz Trans xyz Rot	xz Trans xz Rot
2 <sup>nd</sup> & 6 <sup>th</sup> Speed	1250Nm	xyz Trans xz Rot	xz Trans xz Rot	xz Trans xz Rot	xyz Trans xyz Rot	xz Trans xz Rot	xz Trans xz Rot
3 <sup>rd</sup> & 7 <sup>th</sup> Speed	1250Nm	xyz Trans xz Rot	xz Trans xz Rot	xyz Trans xz Rot	xyz Trans xz Rot	xyz Trans xz Rot	xyz Trans xz Rot
4 <sup>th</sup> & 8 <sup>th</sup> Speed	1250Nm	xyz Trans xz Rot	xz Trans xz Rot	xyz Trans xyz Rot	xz Trans xz Rot	xz Trans xz Rot	xz Trans xz Rot
Rev. Speed	1250Nm	xyz Trans xz Rot	xz Trans xz Rot	xz Trans xz Rot	xz Trans xz Rot	xz Trans xz Rot	xyz Trans xyz Rot

FEA stress analysis are performed for gear 1, gear 2, gear 4 and reverse gears, for each gear group 3 analysis as tangential, radial and axial loading, in total 12 stress data are obtained. This procedure is followed for splined and interference fitted layshaft. Gravitational load is introduced as constant mean stress to splined layshaft and interference fit pressure + gravitational load is introduced as constant mean stress for interference fitted layshaft analysis.



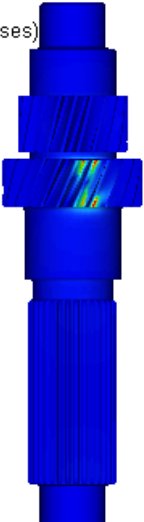


Table 7.4 shows each applied forces stress result on layshaft. The stress colour contours are not communized due to the wide variety of the results. The only difference for splined solution, for the second gear's axial load is flowed over fourth and third gear on layshaft and carried by bearing one which is on the left side of Figure 7.13. This axial load do not creates stress on layshaft, for this reason this analysis is skipped.

---

Table 7.5 shows the stress results for constructed Interference fitted layshaft assembly. Apart from the splined connection the axial loads caused by third, fourth and second gears are carried by the interference fit connection. Due to the tight connection of IF. While constructing the IF layshaft the mesh portion of the first and reverse gear are sustained and the spline geometry mesh is created. Therefore the stress results showed no small deviation on these gears.



Table 7.4 Splined Layshaft stress analysis result table

<p>Contour Plot Element Stresses (2D &amp; 3D)(vonMises) Global System Advanced Average</p>  <p>6.088E+02 5.411E+02 4.735E+02 4.058E+02 3.382E+02 2.706E+02 2.029E+02 1.353E+02 6.764E+01 0.000E+00</p> <p>No result</p> <p>Max = 6.088E+02 Grids 7686125 Min = 3.436E-02 Grids 7696622</p>	<p>Contour Plot Element Stresses (2D &amp; 3D)(vonMises) Global System Advanced Average</p>  <p>4.770E+02 4.240E+02 3.710E+02 3.180E+02 2.650E+02 2.120E+02 1.590E+02 1.060E+02 5.300E+01 0.000E+00</p> <p>No result</p> <p>Max = 4.770E+02 Grids 7792411 Min = 5.429E-03 Grids 8197436</p>
<p>Layshaft splined 1st gear torsion</p> <p>Contour Plot Element Stresses (2D &amp; 3D)(vonMises) Global System Advanced Average</p>  <p>1.350E+03 1.200E+03 1.050E+03 9.000E+02 7.500E+02 6.000E+02 4.500E+02 3.000E+02 1.500E+02 0.000E+00</p> <p>No result</p> <p>Max = 1.998E+03 Grids 7674276 Min = 1.320E-02 Grids 7696661</p>	<p>Layshaft splined 1st gear bending</p> <p>Contour Plot Element Stresses (2D &amp; 3D)(vonMises) Global System Advanced Average</p>  <p>4.711E+02 4.187E+02 3.664E+02 3.140E+02 2.617E+02 2.094E+02 1.570E+02 1.047E+02 5.234E+01 0.000E+00</p> <p>No result</p> <p>Max = 4.711E+02 Grids 7827049 Min = 1.090E-06 Grids 8310108</p>
<p>Layshaft splined 1st gear axial</p> <p>Contour Plot Element Stresses (2D &amp; 3D)(vonMises) Global System Advanced Average</p>  <p>6.769E+02 6.017E+02 5.265E+02 4.512E+02 3.760E+02 3.008E+02 2.256E+02 1.504E+02 7.521E+01 0.000E+00</p> <p>No result</p> <p>Max = 6.769E+02 Grids 7792411 Min = 5.034E-03 Grids 7680450</p>	<p>Layshaft splined 2nd gear torsion</p> <p>Axial load in splined connection carried by bearing 1st.</p>
<p>Layshaft splined 2nd gear bending</p>	<p>Layshaft splined 2nd gear axial</p>

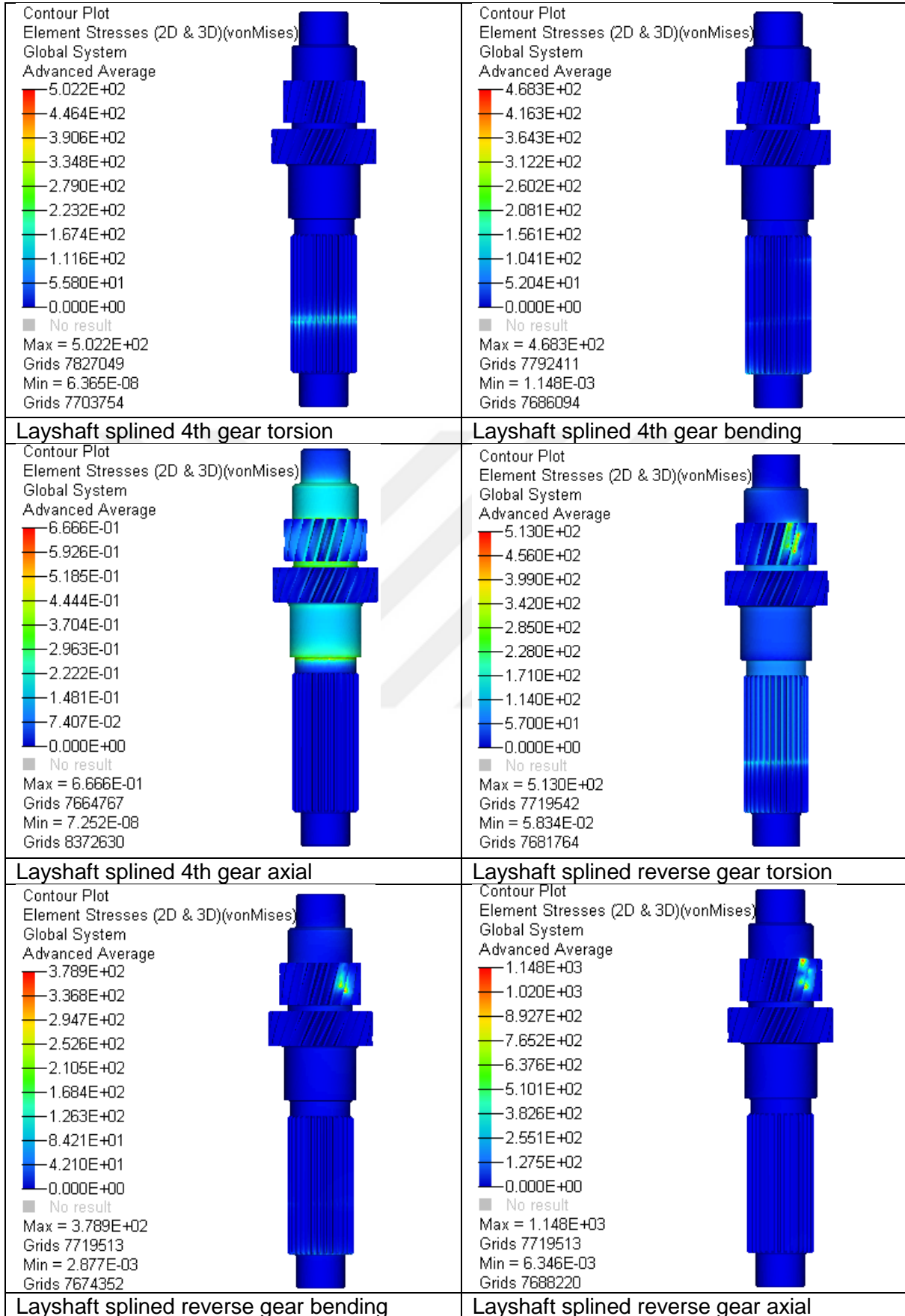



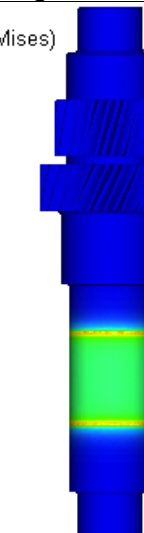
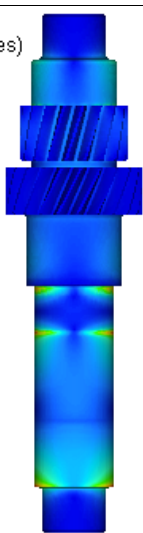
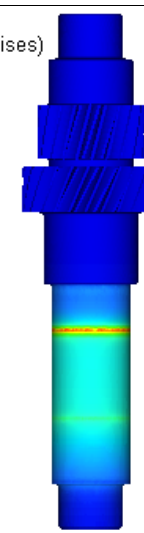
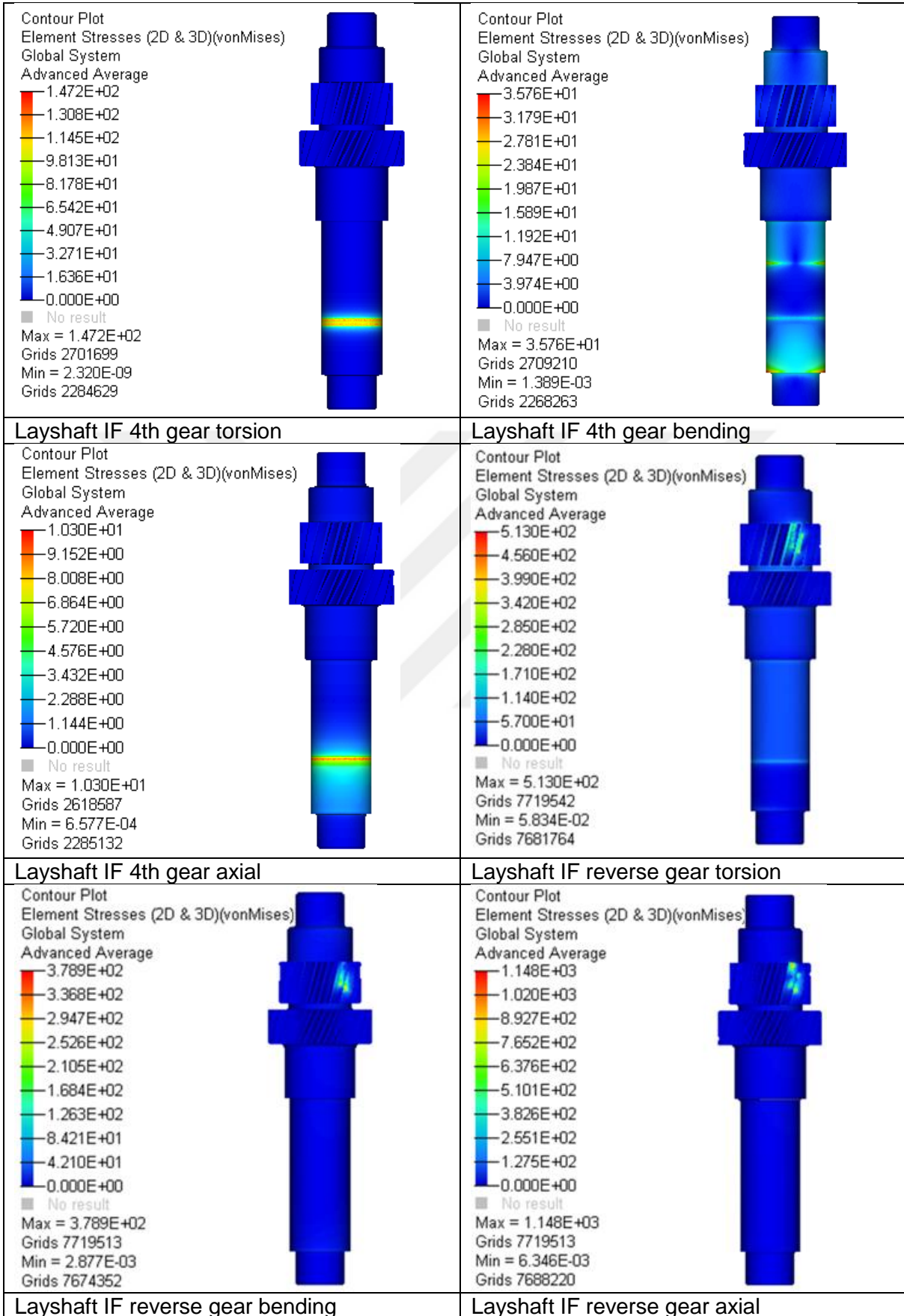




Table 7.5 IF Layshaft stress analysis results table

<p>Contour Plot Element Stresses (2D &amp; 3D)(vonMises) Global System Advanced Average</p>  <p>6.088E+02 5.411E+02 4.735E+02 4.058E+02 3.382E+02 2.706E+02 2.029E+02 1.353E+02 6.764E+01 0.000E+00</p> <p>No result Max = 6.088E+02 Grids 7686125 Min = 3.436E-02 Grids 7696622</p>	<p>Contour Plot Element Stresses (2D &amp; 3D)(vonMises) Global System Advanced Average</p>  <p>4.770E+02 4.240E+02 3.710E+02 3.180E+02 2.650E+02 2.120E+02 1.590E+02 1.060E+02 5.300E+01 0.000E+00</p> <p>No result Max = 4.770E+02 Grids 7792411 Min = 5.429E-03 Grids 8197436</p>
<p>Layshaft IF 1st gear torsion</p> <p>Contour Plot Element Stresses (2D &amp; 3D)(vonMises) Global System Advanced Average</p>  <p>1.350E+03 1.200E+03 1.050E+03 9.000E+02 7.500E+02 6.000E+02 4.500E+02 3.000E+02 1.500E+02 0.000E+00</p> <p>No result Max = 1.998E+03 Grids 7674276 Min = 1.320E-02 Grids 7696661</p>	<p>Layshaft IF 1st gear bending</p> <p>Contour Plot Element Stresses (2D &amp; 3D)(vonMises) Global System Advanced Average</p>  <p>1.353E+02 1.203E+02 1.053E+02 9.023E+01 7.519E+01 6.015E+01 4.511E+01 3.008E+01 1.504E+01 0.000E+00</p> <p>No result Max = 1.353E+02 Grids 2701699 Min = 5.403E-08 Grids 2266938</p>
<p>Layshaft IF 1st gear axial</p> <p>Contour Plot Element Stresses (2D &amp; 3D)(vonMises) Global System Advanced Average</p>  <p>4.569E+01 4.062E+01 3.554E+01 3.046E+01 2.539E+01 2.031E+01 1.523E+01 1.015E+01 5.077E+00 0.000E+00</p> <p>No result Max = 4.569E+01 Grids 2709210 Min = 8.608E-03 Grids 2284762</p>	<p>Layshaft IF 2nd gear torsion</p> <p>Contour Plot Element Stresses (2D &amp; 3D)(vonMises) Global System Advanced Average</p>  <p>1.267E+01 1.126E+01 9.852E+00 8.444E+00 7.037E+00 5.630E+00 4.222E+00 2.815E+00 1.407E+00 0.000E+00</p> <p>No result Max = 1.267E+01 Grids 2324419 Min = 4.090E-07 Grids 2482699</p>
<p>Layshaft IF 2nd gear bending</p>	<p>Layshaft IF 2nd gear axial</p>



## 7.5.2 Layshaft assembly comparison

After performing stress analysis on two different layshaft proposal designs, one distinct difference between two design options is the occurred stress type on the effective connection surface. On the surface of IF design compression stress (Figure 7.14) is beneficial for fatigue life improvement. The stress at spline roots (Figure 7.15) are tensional and tensile stress is the main reason of fatigue failure for splined connections. This could be accounted as one the superiority of interference fitted connections.

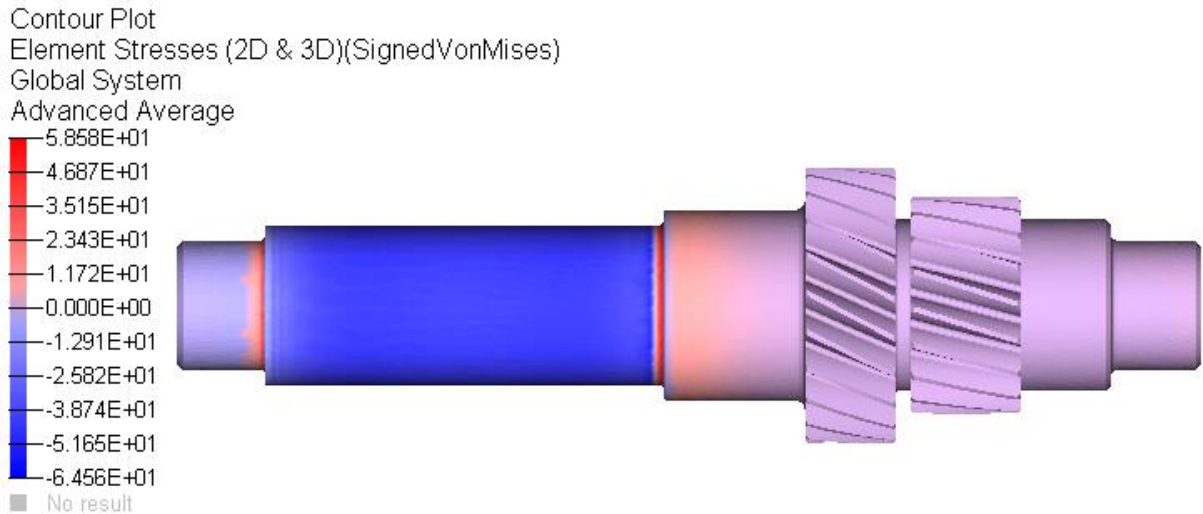


Figure 7.14 Layshaft compression stress on the surface

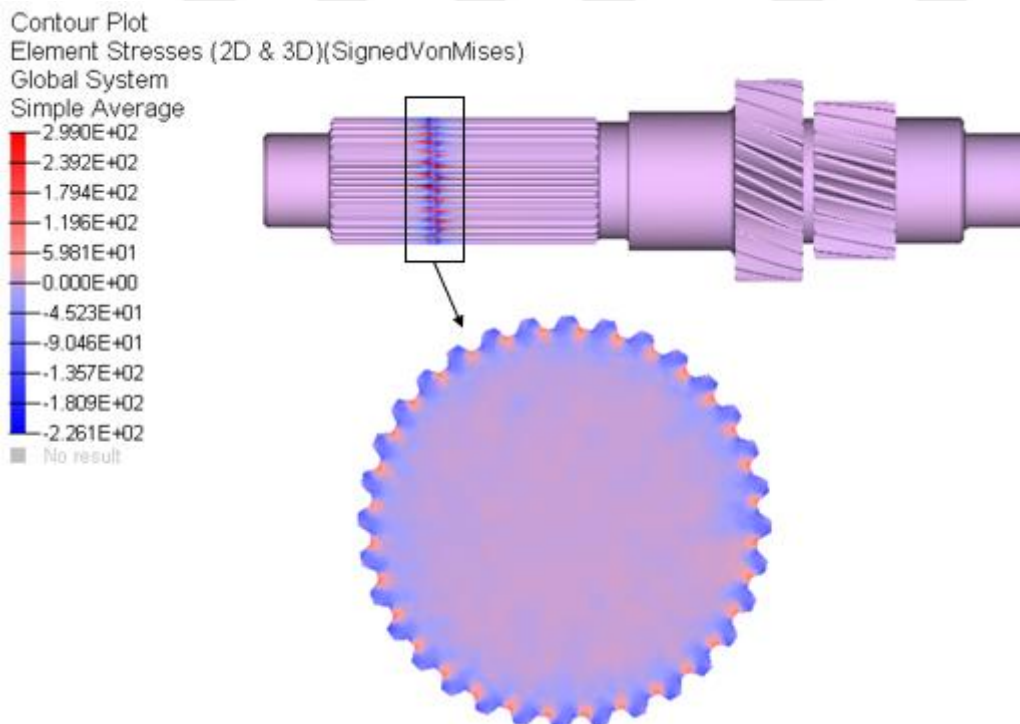


Figure 7.15 Torsional loading of 4th gear, tension at spline roots

### 7.5.3 Mission Profile of Transmission

Before calculation of the durability assessment, transmission design duty cycle is estimated for each gear as in Table 7.6. From this point of view an estimated vehicle mileage could be made with respect to average engine speed. Engine sweet point for maximum torque extraction is between 1200 – 1700 rpm. Highest vehicle speed achieved at 2200 rpm of engine crank speed. Average rpm value of 1700 rpm is taken for further mileage estimation. Vehicle's static speed at 1700 rpm could be calculated easily with Equation 7.5.

Vehicle speed calculation:

$$Velocity_{veh} = \frac{ICE \text{ rpm}}{i_{trans.} \times i_{diff} \times i_{wheel \text{ hub}}} \times circum_{\text{-}tire} \times \left(\frac{60}{1000}\right) \frac{km}{h} \text{converter} \quad \text{Equation 7.5}$$

Table 7.6 Estimated duty cycle of off road vehicle and its driveline

Gear	Per-cent	8+1 TM Estimated Required Minimum Lifetime (Hours)	Layshaft in service	Percent	Lifetime in Hours
1. Gear	8%	4000	1st+5th Gear	25%	12500
2. Gear	9%	4500	2nd+6th Gear	25%	12500
3. Gear	10%	5000	4th+8th Gear	25%	12500
4. Gear	13%	6500	3rd+7th Gear	25%	12500
5. Gear	17%	8500	Rev. Gear	1%	500
6. Gear	16%	8000	Total Lay un- der Torque	74%	38000
7. Gear	15%	7500			
8. Gear	12%	6000			
Reverse Gear	1%	500			
<b>Total Forward</b>	<b>100%</b>	<b>50500</b>			

The calculated service hours above in Table 7.6 is an estimation of duty cycle that the intended off road vehicle will experience on duty. This is a rough estimation and in theory it has no experimental background rather than company experience from its agricultural business. Due to the missing mission profile and the road load data which is not possible to collect without a vehicle. The total cycle for layshaft life estimation is categorized with the torque flow as 1<sup>st</sup> and 5<sup>th</sup> gear, 2<sup>nd</sup> and 6<sup>th</sup> gear, 4<sup>th</sup> and 8<sup>th</sup> gear and a reverse gear. Each gear couples assumed to be in operation as 12500 hours. By this total transmission life in hours is 50000 hours forward and 500 hours reverse capacity.

Normally automotive companies follows the trend of power train development for their next generation vehicles with the help of existing vehicle platforms or follows the next generation vehicle development with the data of existing power train combination. This is one of the drawback for the companies face with which is in development project of both vehicle and its power-train from scratch without past experience.

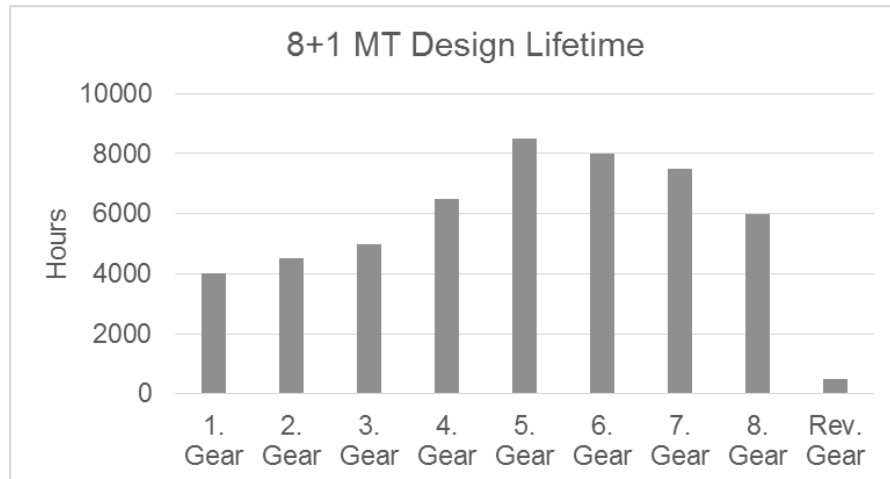


Figure 7.16 Estimated duty cycle of transmission

The table below Table 7.7 the layshaft load cycle is calculated with determined average 1700 rpm transmission input value. layshaft's rpm is calculated as follows.

$$\frac{n_{ICE}}{n_{layshaft}} = \frac{z_{input shaft}}{z_{layshaft}} \quad \text{Equation 7.6}$$

$$\frac{1700 \text{ rpm}}{n_{layshaft}} = \frac{40}{31} \rightarrow n_{lay} = 1317.5 \text{ rpm}$$

For every gear portion 988,125,000 cycle will be accepted as minimum limit cycle for the achievement of layshaft design in post fatigue analysis.

Table 7.7 Layshaft duty cycle with torque flow

Layshaft in service	Percent	Lifetime in Hours	Equivalence Lay Cycle with Torque
1st+5th	25%	12500	988,125,000
2nd+6th	25%	12500	988,125,000
4th+8th	25%	12500	988,125,000
rev	1%	500	39,525,000
<b>Total Lay in Service</b>	<b>74%</b>	<b>38000</b>	<b>3,003,900,000</b>

From operation hours of each gear, the total vehicle mileage could be estimated by considering average ICE rpm value (1700 rpm) with the help of Equation 7.5 see Table 7.8.

Table 7.8 Static speeds at 1700 rpm for each gear selection

	Shifts	Ratio	Velocity @ 1700 rpm	Mileage in km
<b>Low</b>	1st Gear	<b>8.854</b>	6.9 km/h	27,600 km
	2nd Gear	<b>5.971</b>	10.3 km/h	46,350 km
	3rd Gear	<b>4.194</b>	14.6 km/h	73,000 km
	4th Gear	<b>2.982</b>	20.5 km/h	133,250 km
<b>Hi</b>	5th Gear	<b>2.111</b>	29.0 km/h	246,500 km
	6th Gear	<b>1.424</b>	43.0 km/h	344,000 km
	7th Gear	<b>1.000</b>	61.3 km/h	459,750 km
	8th Gear	<b>0.711</b>	86.2 km/h	517,200 km
	Reverse	<b>9.319</b>	6.6 km/h	3,300 km
<b>Total Mileage</b>				<b>1,847,650 km</b>

Though companies do not provide warranty over one million km mileage, 1,000,000 km is accepted as duty life of a heavy commercial vehicle. Of course there are many vehicles on the road with over million km. For power train applications, they must provide enough durability as much as the vehicle, otherwise this design categorized as over engineered design. Despite this fact, engineers always prefer to stay in safe side especially in the first prototyping and first product launches.

By considering the safety parameters 1,847,650 km mileage design aim could be considered non objectionable especially with the lack of similar design experience.

#### 7.5.4 Post Fatigue Life Analysis

Torsion, bending and compression causes multi directional loading of the layshaft, as consequence, it is exposed to multiaxial loading which is classified as multiaxial fatigue investigation. From this aspect as it is described as FEMFAT module utilization in Figure 2.19, two of the module is applicable for this project. The one is Channel Max and the other is Trans Max. These two modules allows to investigate multiaxial stress loading of components. Max notation comes from multiaxial. Channel Max requires load time histories along with related stress data from FEA, for each stress data there is one channel that the load history could be defined by time. For this project we do not have a time dependent load history for respected FEA stress result, at this point Trans Max (transient multiaxial stress module) is utilized. With this module the sequences of the load cases with constant mean stress are introduced to the software.

Fatigue related material data such as Young's modulus, elongation at rupture A5, cyclic hardening coefficient K', cyclic hardening exponent n', slope of S-N curve, cycle limit of endurance, survival probability, thickness of specimen, roughness of specimen, temperature of specimen, fatigue strength coefficient could be defined through material definition section see Table 7.9.

For our application stress controlled FEMFAT ECS material generator utilized which predicts to material behavior based on FKM guideline. From the material class selection of the material generator, Case Hardening Steels is defined and for the materials 18CrNiMo7-6, 20NiCrMo2-2 and 20MnCr5, ultimate tensile strength and yield points are provided by experimental work.

Table 7.9 FEMFAT material definition parameters

<b>FEMFAT Matetial</b>	<b>18CrNiMo7-6 with CHD</b>	<b>20MnCr5 with CHD</b>	<b>20NiCrMo2-2 with CHD</b>
UTS	1465 MPa	1245 MPa	1245 MPa
Yield	1175 MPa	1165 MPa	1230 MPa
Endurance Limit	780 MPa	700 MPa	555 MPa
Rz	6.3 $\mu\text{m}$	6.3 $\mu\text{m}$	6.3 $\mu\text{m}$
K' Cyclic Hardening Coeff	2358.65 MPa	2004.450073	2004.450073
n' Cyclic Hardening exponent	0.110000	0.110000	0.110000
Sigma'f Fatigue strength coeff	3106.57	2787.952393	2210.447998
b Fatigue strength exponent	-0.090909	-0.090909	-0.090909
Epsilon'f Fatigue Ductility coeff:	12.230384	20.074156	2.433481
c Fatigue ductility exponent	-0.826446	-0.826446	-0.826446

The software's approximated endurance limits for each material is corrected with the test result which are obtained by rotating bending fatigue test. See Figure 6.22, Figure 6.23, and Figure 6.24 for corresponded endurance limits with dashed lines which are test. Continues lines represents initial FEMFAT material generator based on FKM guideline.

Previously obtained stress data from FEA analysis are superimposed in post fatigue software FEMFAT Trans Max as time steps to investigate the effect of multiaxial fatigue on structure. For splined layshaft gravity stress result is introduced as constant stress and for interference layshaft, both gravity and interference fit pressure are introduced as constant stress.

While on the visualization of the results the required layshaft cycle with torque flow is accepted as reference value for colour contour representation see Table 7.7. Minimum required cycle limit is for reverse gear, pink colour is used to highlight the locations which has 39,525,000 and lower. The red colour on post visualization will help to identify weak spots. Red colour is used to highlight locations endures lower than 988,125,000. All gear selection related stresses results are included in post investigation so basically searching for min 988,125,000 cycle endurance will cover the all the gear selections for layshaft.

After the experimental work, post fatigue simulations are run with modified miner rule for the two materials 18CrNiMo7-6 and 20NiCrMo2-2 which are highest and the lowest endurance strengths. Analysis results are tabulated in Table 7.10, Table 7.11 for interference fitted construction with two mentioned materials and splined layshaft analysis results are tabulated in Table 7.12 and Table 7.13 for two different materials. It was clearly seen that the weakest point is the gear portion. The colour contour is drawn with inverse damage ( $1/\text{Damage}$ ) in logarithmic scale. This representation shows the remaining life cycle of component with the same loading that is used as input.

For each material group, both designs has same lowest inverse damage value, this can be explained by the utilization of same mesh on the entire layshaft which is almost identical apart from the splined portion. The distinct difference of the both designs, splined layshaft presented a weak point on the portion of third gear's connected splines. The spline at this point is torque input to the layshaft for all the gear combinations. Except the gear portion overall shaft presents



enough durability. The low endurance on gears could lead to failures like pitting, scuffing and tooth root breakage.

Table 7.10 FEMFAT Layshaft IF with 18CrNiMo7-6

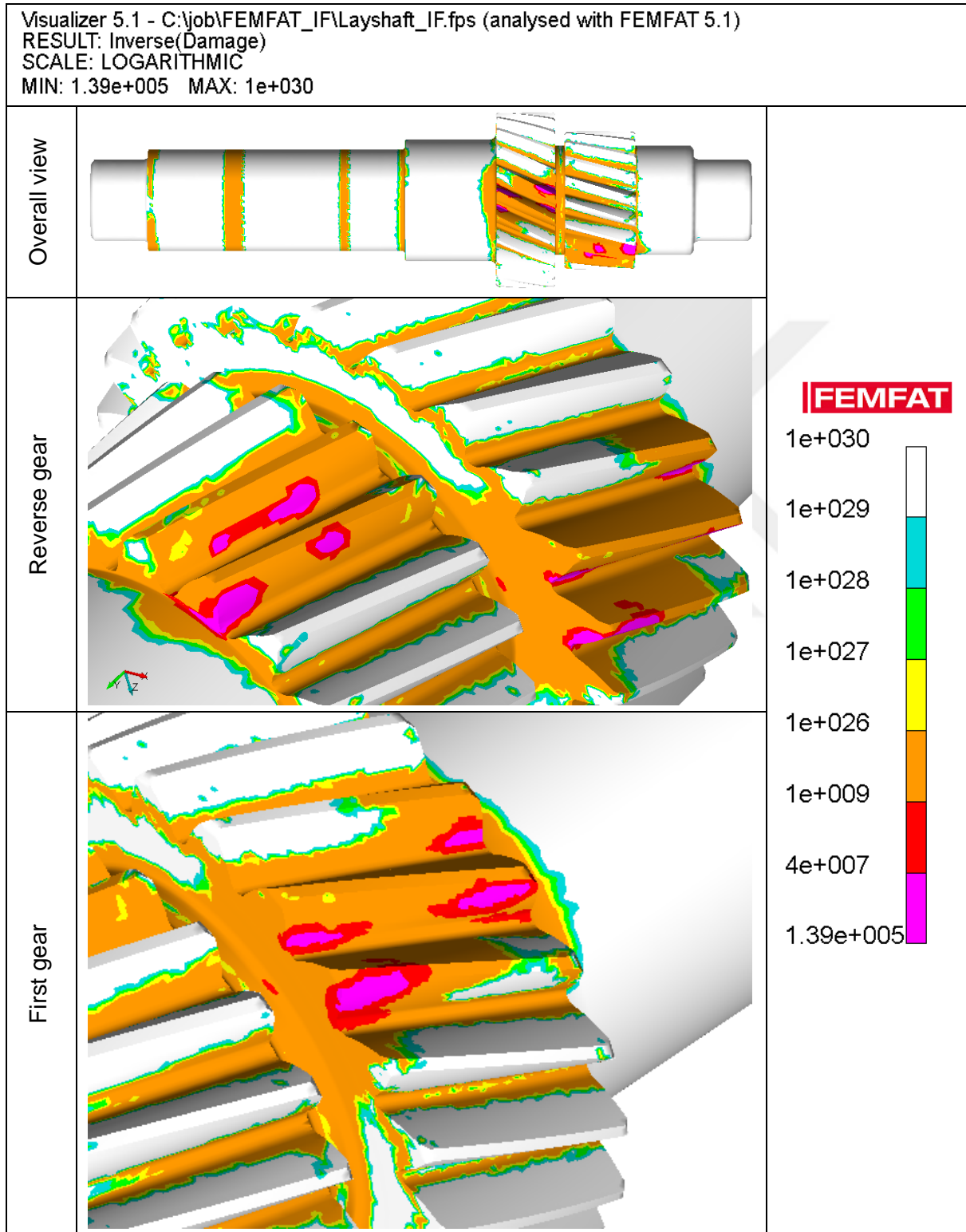




Table 7.11 FEMFAT Layshaft IF with 20NiCrMo2-2

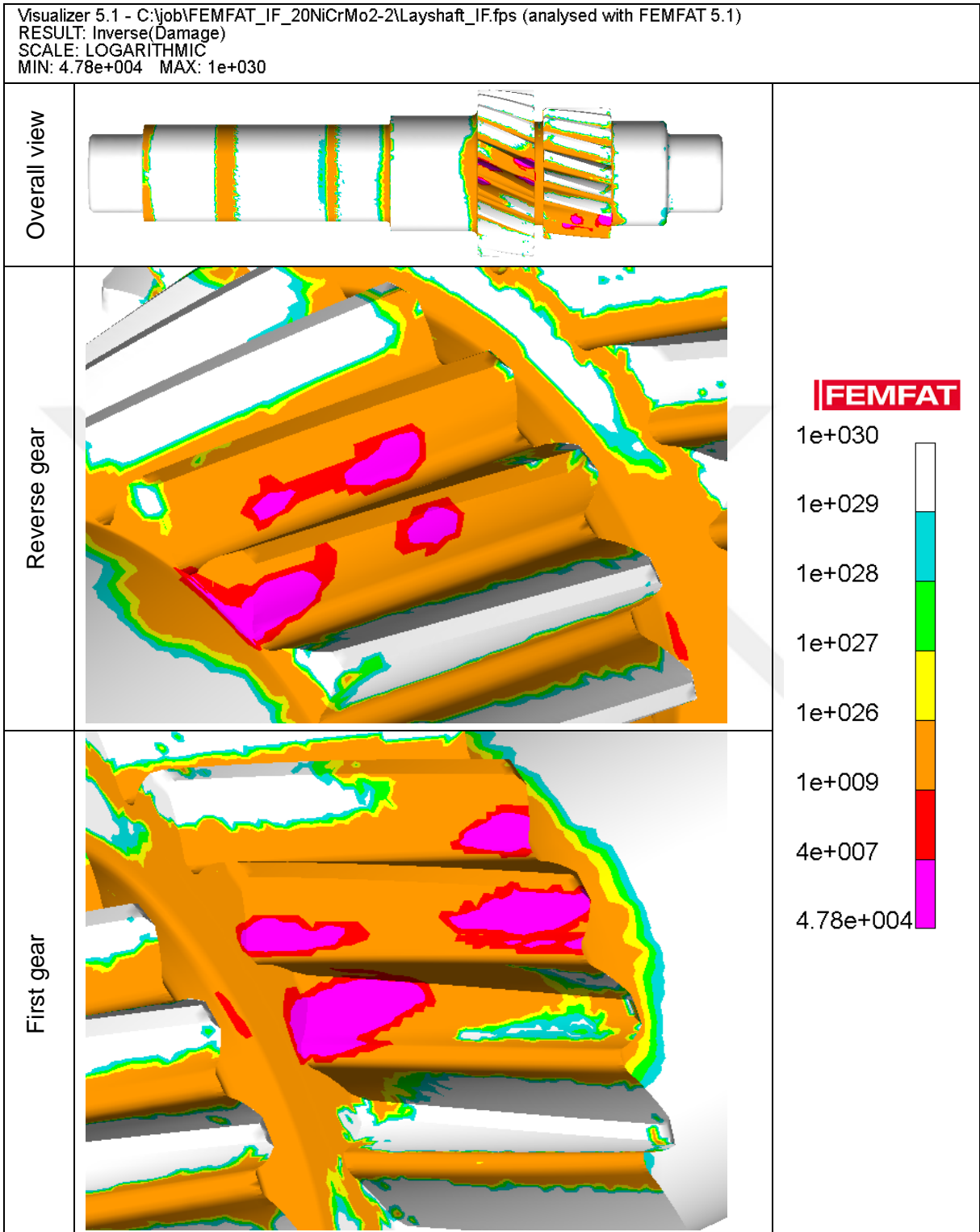


Table 7.12 FEMFAT Layshaft splined with 18CrNiMo7-6

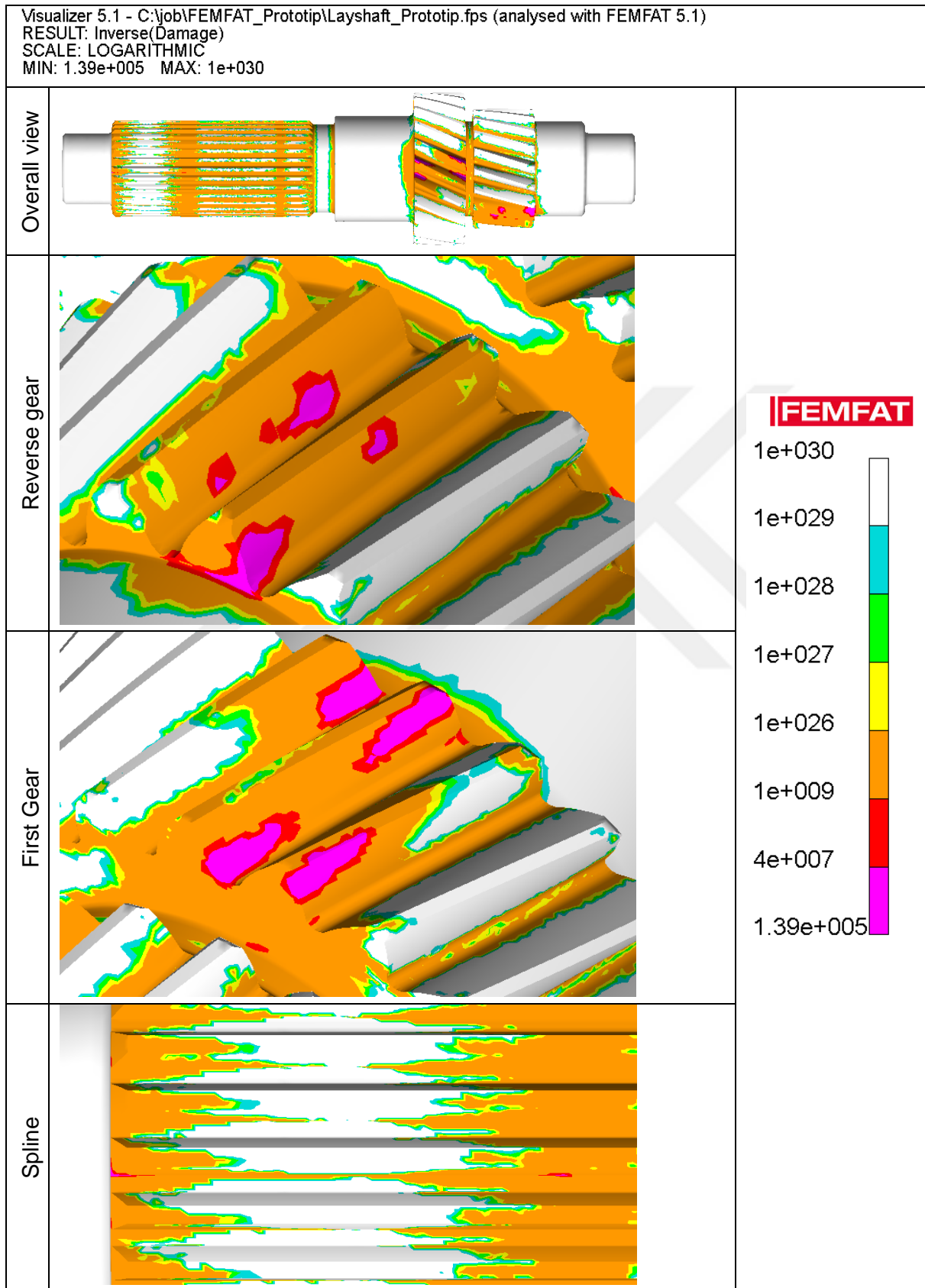
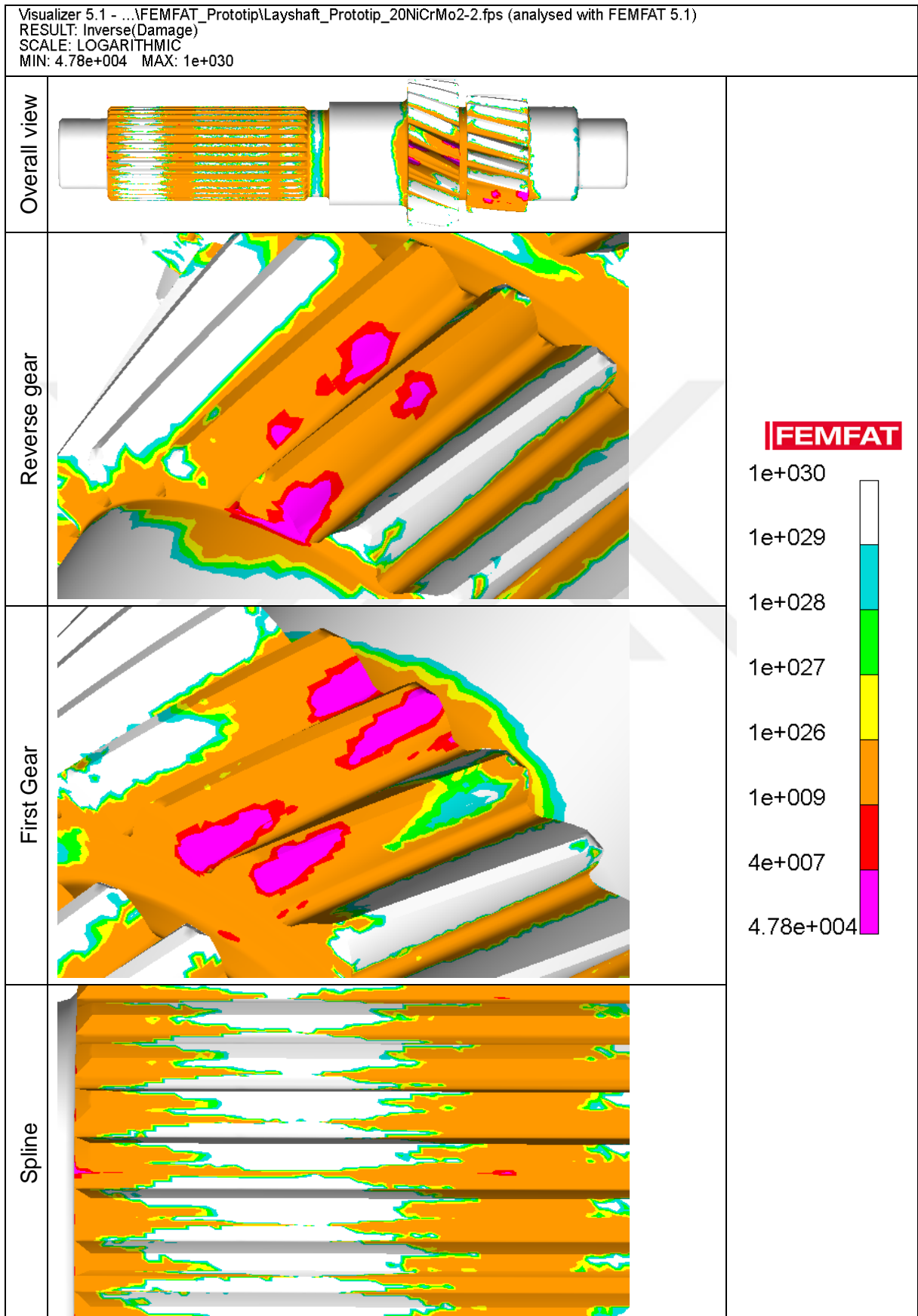


Table 7.13 FEMFAT Layshaft splined with 20NiCrMo2-2



Based on the results which calculates damage accumulation and then inverts the calculated damage to show remaining cycle, one of the weak point is the gear to shaft fillets both on first gear and the reverse gear side. Based on these radii highly stressed radii, this portion of the shaft is optimized. The fillet radius as 1mm at first later it is increased to 3 mm on each side.

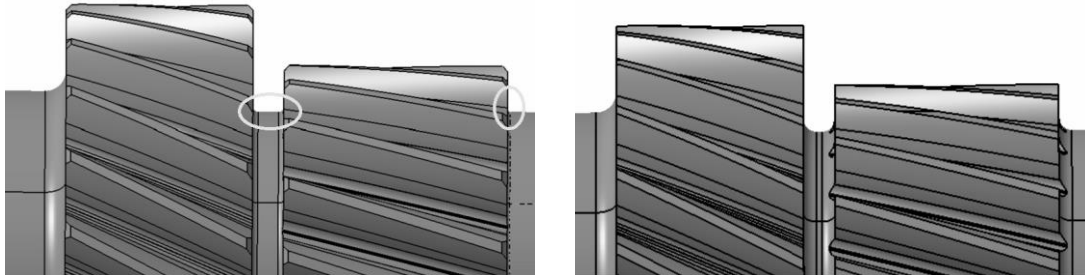


Figure 7.17 Left the first analysed layshaft, right improvement proposal

Important weakness of the design is meshed tooth itself. Reverse gear doesn't look much critical when it is compared to the required life cycle. But first gear, which also serves as torque flow path for the 5<sup>th</sup> gear is critical and more precautions must be taken. Tooth micro geometry modifications such as, crowning, tip relief etc. could eliminates the stress concentration on edges and improves the gear failures.

## 8 Results & Discussion

Material characterization through rotating bending testing is partially successful since the complete SN curve couldn't be obtained, however the endurance limit for the case hardened specimens was obtained. This gave opportunity to evaluate materials amongst themselves in terms of their strengths under cyclic loading. These endurance values are also utilized in post fatigue process FEMFAT software.

From the material point of view 18CrNiMo7-6 represents better fatigue behaviour than the other two materials but it comes with a cost around € 7000 than the other two materials for the planned batch size of production which is revealed at section 5. 20MnCr5 and 20NiCrMo2-2 cost almost the same and 20MnCr5 serves better fatigue behaviour, from that point 20MnCr5 is so far the ideal material in our design with the help of gear parameter improvements.

The obtained stresses under exposed forces on layshaft by the assembled gears are almost identical for the splined and interference fitted layshaft since the highest stress value is occurred at shaft's on build gear portion.

For the reverse gear portion the deviation from its duty cycle is relatively smaller than first gear. Reverse gears are mostly excluded from fatigue durability searches. For this reason, first gear could be the failure mode of this transmission and its parameters must be reviewed.

The interference fit connection produces pre compression on the layshaft component, which is good for better fatigue behaviour. This connection exhibits better performance under cyclic loading than the splined connection.

Despite the better performance of IF connection, the upper engineering management is not welcomed warmly the interference fit connection solution, because of the previously designed interference fit connections for agricultural tractor which were failed at the first test on the field. Due to this reality among the two of the design alternatives for prototyping, the splined solution Figure 8.1 is produced. The work also revealed the reason of common trend to the interference fit solution.



Figure 8.1 Manufactured prototype layshaft with spline connection

In general changing material will not change the elasticity so these three materials are almost identical at the linear portion. For that reason shaft deflection will be the same for three of them, therefore material selection will only affect the durability of the component.

## 8.1 Future Work

Testing was performed only in material basis. The ideal design could be verified by performing the real life duty test of the layshaft. One way is making prototype of the complete transmission and running it on test bench. Another way is performing vehicle test on the field with newly developed vehicle. Test bench preparation is still continuing within the company. With the help of rig tests the proposed numerical approach could be compared with the real condition will be improved to make more reliable fatigue estimations on the product development phase.

A common approach for vehicle and powertrain development is keeping one of these from previous design and implementing a new design either for powertrain or vehicle. In other words when one the dynamics of these two main subsystems of the vehicle is known it would be easier to estimate the applied forces on one of these systems. The one assembled prototype of the vehicle will provide a load data for ongoing development of the transmission.



## 9 Bibliography

Altair Engineering, Inc., 2015. *Practical Aspects of Finite Element Simulation A Study Guide*. Michigan, USA: Altair University.

Bathias, C. & Pineau, A., 2011. *Fatigue of Materials and Structures Application to Design and Damage*. London: John Wiley & Sons, Inc..

Brain, M., n.d. *How Stuff Works*. [Online]

Available at: <http://auto.howstuffworks.com/transmission.htm>

[Accessed 15 07 2016].

BS ISO 1143:, 2010. *BS ISO 1143:2010 Metallic Materials - Rotating bar bending fatigue testing*, Geneva Switzerland: ISO copyright office.

Budynas, N., 2006. *Shigley's Mechanical Engineering Design*. Eight ed. s.l.:McGraw-Hill.

Budynas, R. G. & Nisbett, J. K., 2011. *Shigley's Mechanical Engineering Design*. New York: McGraw-Hill.

Challister, W. D. J., 2007. *Material Science and Engineering*. New York: John Wiley & Sons, Inc..

Chapetti, M. D. & Guerrero, A. O., 2013. Estimation of Notch Sensitivity and Size Effects on Fatigue Resistance. *Procedia Engineering* 66, pp. 323-333.

Dassault Systemes, 2006. *ABAQUS 2016 Analysis User's Guide Volume IV Elements*, s.l.: Dassault Systemes.

Dassault Systemes, 2011. *SIMULIA UK RUM 2011*, South Gloucestershire: SIMULIA.

Dassault Systemes, 2016. *Abaqus 2016 Analysis User's Guide Volume V*, s.l.: Dassault Systemes SIMULIA.

Fatemi, A., n.d. *Cyclic Deformation and strain-life approach*, Ohio: University of Toledo.

Fatemi, A., n.d. *Fatigue Design Methods*, Ohio: University of Toledo.

Fatemi, A., n.d. *Fatigue from Variable Amplitude Loading*, Ohio: University of Toledo.

Fatemi, A., n.d. *Fatigue test an S-N approach*, Ohio: University of Toledo.

Fatemi, A., n.d. *Fundamentals of LEFM and Application to Fatigue Crack Growth*, Ohio: University of Toledo.

Fatemi, A., n.d. *Introduction to Mechanical Failure Modes*, Ohio: University of Toledo.

Fatemi, A., n.d. *Macro/Micro aspects of fatigue of metals*, Ohio: University of Toledo.

Fatemi, A., n.d. *Multiaxial Fatigue Loading*, Ohio: University of Toledo.

Fatemi, A., n.d. *Notches and Their Effects*, Ohio: University of Toledo.

Fatemi, A., n.d. *Residual Stresses and Their Effects on Fatigue Resistance*, Ohio: University of Toledo.

- Fatemi, A., Stephens, R. I., Stephens, R. I. & Fuchs, H. O., 2001. *Metal Fatigue in Engineering*. USA & Canada: John Wiley & Sons, Inc..
- Fischer, R. et al., 2015. *The Automotive Transmission Book*. Switzerland: Springer International Publishing.
- Frost, N. E., 1959. A relation between the critical alternating propagation stress and crack length for mild steel. *Proc Instn Mech Engrs*, pp. 173: 811-836.
- Gaier, C., 2010. *Multi-axial Fatigue Analysis with the FE Post-processor FEMFAT*. Örebro, ECS MAGNA.
- Genel, K. & Demirkol, M., 1998. Effect of case hardening depth on fatigue performance of AISI 8620 carburized steel. *International Journal of Fatigue*, pp. 207-212.
- General Motors Company, 1939. *Generations of GM History*. [Online] Available at: [https://history.gmheritagecenter.com/wiki/index.php/1939,\\_The\\_First\\_Fully\\_Automatic\\_Transmission](https://history.gmheritagecenter.com/wiki/index.php/1939,_The_First_Fully_Automatic_Transmission) [Accessed 20 July 2016].
- Gillespie, T. D., 1992. *Fundamentals of Vehicle Dynamics*. Warrendale, PA: Society of Automotive Engineers, Inc..
- Göksenli, A. & Eryurek, I., 2009. Failure analysis of an elevator drive shaft. *Engineering Failure Analysis*, pp. 1011-1019.
- Hoerbiger Antriebstechnik GmbH, n.d. *HOERBIGER Synchronizers*. [Online] Available at: <http://www.hoerbiger.com/en-1/pages/149> [Accessed 19 July 2016].
- Johansen, S., 2013. *Structural Topology Optimization Basic Theory, Methods and Applications*, Trondheim: Norwegian University of Science and Technology.
- Kandreegula, S. K. et al., 2016. Design and Optimization of Web Fillets for Commercial Vehicle Crankshaft for Improving SCF and Theoretically Correlated. *SAE International*.
- Klebanov, B. M., Barlam, D. M. & Nystrom, F. E., 2007. *Machine Elements Life & Design*. New York: CRC Press Taylor & Francis Group.
- Koechlin, S., 2015. *FKM Guideline : strengths, limitations and experimental validation*. Angoulême, FRANCE, ELSEVIER, p. 309 – 319.
- Lee, J.-L., Pan, J., Hathaway, R. & Barkey, M., 2005. *Fatigue Testing & Analysis*. Oxford, UK;: Elsevier.
- Marini, M. & Ismail, A. B., 2011. TORSIONAL DEFORMATION AND FATIGUE BEHAVIOUR OF 6061 ALUMINIUM ALLOY. *IJUM Engineering Journal*, pp. 21-32.
- Naunheimer, H., Bertsche, B., Ryborz, J. & Novak, W., 2011. *Automotive Transmissions Fundamentals, Selection, Design and Application*. Heidelberg: Springer.
- Norberg, E. & Lövgren, S., 2011. *Topology Optimization of Vehicle Body Structure for Improved Ride & Handling*, s.l.: Linköpings Universitet.



- R.A.Gujar & S.V.Bhaskar, 2013. Shaft Design under Fatigue Loading by Using Modified Goodman Method. *International Journal of Engineering Research and Applications*, pp. 1061-1066.
- Rutten, J., 2005. *Design of a New Transmission Concept*, Stuttgart: Eindhoven University of Technology.
- Schijve, J., 2001. *Fatigue of Structures and Materials*. Dordrecht: Kluwer Academic Publisher.
- Shen, L., 2012. *Fretting and Plain Fatigue Competition Mechanism and Prediction in Spline Shaft-Hub Connection*, Liuyang: PAPIERFLIEGER VERLAG GmbH.
- Sigmund, O., 2001. A 99 line topology optimization code written in Matlab. *Struct Multidisc Optim* 21, pp. 120-127.
- Socie, D. F., 2002. *Fatigue Made Easy - Historical Intro*, Illinois: University of Illinois at Urbana-Champaign.
- Socie, D. F., 2003-2005. *Probabilistic Aspects of Fatigue*, Illinois: University of Illinois at Urbana-Champaign.
- Socie, D. F., 2003. *Multiaxial Fatigue*, Illinois: University of Illinois at Urbana-Champaign.
- Spittel, M. & Spittel, T., 2009. Metal Forming Data. Part 1: Ferrous alloys. In: *Metal Forming Data of Ferrous Alloys - deformation behaviour*. Berlin Heidelberg: SpringerMaterials – The Landolt-Börnstein Database, pp. 984-989.
- Srivastava, N. & Haque, I., 2009. A review on belt and chain continuously variable transmissions (CVT): Dynamics and Control. *Mechanism and Machine Theory*, pp. 19-41.
- Stephens, R. I., Fatemi, A., Stephens, R. R. & Fuchs, H. O., 2001. *Metal Fatigue in Engineering*. Second ed. Canada: John Wiley & Sons Inc..
- Tanaka, K. & Akinawa, Y., 1987. *Notch geometry effect on propagation of short fatigue cracks in notched components*. s.l., s.n., pp. 739-748.
- Temiz, V., n.d. *Lecture Notes: Mil göbek bağlantıları*. [Online] Available at: <http://web.itu.edu.tr/temizv/Sunular/Sunular.htm> [Accessed 04 06 2016].
- Thankachan, D. P. & Purushothaman, P., 2014. Optimum Material and Process Modification to Reduce Lead Time of Pedestal Manufacturing Used in Gearbox Assembly. *International Journal of Engineering Research and Technology*, pp. 2036-2041.
- Tovo, R. et al., 2014. Experimental Investigation of the Multiaxial Fatigue Strength of Ductile Cast Iron. *Theoretical and Applied Fracture Mechanics*, pp. 60-67.
- Ural, A., Khrisnan, V. R. & Papoulina, K. D., 2009. A cohesive zone model for fatigue crack growth allowing for crack retardation. *International Journal of Solids and Structures*, pp. 2453-2462.
- WALTHER, P. D.-I. H. F., 2014. *Fatigue Behaviour*, Dortmund: TU Dortmund.

Yao, C.-H., 2008. *Automotive Transmissions: Efficiently Transferring Power from Engine to Wheels*. [Online]

Available at: <http://www.wesrch.com/energy/mobile/paper-details/pdf-TR1SVVIMGEXUL-automotive-transmissions-efficiently-transferring-power-from-engine-to-wheels>

[Accessed 15 July 2016].

